Universidade de Aveiro Departamento de Química
2018

LUÍS FILIPE FIGUEIREDO MENDES

ESTUDO METABOLÓMICO DA REPROGRAMAÇÃO METABÓLICA INDUZIDA POR FLAVONOIDES EM MACRÓFAGOS HUMANOS

METABOLOMICS STUDY OF FLAVONOID-INDUCED METABOLIC REPROGRAMMING IN HUMAN MACROPHAGES

Universidade de Aveiro Departamento de Química
2018

LUÍS FILIPE FIGUEIREDO MENDES

ESTUDO METABOLÓMICO DA REPROGRAMAÇÃO METABÓLICA INDUZIDA POR FLAVONOIDES EM MACRÓFAGOS HUMANOS

METABOLOMICS STUDY OF FLAVONOID-INDUCED METABOLIC REPROGRAMMING IN HUMAN MACROPHAGES

Dissertação apresentada à Universidade de Aveiro para cumprimento dos requisitos necessários à obtenção do grau de Mestre em Bioquímica, ramo Métodos Biomoleculares, realizada sob a orientação científica da Doutora Iola Melissa Fernandes Duarte, Investigadora Principal do CICECO- Instituto de Materiais de Aveiro, Departamento de Química da Universidade de Aveiro e sob a coorientação do Doutor Vítor Gaspar, Investigador Pós-Doutoral do CICECO - Instituto de Materiais de Aveiro, Departamento de Química da Universidade de Aveiro.

o júri

presidente

Professor Doutor Mário Manuel Quialheiro Simões
Professor Auxiliar, Departamento de Química, Universidade de Aveiro

Professora Doutora Catarina Rodrigues de Almeida
Professora Auxiliar, Departamento de Ciências Médicas,
Universidade de Aveiro

Doutora Iola Melissa Fernandes Duarte
Investigadora Principal, Departamento de Química, Universidade de Aveiro

agradecimentos

Em primeiro lugar queria agradecer à minha orientadora, Doutora Iola Duarte, principalmente pelo acompanhamento e boa disposição sempre presentes ao longo deste precurso, e por ter despertado o meu interesse na área da metabolómica e na técnica de RMN ao longo destes últimos anos. Ao meu coorientador, Doutor Vítor Gaspar, por ter demonstrado muita paciência, dedicação e disponibilidade na transmissão de conhecimentos em vários contextos, em especial na cultura de células. Queria também agradecer ao Professor João Mano, pela disponibilização de condições e recursos necessários à realização deste trabalho. Ao Tiago Conde, com quem partilhei a maior parte do tempo dedicado à execução deste trabalho. Agradeço também à Universidade de Aveiro e a todos os professores que fizeram parte do meu percurso académico ao longo da licenciatura e do mestrado.

A todas as amizades que fiz ao longo do tempo, em especial à Rita Futre, que felizmente me convenceu a continuar para o mestrado. Sempre com uma veia artística de qualidade elevadíssima que proporcionou muitos risos e facilitou bastante o que seria, de outra forma, um percurso bastante mais árduo para mim.

À minha família, pelo apoio que me deram ao longo do que certamente foi um tempo tão cansativo para eles quanto para mim, e por esta oportunidade que me puderam proporcionar.

palavras-chave

Inflamação, macrófagos derivados de THP-1, metabolismo celular, bioflavonóides, Ressonância Magnética Nuclear (RMN), metabolómica.

resumo

A capacidade dos macrófagos alterarem o seu fenótipo entre estados pro-inflamatórios (tipo-M1) e anti-inflamatórios (tipo-M2), faz com que a sua modulação seja uma estratégia promissora para mitigar a inflamação excessiva e/ou crónica. Os bioflavonóides são compostos naturais com atividade anti-inflamatória bem documentada. No entanto, pouco se sabe acerca dos seus efeitos metabólicos em macrófagos humanos. Nesta tese, utilizou-se a metabolómica baseada em RMN para averiguar de que forma diferentes bioflavonóides (Quercetina, Naringenina e Naringina) modulam o metabolismo de macrófagos humanos, com vista a compreender melhor os seus mecanismos de ação. Macrófagos derivados de monócitos humanos THP-1 foram cultivados *in vitro* e tratados com cada flavonóide, tanto no estado não-polarizado (M0) como após uma pré-polarização com LPS/IFN-γ (M1). A estimulação com IL-4/IL-13 (M2) foi também empregue para comparação. As frações polares das células foram obtidas por extração com solventes orgânicos e subsequentemente analisadas por espetroscopia de RMN-^{1}H. Perto de 50 metabolitos intracelulares foram identificados (endometaboloma), sendo que a análise dos meios de cultura (exometaboloma) foi útil para estudar padrões de consumo e excreção. O estudo dos perfis metabólicos através de análise multivariada e quantitativa revelou variações consistentes perante os diferentes estímulos fornecidos aos macrófagos. Os três flavonóides causaram diferentes alterações metabólicas, sendo que o maior impacto foi observado para a Quercetina e o menor para a Naringina. Os principais efeitos partilhados por todos os flavonóides, especialmente em macrófagos pré-polarizados para M1, incluíram diminuição do consumo de glucose e das reservas energéticas (ATP, UTP, fosfocreatina). Outros efeitos foram muito específicos dependendo do flavonóide, nomeadamente a modulação do ciclo TCA e do metabolismo de aminoácidos, a resposta anti-oxidante e variações em metabolitos associados às membranas. De forma geral, este estudo demonstrou que, apesar de apresentarem capacidade semelhante de atenuar a atividade pró-inflamatória de macrófagos, os três flavonóides afetaram o metabolismo celular de formas distintas. Em estudos futuros, será importante avaliar a expressão/atividade de enzimas metabólicas chave, de modo a incrementar o conhecimento atual sobre a modulação do metabolismo de macrófagos mediada por flavonóides. Este conhecimento deverá pois suportar o desenvolvimento de flavonóides como fármacos imunomodulatórios, especialmente direcionados para a atenuação e/ou resolução da inflamação, por exemplo, no contexto de doenças associadas a inflamação crónica ou da rejeição de biomateriais implantados.

keywords

Inflammation, THP-1 macrophages, cell metabolism, bioflavonoids, Nuclear Magnetic Resonance (NMR), metabolomics.

abstract

The ability of macrophages to change between pro-inflammatory (M1-like) and anti-inflammatory (M2-like) phenotypes makes their modulation an attractive therapeutic strategy to mitigate excessive and/or chronic inflammation. Bioflavonoids are natural compounds with well documented anti-inflammatory activity. However, little is known about their molecular and metabolic effects on human macrophages. In this thesis, NMR metabolomics has been used to assess how different bioflavonoids (Quercetin, Naringenin and Naringin) modulate the metabolism of human macrophages, with a view to better understand their modes of action. *In vitro*-cultured macrophages differentiated from human THP-1 monocytes were treated with each flavonoid, both in the uncommitted state (M0) or after pre-polarization with LPS/IFN-γ (M1). Treatment with IL-4/IL-13 (M2) was also carried out for comparison. Cells were solvent-extracted to obtain the polar fractions and subsequently analysed by ^{1}H NMR spectroscopy. Near 50 intracellular metabolites were detected (endometabolome), whereas analysis of cells-conditioned culture medium (exometabolome) was useful to assess consumption and excretion patterns. Multivariate analysis and discrete quantitative assessments of metabolic profiles revealed consistent variations upon macrophage exposure to the different stimuli. The three flavonoids produced pronounced metabolic alterations, with the strongest impact being observed for Quercetin and the mildest for Naringin. The main effects shared by all flavonoids, especially in M1 pre-polarized macrophages, comprised downregulation of glucose uptake and decreased energetic pools (ATP, UTP, phosphocreatine). Other effects were highly flavonoid-specific, namely TCA cycle modulation and amino acid metabolism, antioxidant response and variations in membrane-related metabolites. Overall, this work has shown that, although sharing similar ability to attenuate pro-inflammatory activity of macrophages, the three flavonoids affect macrophage metabolism in distinct ways. Future studies should entail assessment of key metabolic enzymes to further advance current understanding on flavonoid-mediated modulation of macrophage metabolism. This knowledge is expected to support the development of flavonoids as immunomodulatory drugs, especially aimed at attenuating and/or resolving inflammation, for instance, in the context of chronic inflammatory diseases or the rejection of biomaterial implants.

List of abbreviations and acronyms

2-DG	2-Deoxyglucose
AASS	Aspartate-argininosuccinate shunt
ACLY	ATP-citrate lyase
AICAR	5-aminoimidazole-4-carboxamide-1-β-D-ribofuranose
AKI	Acute kidney injury
AMP	Adenosine monophosphate
AMPK	Adenosine monophosphate-activated protein kinase
ASS	Argininosuccinate synthase
ATP	Adenosine triphosphate
BMDM	Bone marrow-derived macrophages
BPS	Bisphenol S
CAD	Coronary artery disease
CARKL	Carbohydrate kinase-like protein
CIC	Citrate carrier
CPT1A	Carnitine palmitoyltransferase 1A
DAMPs	Danger-associated molecular patterns
DCA	Dichloroacetate
DI	Dimethyl itaconate
DMM	Dimethyl malonate
DMSO	Dimethyl Sulfoxide
DON	Deoxynivalenol

ECAR	Extracellular acidification rate
ETC	Electron transport chain
ER	Endoplasmic reticulum
FAO	Fatty acid oxidation
FAS	Fatty acid synthesis
G3P	Glycerol-3-phosphate
G6P	Glucose-6-phosphate
G6PD	Glucose-6-phosphate dehydrogenase
GAPDH	Glyceraldehyde-3-phosphate dehydrogenase
GB	Glabridin
GM-CSF	Granulocyte-macrophage colony-stimulating factor
GSH	Reduced glutathione
HBP	Hexosamine biosynthesis pathway
HEL	Helenalin
HFO	Heavy Fuel Oil
HIF-1	Hypoxia inducible factor 1
HK1	Hexokinase 1
HLA-DR	Human leukocyte antigen – antigen D related
HMDB	Human Metabolome Database
IDH	Isocitrate dehydrogenase
IFN-β/ γ	Interferon beta/gamma
iNOS	Inducible nitric oxide synthase
IRF-1/4	Interferon regulatory factor ¼
Irg1	Immunoresponsive gene 1

LPS	Lipopolysaccharide
M-CSF	Macrophage colony-stimulating factor
mTOR	Mechanistic target for rapamycin
MVA	Multivariate Analysis
NAD	Nicotinamide adenine dinucleotide
NADPH	Nicotinamide adenine dinucleotide phosphate
Nar	Naringin
NF-kB	Nuclear factor kappa B
Ngn	Naringenin
NLRP2	NLR family pyrin domain containing 2
NO	Nitric oxide
NOX	NADP oxidase
OCR	Oxygen consumption rate
PAMPs	Pathogen-associated molecular patterns
PBMC	Peripheral blood mononuclear cells
PCA	Principal Component Analysis
PDH	Pyruvate dehydrogenase
PDK1	Pyruvate dehydrogenase kinase 1
PEP	Phosphoenolpyruvate
PFK	Phosphofructokinase
PFKFB2	6-phosphofructo-2-kinase/fructose-2,6-biphosphatase 3
PG	Prostaglandin
PHD	Prolyl hydroxylase
PI3K	Phosphatidylinositol 3-kinase

PKM2	Pyruvate kinase M2
PLS-DA	Partial Least Squares - Discriminant Analysis
PPP	Pentose phosphate pathway
Que	Quercetin
RNS	Reactive nitrogen species
ROS	Reactive oxygen species
RTC	Reverse electron transport chain
SDH	Succinate dehydrogenase
TAM	Tumor associated macrophages
TCA	Tricarboxylic acid cycle
TGF-β	Transforming growth factor β
TLR4	Toll like receptor 4
TNF-α	Tumor necrosis factor α
USPIO	Ultrasmall superparamagnetic Iron oxides
VEGF	Vascular endothelial growth factor
VHL	Von Hippel-Lindau factor

Index

Figures list

Tables list

Supplementary Information

CHAPTER 1

INTRODUCTION

1. Introduction

1.1. Macrophage plasticity, polarization and metabolism

Macrophages are specialized white blood cells with high phagocytic activity, which are a part of the mononuclear phagocytic system (MPS).[1,2] The MPS consists of cells from hematopoietic origin, including tissue resident macrophages and circulating monocytes, which are essential for the innate immune response.[2] Most tissue resident macrophages are established during embryogenesis and maintained by *in situ* proliferation, and are present at most tissues throughout the body, where they can exert specific functions.[3] In the context of inflammation, macrophages can also differentiate from circulating monocytes that are recruited to the inflamed site.[3,4]

The main functions exerted by macrophages include maintaining tissue homeostasis, immune surveillance, including defence against pathogens, and orchestration of inflammation.[2,5] In order to maintain tissue homeostasis, macrophages clear considerable amounts of erythrocytes in the blood every day, allowing for iron and haemoglobin recycling[5], while also ensuring that apoptotic cells and cellular debris originated from tissue damage or remodelling are cleared from the tissue.[6,7] Macrophages are also associated with pathogen detection and clearance through phagocytosis, proving to be an effective host defence mechanism for the host against harmful organisms like bacteria, fungi or viruses.[8] Indeed, tissue resident macrophages are among the first responders to tissue injury or an infectious pathogen. They recognize molecular patterns like PAMPs (pathogen-associated molecular patterns) and DAMPs (danger-associated molecular patterns), followed by secretion of chemical signals, like cytokines and chemokines, that can modulate other immune cells and contribute to the inflammatory response.[9,10] This process is highly regulated and involves communication between different leukocytes.[2] Tissue resident macrophages can also stimulate the influx of inflammatory leukocytes into the affected tissue, where circulating monocytes and neutrophils are the first cells to arrive.[4] After infiltrating the tissue, monocytes differentiate into mature macrophages which contribute to the development and resolution of inflammation, pathogen clearance and restoring

of tissue homeostasis.[4] Moreover, these macrophages are capable of interacting and modulating the activity of other immune cells, such as T lymphocytes.[2] One of the mechanisms through which these white blood cells interact involves macrophages presenting the antigens associated with the phagocytized pathogen, which leads to the activation of effector T lymphocytes, bridging the innate and adaptive immune response.[2]

1.1.1. Canonical stimuli of macrophage polarization

To perform such a wide variety of functions, macrophages adopt various polarization (or activation) states.[11] Indeed, macrophages have the ability to sense molecular mediators and danger signals in their local microenvironment[9], resulting in the expression of different phenotypes that consequently play different roles in the immune response, specifically regarding inflammation.[12] In early stages of inflammation, macrophages display a more pro-inflammatory phenotype, being generally designated as M1 macrophages (classically activated).[13] With time, macrophages tend to shift their functional phenotype towards a more anti-inflammatory state known as M2 (alternatively activated),which help to resolve inflammation and regenerate the tissue.[13] The M2 phenotype can be further divided into four subtypes (M2a, M2b, M2c and M2d), which can be obtained through different polarization stimuli and differ in their cytokine expression profiles (figure 1).[14] It is, however, important to mention that categorizing macrophages strictly as M1 or M2 is an oversimplified notion, as these phenotypes are two opposite extremes in a wide range of functional states.[15]

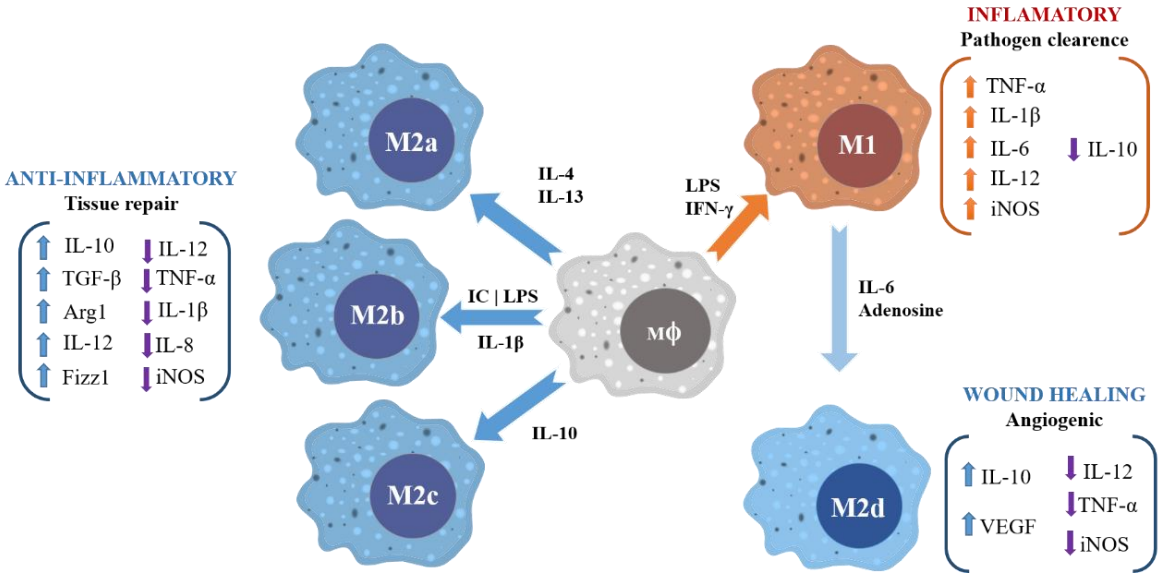

Figure 1: Differential macrophage polarization into different phenotypes upon exposure to various stimuli. Classical activation (M1) induced by LPS and IFN-γ (red). Alternative activation (blue) induced by different stimuli according to M2 subtype: M2a - IL-4 and IL-13; M2b – Immune Complex (IC), LPS and IL-1β; M2c - IL-10; M2d – IL-6 and adenosine. Adapted from[14,16,17].

The polarization shift towards the M1 phenotype can be triggered by molecular patterns present in external pathogens, such as bacterial cell wall lipopolysaccharides (LPS) and peptidoglycans, or endogenous secretion of cytokines like IFN-γ by T-cells.[17] LPS signal transduction is strongly associated with toll like receptors (TLR's) present in macrophage membranes, with TLR4 having a fundamental role in its regulation.[18,19] A study using mouse macrophages (RAW 264.7 cells) showed that manipulation of either the tridimensional structure or expression levels of TLR4 in these cells caused significant alterations on their response to LPS stimulation.[19] Regarding IFN-γ stimulation, it has been demonstrated that IFN regulatory factor (IRF1) and IFN-β play an essential part in the signaling pathway, with M1 markers being decreased after knockdown of IRF1 and IFN-β in human monocyte derived macrophages (U937 monocytes).[20]

Throughout the years, several studies have been conducted to assess which stimuli are most effective to selectively activate macrophages *in vitro* into the M1 phenotype.[12,21–25] One of the most commonly used stimuli for *in vitro* M1 polarization is based on the combination of LPS and IFN-γ,[20] which is the stimulus chosen in this present work as the canonical M1 macrophage polarization.

M2 macrophages present an additional challenge regarding stimulation and phenotypic characterization, given the four different subsets identified. Briefly, the M2a phenotype is achieved through IL-4 and IL-13 stimulation, the M2b by immune complexes, TLR and IL-1R agonists, the M2c with IL-10 stimulation, and M2d through IL-6 and adenosines.[14,16] Displaying different cytokine expression profiles, these subsets can have different contributions in the context of inflammation or tissue regeneration.[14] An example of this is M2b being functionally anti-inflammatory but retaining high levels of pro-inflammatory cytokines like IL-12, and M2c being the biggest contributor for IL-10 production amongst the subtypes.[26] In this context, a study by Tang and colleagues showed that in mice with acute lung injury (ALI), M2c macrophages were more effective at reducing fibrosis in the lung when compared to M2a macrophages.[26] More detailed information can be found in recent reviews, highlighting the differences between these subsets.[14,16,17]

In vitro studies often use a combination of IL-4 and IL-13 to polarize macrophages towards the prototypical M2 phenotype[12,17,21], this stimuli having been chosen for M2 polarization in the present work. Interleukins IL-4 and IL-13 are mainly released by T-helper type 2 cells after antigen recognition, although many other immune cells have the ability to secrete these cytokines after specific stimulation.[27] IL-4 binds strongly with IL-4Rα in the macrophage membrane, which triggers a series of signaling pathways that ultimately leads to the phenotypical alterations seen in M2 macrophages.[28] Sharing around 25% homology with IL-4, IL-13 can also exert similar biochemical effects, specifically regarding the inflammatory and immune responses.[29]

Highlighting the importance of these interleukins, a study using mice with acute kidney injury (AKI) showed that deletion of IL-4/IL-13 or inhibition of downstream components in the signaling cascade caused delayed recovery from injury and had

a significant increase in M1 macrophage markers with a decrease in M2 markers.[30] This corroborates the role of alternatively activated macrophages in tissue repair and strongly indicates that IL-4 and IL-13 are essential for driving the polarization towards the M2 phenotype (specifically, M2a).[30]

Overall, dysregulation of this process of differential activation in macrophages can lead to chronic inflammation, where the affected tissue can suffer persistent damage and/or contribute to disease progression.[31–35] This is now recognized to underlie a number of diseases, including cancer,[31] coronary artery disease[35] and some auto-immune diseases like rheumatoid arthritis[32] and multiple sclerosis[33], while also displaying other negative health impacts, such as the rejection of implanted biomaterials.[34,36] Hence, multiple efforts have been conducted to further understand the mechanisms underlying macrophage polarization and to develop strategies to modulate this process.[13]

1.1.2. Phenotypic markers of macrophage polarization

The distinction between M1 and M2 polarized macrophages can be assessed by the different expression of several biological molecules, including membrane surface receptors, cytokines and intracellular enzymes, such as iNOS or arginase-1 (Table 1).[37] By identifying/quantifying some of these molecules and associating them to one phenotype or the other, polarization markers may be established. It should be underlined, however, that such markers are dependent on the cells' origin, varying significantly between murine and human macrophages.[12]

Table 1: Common polarization biomarkers (mouse and human), cytokines and chemokines expressed in M1 and M2 macrophages. Adapted from[12,16,21,38].

	Cell surface markers	Enzymes/ Proteins	Cytokines	Chemokines	Refs
M1	CD64 CD68 CD80 CD86 TLR2 TLR4 IL-1R HLA-DR	iNOS [a]	IL-6 IL-8 IL-12 IL-23 TNF-α IL-1β	CCL2 CCL3 CCL4 CCL5 CCL8 CCL9 CCL10 CCL11	[12] [16] [21] [38]
M2	CD36 CD163 CD206 CD209 CD200R IL-1R II	Arg-1 [a] Ym 1/2 [a] Fizz1[a]	IL-10 IL-1Rα TGF-β	CCL17 CCL22 CCL24	[12] [16] [21] [38]

[a] *Murine only*

1.1.2.1. Cell surface markers

One of the most commonly used methods to characterize macrophage *in vitro* polarization is based on the analysis of expressed cell surface antigens through flow cytometry analysis.[39] Using human macrophages derived from peripheral blood mononuclear cells (PBMC), Tarique and colleagues showed that macrophages could be separated into different populations, according to cell surface receptors expression.[12] An increased expression of CD80 (a T-lymphocyte activation antigen) and CD64 (high affinity Fcγ receptor I) was strongly associated with human macrophage stimulation in culture with a combination of LPS and IFN-γ.[12] This increase in the $CD80^{+}CD64^{+}$ population highlighted these two surface receptors as good markers for identification of classical activation of macrophages.[12] On the other hand, the expression of CD11b (ITGAM – Integrin Alpha M) and CD209 (DC-SIGN - Dendritic Cell-Specific Intercellular adhesion molecule-3-Grabbing Non-integrin) was significantly higher in macrophages stimulated with IL-4 and IL-13 when compared to uncommitted macrophages or macrophages stimulated with LPS and IFN-γ, therefore being associated with M2 macrophages.[12]

In another study with macrophages differentiated from THP-1 cells (human monocytic cell line derived from an acute monocytic leukemia patient) the M1 phenotype was associated with CD80 and the receptor HLA-DR (Human leukocyte antigen – antigen D related), whereas M2 macrophages were characterized by increased expression of CD206 (mannose receptor) and CD163 (a hemoglobin scavenger receptor).[21] The heterogeneity seen in surface markers used for macrophage phenotypic differentiation throughout literature studies can be associated with a lack of consensus regarding some of the methodological steps, such as the type, concentration or duration of the polarization stimuli used, cell type, culture media, etc. Additionally, even though murine macrophages are better characterized thus far when compared to humans, as mentioned before, extrapolation between polarization surface markers in murine and human macrophages may not be possible.[12]

1.1.2.2. iNOS and Arginase-1

The enzymes iNOS and arginase-1 are involved in arginine metabolism and can also be used as polarization markers due to their differential expression in activated macrophages and strong contribution to functional phenotype differences.[40] iNOS (inducible nitric oxide synthase) is an enzyme associated with nitric oxide (NO) production.[41] An increase in NO production caused by a higher iNOS expression is commonly seen in murine M1 macrophages, being associated with anti-microbial effects.[9] There is however, a lack of consensus regarding whether or not human macrophages display this increase in iNOS expression after M1 stimulation, suggesting that iNOS is a good marker for murine models, but not necessarily for human macrophages.[21,42]

A similar situation occurs with arginase-1 expression, as there are uncertainties regarding its use as a polarization marker for alternatively activated (M2) human macrophages.[43,44] Indeed, while some studies reported that arginase-1 is not increased in human M2 macrophages[44–46], others have shown that arginase-1 expression can be used as a polarization marker due to its differential increase in M2 macrophages when compared to M1 macrophages.[47–49] This

discrepancy over the expression of both iNOS and arginase-1 in activated human macrophages has been reviewed before, where some research papers from both sides of the argument have been mentioned, stating that the opposing results may be due to several methodological disparities between studies and macrophage models, further contributing to the idea that standardization could be beneficial for overall progress in studying macrophages in the context of inflammation.[42,43]

1.1.2.3. Cytokines and chemokines

One of the most important phenotypic differences between M1 and M2 macrophages and its variants, is the production and excretion of cytokines to the extracellular medium at the inflammation or implantation site.[50] Several pro-inflammatory cytokines are released by activated M1 macrophages, including various interleukins, like IL-1β, IL-6, IL-8, IL-12; tumor necrosis factors, such as TNF-α, and growth factors like VEGF.[10] A study by Schutte and colleagues using THP-1 derived macrophages showed that after stimulation with LPS, macrophages showed a general increase in pro-inflammatory cytokines and also an increase in anti-wound healing cytokines, including several of those mentioned before, being therefore consistent with an M1 phenotype.[51]

In M2 macrophage subtypes, most pro-inflammatory cytokine levels are decreased and anti-inflammatory cytokines like IL-10[52] and TGF-β are released,[53] with the exception of M2b, which retains a high expression of pro-inflammatory cytokines,[14] as mentioned earlier. A study conducted by Song and colleagues using macrophages differentiated from human PBMCs showed that after *in vitro* stimulation with IL-4, more collagen was produced by cultured fibroblasts in response to the increase in TGF- β secreted by macrophages.[53] This mechanism is involved in tissue repair, which is associated with M2 macrophage subtypes.[53] IL-10 is a potent anti-inflammatory cytokine, responsible for maintaining/restoring homeostasis by preventing an over prolonged and consequently detrimental inflammatory response.[13,54,55] It has been shown that impaired expression of IL-10 can lead to more effective pathogen clearance, but it can also imply an imbalance in inflammation homeostasis, leading to persistent inflammation. Indeed, it is widely

recognized that both TGF-β and IL-10 are essential modulators of the inflammatory response, being involved in the resolution of inflammation and tissue repair.[51,52]

Chemokines are small cytokines that also play an essential role in inflammation by mediating macrophage chemotaxis, stimulating immune cell migration and targeting inflamed tissue.[56] This migration towards chemotactic agents is different in M1 and M2 macrophages, consequently contributing to further phenotypic differences between the two phenotypes.[56] A study by Vogel and colleagues using human macrophages derived from PBMCs showed that in comparison to M1, IL-4 stimulated M2 macrophages migrate faster and to longer distances when attracted by several chemokines like CCL5 and CXCL12.[57] Some reviews have listed several differences regarding macrophages direct chemokine secretion, indicating higher levels of pro-inflammatory chemokines in M1 macrophages, including CCL5, CXCL9 and CXCL10, amongst several others.[14,58] Regarding M2 macrophages, it has been shown that stimulation with IL-4 can up-regulate chemokines (e.g., CCL17, CCL22 and CCL24), which recruit immune cells involved in tissue repair and inflammation resolution, therefore contributing to the anti-inflammatory effect reported for alternatively activated macrophages.[14,57,59]

1.1.3. Metabolic features of differentially activated macrophages

It has recently come to light that macrophages at different polarization states require distinct metabolic programs to express their functional phenotypes and perform their effector functions.[60–64] Activation-dependent alterations have been reported in several metabolic pathways, including glycolysis,[65] amino acid metabolism (with arginine playing an essential role),[66] OXPHOS and TCA cycle,[67] PPP[68] and lipid metabolic pathways, including fatty acid oxidation (FAO) and fatty acid synthesis (FA synthesis).[69]

A summarized representation of metabolism regulation in differentially activated macrophages is shown in Figure 2. Overall, M1 macrophages are characterized by increased glycolysis and pentose phosphate pathway (PPP), with a truncated TCA cycle and impaired OXPHOS, while M2 macrophages have been shown to display a normal TCA cycle and OXPHOS.[62] Lipid metabolism has also been found to play an important role in macrophage differential activation, although some conflicting data exists regarding the relative importance of FA synthesis and oxidation in each phenotype.[60–63,70,71]

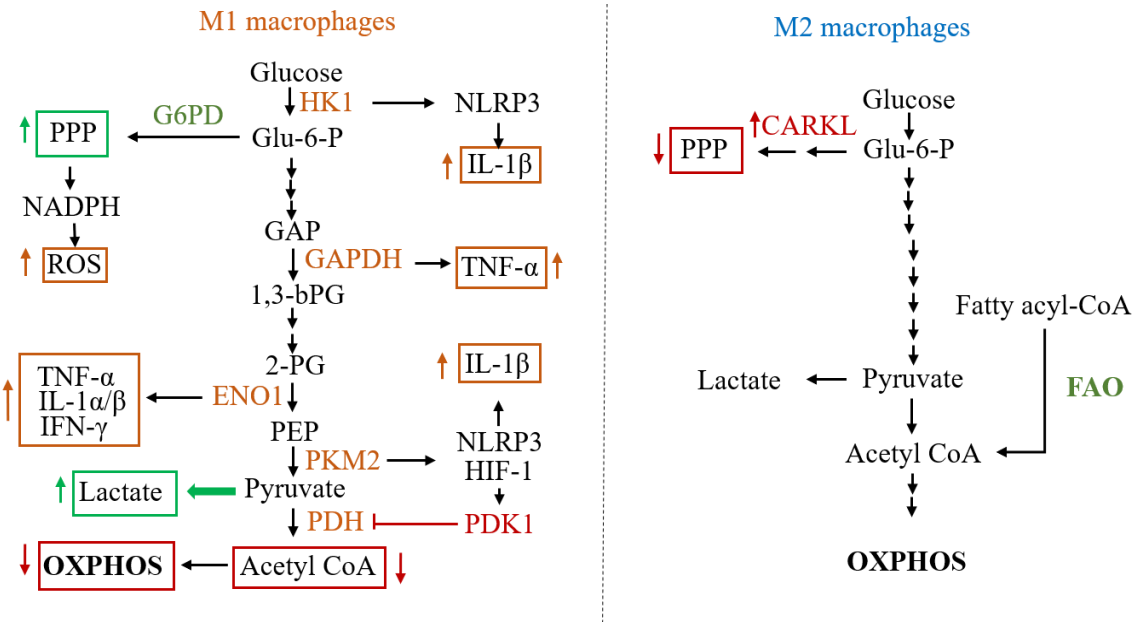

Figure 2: Schematic representation of metabolic differences between M1 and M2 macrophages. Glycolysis is increased in both phenotypes, albeit with more prevalence in M1, with several glycolytic enzymes and intermediates contributing to the pro-inflammatory phenotype. Unlike M1, which heavily rely on aerobic glycolysis, M2 macrophages display a normal OXPHOS and use FAO as a supplementary source of energy. PPP is unaltered/suppressed in M2 due to increased CARKL expression. Adapted from[61,62].

1.1.3.1. Glycolysis and its regulation in polarized macrophages

Glycolysis is the metabolic pathway through which glucose is transformed into pyruvate, with the concomitant production of NADH and ATP.[63,72] Pyruvate can then be oxidized into acetyl-coA and enter the TCA cycle, or it can be converted into lactate, especially if oxygen supply is low.[60] In addition to a small energetic yield (2 ATP molecules per each glucose molecule), glycolysis provides cells with several intermediate metabolites that can be used for various biosynthetic processes,[72] including the biosynthesis of amino acid,[73] lipids[74] and nucleotides.[75]

Similarly to tumor cells, pro-inflammatory macrophages heavily rely on glycolysis for energy generation, instead of OXPHOS, even when physiological amounts of oxygen are available.[62] Considering the normoxic environment, this process is known as aerobic glycolysis, being commonly referred to as the Warburg effect.[76,77] Moreover, M1 macrophages show impaired mitochondrial respiration, further indicating how important glycolysis is in this context.[62,78]

A study by Gleeson and colleagues using human monocyte-derived macrophages showed that after stimulation with *Mycobacterium tuberculosis*, a significant increase in lactate was detected, reflecting an increase in glycolytic activity.[76] Additionally, a study by Venter and colleagues using a murine macrophage cell line (RAW 264.7) determined that glycolysis was indispensable for LPS-induced macrophages' phagocytic activity. Indeed, macrophage migration and phagocytosis were clearly impaired in the presence of 2-deoxyglucose (2-DG), a known glycolytic inhibitor.[79] On the other hand, inhibiting OXPHOS with oligomycin, produced much less relevant alterations, which is consistent with glycolysis being the major source of energy in M1 macrophages.[79] Both studies showed that pro-inflammatory stimuli (*M. tuberculosis* in the first study and LPS in the second), drive an alteration in glucose metabolism, specifically favoring glycolysis instead of mitochondrial respiration, even in the presence of normal levels of oxygen.[76,79]

The role of glycolysis in M2 macrophage subtypes has been less extensively investigated compared to M1 macrophages. Still, some studies have reported an increased glycolytic rate in IL-4 or M-CSF induced macrophages, suggesting it to

be relevant to the functional phenotype expressed.[80–82] However, M2 macrophages were not seen to display an impairment in OXPHOS (unlike M1) and the increase in glycolytic rate wasn't as pronounced.[62,83] A study conducted by Zhao and colleagues used murine bone marrow-derived macrophages (BMDM) polarized into M2 macrophages with IL-4.[80] After stimulation, macrophages showed an increased expression in the glucose transporter GLUT-1 (consequently with a higher glucose uptake) and also increased levels of glycolytic enzymes.[80] To further establish the role of glycolysis in the functional phenotype, they used 2-DG to inhibit glycolysis, which caused decreased expression of several murine M2 markers, including arginase-1, thus indicating that glycolysis is necessary for M2 phenotype establishment.[80] Increased glycolytic rate has also been reported in human macrophages derived from PBMCs which were differentiated and polarized towards an anti-inflammatory (M2) phenotype by using M-CSF *in vitro*. In that study, inhibition of glycolysis led to impaired secretion of various cytokines, with macrophages not displaying their usual cytokine production patterns.[82] By later exposing the already polarized M2 macrophages to LPS, they showed that there was an increase in pro-inflammatory cytokines, like IL-6.[82] This was coupled with an additional increase in glycolysis, indicating that in response to a pathogenic stimuli (in this case LPS), M2 macrophages can display a slightly more pro-inflammatory behavior, hence showing some phenotypic plasticity according to the microenvironment.[82] Altogether, existing studies indicate that glycolysis plays a major role in the regulation of both M1 and M2 macrophages, with a greater impact on M1 macrophages due to the concomitant impairment in OXPHOS (not seen in M2 macrophages).

Several enzymes from the glycolytic metabolic pathway have been implicated in the pro-inflammatory phenotype displayed by M1 macrophages, including hexokinase 1 (HK1), enolase, pyruvate kinase M2 (PKM2), amongst others.[62] Both hexokinase 1 (HK1) and pyruvate kinase M2 (PKM2) are associated with the activation of the NLRP3 inflammasome, which is a multi-protein complex mainly responsible for the activation of inflammatory caspases and maturation of IL-1β, a pro-inflammatory cytokine.[84–87] In murine BMDM cells, PKM2 inhibition with Shikonin resulted in a significant suppression of the NLRP3 inflammasome and

decreased secretion of IL-1β, hindering the inflammatory state.[86] Additionally, a study by Palsson and colleagues using murine BMDM cells showed that PKM2 could stabilize HIF-1 (hypoxia inducible factor 1), which is a known positive regulator for IL-1β.[87] A third role for PKM2 in this context is its ability to phosphorylate and consequently activate STAT3, which in turn can boost the production of pro-inflammatory cytokines IL-6 and IL-1β.[88] Enolase has also been implicated in an increased inflammatory state, specifically regarding synovial inflammation in rheumatoid arthritis, with pro-inflammatory cytokines TNF-α and IL-1α/β levels being particularly affected.[89] In a study using THP-1 cells, the enzyme glyceraldehyde 3-phosphate dehydrogenase (GAPDH) has been proposed as an important mediator between glycolysis and inflammation, since GAPDH can interact with TNF-α mRNA, suppressing TNF-α levels post-transcriptionally.[90] However, when GAPDH is engaged in the glycolytic pathway, its availability for TNF-α mRNA suppression is lower, which results in higher levels of TNF-α, therefore contributing to a more pro-inflammatory state.[91]

In terms of regulatory mechanisms, some signaling pathways have been referred to be involved in glycolysis upregulation during macrophage activation. In human monocytic cells, specifically THP-1 (cell line) and PBMC (isolated from blood from healthy volunteers), it has been shown that LPS can induce phosphorylation (activation) of the Ser and Thr kinase (AKT) through the phosphatidylinositol 3-kinase (PI3K)-AKT signaling pathway, triggered by TLR-4 receptor stimulation.[91] One of the ways through which AKT (or protein kinase B-PKB) regulates glucose metabolism is by promoting the translocation of glucose transporters to the surface membrane, increasing glucose cell uptake, thus feeding more substrate to the glycolytic pathway.[92] In regard to macrophage stimulation with IL-4 (to induce M2-like phenotype), PI3K-AKT has also been found activated, impacting on glucose metabolism.[93] A study by Covarrubias and colleagues using BMDM cells showed that AKT inhibition resulted in a diminished increase in glucose uptake by IL-4 stimulated macrophages when compared to macrophages without AKT inhibition.[94] Additionally, by inhibiting glycolysis with 2-DG, they showed a reduced expression of M2 associated genes, which means that AKT is not only contributing to increased glucose uptake and metabolism, but also to the

enhanced expression of M2 associated genes.[94] Another major role of AKT signaling regards its interaction with mTOR (mechanistic target for rapamycin), which is key to the regulation of macrophage polarization.[93] After activation, AKT can phosphorylate the TSC (tuberous sclerosis complex), inactivating it. Considering how this complex is responsible for negatively regulating mTORC1 (complex 1), AKT leads to mTORC1 activation, which is responsible for increased gene expression linked to the promotion of cell growth and metabolism, regulating various metabolic processes, including glycolysis.[94,95] Further establishing the role of mTOR in glycolytic metabolism regulation, a specific mTOR signaling pathway involving mTORC2 (complex 2) has been implicated in regulating IRF-4 (interferon regulatory factor 4), which is a transcriptional factor responsible for the expression of several genes, including those encoding glycolytic enzymes.[95] A study by Huang and colleagues using IL-4 polarized BMDM cells showed that M2 macrophages with an IRF-4 deficiency displayed an impaired glycolytic rate, subsequent to a significantly decreased expression in glycolytic enzymes.[95]

It may therefore be concluded that glycolysis plays an important role in macrophage activation, both in M1 and M2 phenotypes (albeit with differences regarding its predominance as the cells' main energy provider), and that AKT is a major regulator of glucose metabolism in activated macrophages.[94] Notably, enhanced glycolysis cannot be considered a mere consequence of macrophage activation, but rather as an essential regulating process that is necessary for optimal expression of several genes that contribute to the phenotypical expression in activated macrophages.

1.1.3.2. PPP and oxidative/nitrosative stress in polarized macrophages

The PPP is a metabolic pathway that works in parallel with glycolysis, contributing to the maintenance of the cellular redox balance through NADPH production, and to the promotion of cell proliferation and growth through nucleotide biosynthesis.[75] An increase in this metabolic route has been associated with M1 macrophages, but not with M2 subtypes, indicating its role in macrophage pro-inflammatory activity.[68]

One of the major links between PPP and the inflammatory response is through the production of reactive oxygen species (ROS) and reactive nitrogen species (RNS), associated with oxidative and nitrosative stress promotion, respectively.[96] Reactive species such as nitric oxide (NO) and hydrogen peroxide (H_2O_2) possess anti-microbial effects,[97] thereby aiding macrophage mediated pathogen clearance.[97] In M1 macrophages, it has been shown that increased NADPH production through the PPP is responsible for increased production of ROS and stimulation of gene expression, including enzymes like iNOS and NADP oxidase (NOX), therefore contributing for NO production and enhancing the anti-microbial response.[96] Indeed, LPS stimulation of RAW 264.7 murine macrophages with G6PD repression (Glucose-6-phosphate dehydrogenase - the first enzyme of PPP) caused a significant decrease in pro-inflammatory cytokines and in the levels of both ROS and RNS, hindering the macrophages' pro-inflammatory activity.[96] On the other hand, NADPH is also involved in the formation of glutathione (GSH), a tripeptide with strong antioxidant effect by scavenging ROS and therefore lowering the cellular oxidative stress, possibly working as a countermeasure to prevent the inflammatory response from being overly dominant or prolonged.[68,96]

The enzyme carbohydrate kinase-like protein (CARKL), a sedoheptulose kinase responsible for converting sedoheptulose into sedoheptulose-7-phosphate (S7P), has been identified as a key control point which limits the flux through the PPP.[68] A decrease in CARKL expression was observed both *in vitro* and *in vivo* in human and murine LPS-stimulated macrophages.[68] In M1 polarized RAW 264.7 macrophages, decreased CARKL expression was correlated to enhanced M1 activation, specifically regarding GSH and NADH production.[68] In contrast, IL-4

stimulated macrophages (M2) showed an upregulation in CARKL, and no stimulation of the PPP pathway.[68]

Despite the PPP not being upregulated in IL-4 stimulated macrophages (M2), it has been shown that ROS are still necessary for M2 polarization.[96,98] Blocking ROS production in BMDM cells with BHA (butylated hydroxyanisol) resulted in a decreased expression of several M2 polarization markers after stimulation with M-CSF, indicating that ROS unavailability can actually hamper monocyte differentiation to macrophages, specifically regarding M2 macrophages.[98] Interestingly though, ROS inhibition showed no significant impairment in monocyte differentiation and polarization towards M1 macrophages (in this case, BMDM cells with GM-CSF).[98]

1.1.3.3. TCA cycle in polarized macrophages

One of the major metabolic differences between differentially activated macrophages regards mitochondrial OXPHOS regulation.[99] While M1 macrophages present an impairment in OXPHOS, M2 macrophages use it as their main source of ATP, supplying the cell with the necessary energy for carrying out various biological functions.[99] In M1 macrophages, OXPHOS impairment is associated with tricarboxylic acid (TCA) cycle dysfunction, as shown in Figure 3.[100,101] A first breaking point has been found in the conversion step of isocitrate to α-ketoglutarate, catalyzed by the enzyme isocitrate dehydrogenase (IDH), whereas a second break involves the conversion of succinate to fumarate by succinate dehydrogenase (SDH).[102] These breaks will consequently result in the accumulation of upstream metabolites, namely citrate and isocitrate (resulting from the first break), together with succinate (second break), which are essential for M1 phenotype establishment.[102]

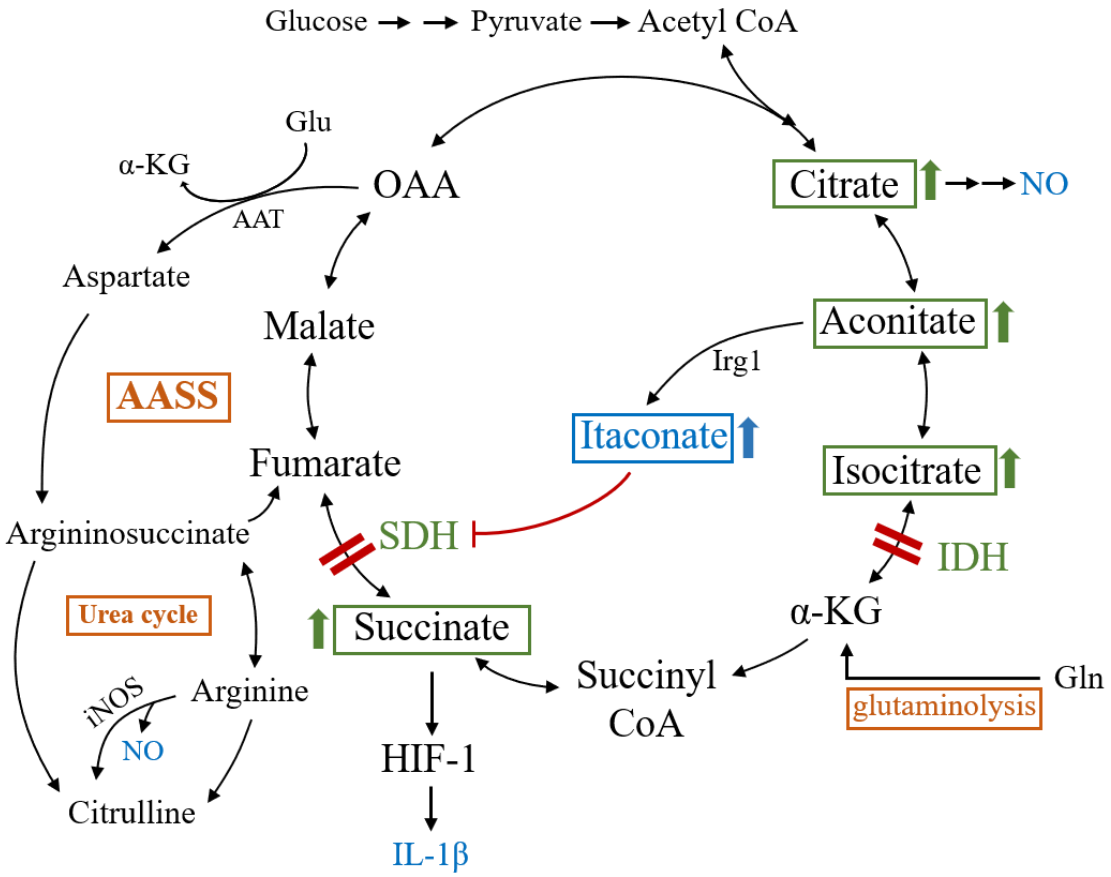

Figure 3: Schematic representation of the altered TCA cycle in M1 macrophages. The first breakpoint in IDH is responsible for citrate, isocitrate and aconitate accumulation. The latter can be further converted to itaconate, which is then involved in the competitive inhibition of SDH and has anti-microbial effects. Succinate accumulation can stabilize HIF-1 and subsequently increase IL-1β levels. The metabolites downstream of the breaks are replenished through anaplerotic pathways, like glutaminolysis or the aspartate-argininosuccinate shunt (AASS). Adapted from[61].

1.1.3.3.1. Succinate metabolism in M1 macrophages

Succinate has been shown to importantly account for the pro-inflammatory phenotype of classically activated (M1) macrophages.[99] In particular, succinate-mediated changes include regulating mechanisms involving transcriptional factors like HIF-1, mitochondrial ROS production, and alterations in amino acid metabolism, specifically regarding glutamine and arginine.[99] Succinate accumulation in the mitochondria of activated inflammatory macrophages is linked with the activation of the transcriptional factor HIF-1 (hypoxia inducible factor), independent of oxygen availability.[99] HIF-1 is composed of two subunits (α and β), whereby the α subunit binds to molecular oxygen and the β subunit interacts with DNA sequences, activating gene transcription involved in several cellular processes like cell proliferation, inflammation and metabolism.[103] It has been shown that SDH inhibition and subsequent succinate accumulation results in inhibition of prolyl hydroxylases (PHD), which are responsible for preventing HIF-1 stabilization.[104] When PHD are active and oxygen is available at physiological levels, HIF-1 is hydroxylated, allowing the association of the VHL (*von hippel-lindau)* factor, which serves as a signal for proteasomal degradation through the ubiquitin-proteasome complex.[105] Besides succinate, other TCA cycle intermediates like fumarate seem to be involved in HIF-1 stabilization through PHD inhibition.[106] HIF-1 has been associated with several roles in the immune response, including regulating inflammatory cytokine expression, NO synthesis, prostaglandins, amongst others.[107] An example of cytokine regulation regards IL-1β production in M1 macrophages (BMDM stimulated with LPS), as it has been found that IL-1β levels were significantly decreased in cells where the HIF-1 pathway was somehow disrupted.[99] Contrarily, macrophages with high succinate levels (and, hence, HIF-1 stabilization) displayed a notorious increase in IL-1β production, contributing to the pro-inflammatory phenotype.[99] Out of many proteins that are differently expressed due to HIF-1 transcriptional regulation, PDK1 (pyruvate dehydrogenase kinase 1) plays a particularly essential role in metabolism by inhibiting the enzymatic complex PDH (pyruvate dehydrogenase).[108] This ensures that pyruvate will not be converted into acetyl-CoA, preventing it from entering the mitochondria and feeding the oxidative pathway, therefore favoring the

fermentative pathway (conversion into lactate).[108] A study by Tan and colleagues using BMDM cells showed that PDK1 knockdown led to a decrease in aerobic glycolysis in M1 macrophages, reducing several aspects of its pro-inflammatory phenotype.[65] In M2 macrophages, PDK1 knockdown led to an enhanced macrophage activation towards a more anti-inflammatory state.[65]

Another major role for succinate in M1 macrophages is associated with its interference with the electron transport chain (ETC) in the mitochondria, contributing to increased levels of ROS production.[101] Indeed, increased succinate mitochondrial levels can lead to excessive reduction in ETC complex II (succinate dehydrogenase),[109] as seen in LPS stimulated macrophages[100] and macrophages subjected to bacterial infections in general.[110] Excessive reduction results in the induction of a reversed electron flow in the ETC (RTC), sending electrons towards complex I, which results in the increased production of superoxide anion,[109] a reactive oxygen species, therefore contributing to the oxidative burst and subsequent anti-microbial effect in M1 macrophages.[100,110] It has been shown in BMDM cells that inhibition of the reverse electron flow with Metformin or inhibition of complex I with Rotenone caused a decrease in both pro-IL-1β and ROS production in LPS stimulated macrophages, hindering the pro-inflammatory response in classically activated macrophages.[111] This indicates that the reversed electron flow in the ETC caused by the increased succinate levels contributes to the inflammatory response not only by increasing ROS production in the complex I, but also through increased expression of pro-inflammatory cytokines like IL-1β.[111]

Finally, TCA cycle impairment at SDH has implications in amino acid metabolism, namely via increased glutaminolysis and activation of the aspartate-argininosuccinate shunt (AASS), as both are used as anaplerotic processes to keep the cycle running.[102,112,113] The AASS in particular is considered to be an essential part of macrophage inflammatory response, as arginine and/or citrulline can fuel NO production via iNOS.[102,114] On the other hand, in M2 macrophages, arginine is converted into ornithine and urea via arginase-1 (urea cycle), decreasing arginine's availability for NO production via iNOS.[115] Additionally, glutamine can also be a nitrogen supplier for the hexosamine biosynthesis pathway (HBP), which is a minor branch from the glycolytic pathway, producing UDP-Glc-NAc.[102] A study

by Jha and colleagues showed that glutamine depletion or inhibition of N-glycosylation in murine BMDMs is associated with decreased expression of M2 phenotypic markers, indicating that glutamine catabolism is essential for M2 polarization.[102]

In spite of the well-established pro-inflammatory role of succinate, recent work has shown that SDH-mediated succinate oxidation is actually necessary for a pro-inflammatory phenotype.[100] By using dimethyl malonate (DMM), a competitive inhibitor for SDH, it was demonstrated that IL-1β mRNA and HIF-1 expression were lowered, while IL-10 was increased, reflecting a more anti-inflammatory phenotype.[100] Hence, it is possible that SDH is not a real breakpoint in the TCA cycle of M1 macrophages as initially thought, and that succinate processing (and the efficiency of SDH oxidation) rather than succinate accumulation in itself, are important for the activation of macrophages in response to inflammatory stimuli.[116]

1.1.3.3.2. Citrate metabolism in M1 macrophages

Citrate can contribute to a pro-inflammatory state in macrophages due to its role as precursor of different mediators that are required for the inflammatory response, including prostaglandins (PG's), NO and ROS.[117] PG production depends on FA synthesis, where citrate may be used as substrate.[117] When citrate is located in the cytosol, it can be converted into acetyl-CoA and oxaloacetate, triggered by the cytosolic enzyme ATP-citrate lyase (ACLY).[118,119] Acetyl-CoA is then used for fatty acid biosynthesis, providing the cell with PG precursors like arachidonic acid.[117] A study by Infantino and colleagues using macrophages derived from human histiocytoma mononuclear cells (U937 cell line) showed increased expression in ACLY after activation with different combinations of pro-inflammatory stimuli.[119] This was associated with the signaling pathway involving TLR-4 stimulation by LPS and subsequent NF-kB activation, causing alterations in the transcription of several genes, including the genes coding for the enzyme ACLY.[119] Considering that M1 polarization causes citrate accumulation in the mitochondrial matrix, and that ACLY is active in the cytosol, citrate first needs to be

transported from the mitochondria to the cytosol.[117] This transportation is mediated by mitochondrial CIC (citrate carrier), which has been found to be upregulated in LPS-stimulated U937 macrophages.[117] The other product obtained from citrate by ACLY is oxaloacetate, which is converted to malate and then to pyruvate via malic enzyme, resulting in the production of NADPH, another potential contributor to the inflammatory response due to increased production of NO and ROS, as already described.[117,119]

Another metabolic route in which citrate can engage is the synthesis of itaconic acid (or itaconate), involving the mitochondrial enzyme cis-aconitic acid decarboxylase, encoded by the immune-responsive gene 1 (*Irg1*).[120] *Igr1* is one the most highly expressed genes in mammalian macrophages during inflammation, so it is not surprising that it plays an essential part in M1 metabolic processes.[116] The *Irg1*-coded enzyme catalyzes the conversion of cis-aconitate, an intermediate of the TCA cycle, into itaconate.[121] This metabolite has been associated with some anti-microbial functions, including the inhibition of the bacterial enzyme isocitrate lyase, which is important for the glyoxylate shunt in both bacteria and fungi.[63,116]

Recently, itaconate has also been postulated to modulate macrophage inflammatory response by controlling succinate levels and TCA cycle remodeling.[116,122] In particular, in RAW 264.7 macrophages, itaconate was shown to act as an endogenous inhibitor of SDH, causing succinate accumulation.[122] In another study, addition of exogenous itaconate to BMDM macrophages was shown to decrease their pro-inflammatory profile, as assessed by the downregulation of an array of pro-inflammatory transcripts.[116] Altogether, the available data highlights a major regulatory role for itaconate regarding succinate levels, mitochondrial respiration and cytokine production in inflammatory macrophages. Additionally, a recent study by Mills and colleagues showed that the activation of transcription factor Nrf2 is required for its anti-inflammatory effects, where itaconate is associated with the alkylation of cysteine residues in proteins, which enable Nrf2 to increase the expression of anti-inflammatory and anti-oxidant genes.[123] Administration of itaconate and a cell-permeable itaconate derivative (4-octyl itaconate) to LPS-stimulated human and murine macrophages (PBMC and BMDM, respectively), resulted in a decrease in Il1b mRNA and pro-IL-1β and HIF-1 protein

levels, indicating a potential anti-inflammatory effect caused by this derivative.[123] This anti-inflammatory potential was also observed *in vivo*, where 4-octyl itaconate prolonged survival and decreased TNF-α and IL-1β levels in an LPS model of sepsis.[123]

The main idea to be summarized here is that TCA cycle rewiring is essential for defining differential macrophage phenotypes and effector functions. This rewiring sets a major role for several TCA cycle metabolites, with particular relevance given to citrate, itaconate, succinate and fumarate, which are essential as signaling molecules and immunomodulators. Taking in consideration that M2 macrophages do not display this complex TCA cycle rewiring, these metabolic differences may be interpreted as hallmarks for macrophage classical activation.

1.1.3.4. Fatty acid metabolism in activated macrophages

Several review articles mention fatty acid oxidation (FAO) and FA synthesis as metabolic regulators in activated macrophages, indicating that lipid metabolism has an intricate and multifaceted role on these cells.[60–63,70] Increased FAO is commonly described as an important feature of M2 macrophages,[61,62] to sustain their energetic needs and anti-inflammatory activity.[70] However, the dependence of M2 macrophages on FAO has been challenged by some studies.[71,124] A study conducted by Namgaladze and colleagues showed that while FAO was deemed necessary for IL-4 mediated M2 phenotype establishment in murine macrophages, it was dispensable in human macrophages (differentiated from monocytes isolated from buffy coats).[71] By inhibiting carnitine palmitoyltransferase 1A (CPT1A - one of the enzymes involved in FAO that oxidizes palmitate), they showed that despite FAO not being active in the cell, there was no suppression in M2 macrophage phenotype expression, which implies that lipid metabolism and its regulation can have considerable differences between species.[71] Fatty acid metabolism has also been implicated in the pro-inflammatory response of M1 macrophages, being linked with increased secretion of pro-inflammatory cytokines (like IL-1β and IL-18) through activation of the NLRP3 inflammasome.[62,125] A study by Moon and colleagues using murine BMDMs and human PBMCs showed that by inhibiting

CPT1A, a decrease in IL-1β and IL-18 was observed, associated with NLRP3 inflammasome suppression.[125] The mechanism involved in NLRP3 activation is related to mitochondrial ROS production, where palmitate oxidation by CPT1A fuels mitochondrial respiration.[125] Additionally, fatty acid synthase (FAS), an essential enzyme associated with lipogenesis, has also been implicated in this signaling pathway, where its inhibition resulted in NLRP3 suppression *in vivo* and in a consequential decrease in IL-1β and IL-18.[126]

In line with these findings, the possibility of targeting macrophage metabolism to modulate macrophage activation and functions emerges as a promising novel strategy that may provide therapeutic benefit in the context of exacerbated inflammation-related disorders and other conditions where persistent inflammation is found.[36,127]

1.2. Immunomodulatory effects of bioflavonoids

The search for naturally occurring compounds that display potential therapeutic benefit has harnessed growing interest in various fields of research, including immunology, as many existing immunoregulatory drugs are commonly associated with potentially serious side effects due to their high toxicity.[128]

One group of natural compounds that has shown great potential in terms of immunomodulatory effects are bioflavonoids.[129–131] In this thesis, the cellular responses of human macrophages to three naturally occurring flavonoids was investigated, namely Quercetin, Naringenin and Naringin. Previous knowledge on their effects towards macrophage activation and metabolism is summarized below.

1.2.1. Bioflavonoids

Bioflavonoids are naturally occurring polyphenolic secondary metabolites that are commonly found in plants.[130,132] These compounds have been the focus of many studies with the intent of establishing their various biological and pharmacological activities, including anti-inflammatory, anti-cancer, antioxidant, anti-microbial, anti-diabetic, anti-ulcer and anti-stress activities.[129–134]

Flavonoids basic structure consists of three carbon rings (C_6-C_3-C_6), more specifically, a benzene ring (A) and a phenyl ring (B), connected by a 3-carbon ring (C) (Figure 4).[132] The majority of flavonoids found in nature are in their glycosylated form, with a sugar moiety linked to the flavonoid aglycone, while also commonly featuring methylated groups, contributing to the immense diversity seen in existing flavonoids.[134] These compounds can be further divided into sub-categories according to the C ring carbon to which the B ring is linked, and regarding the degree of saturation and/or oxidation of the C ring.[135] When the B ring is linked to carbon 3 of the C ring, the compound is classified as an isoflavone and when the link is to the carbon 4, a neoflavonoid.[135] Regarding linkage to position 2, several other subcategories exist depending on the C ring structure.[135] These include, for example, favonols, flavanones, flavones, chalcones and flavanols.[132,135]

Quercetin, one of the compounds assessed in this study, is an example of a flavonol, meaning that in addition to a ketone group in the C ring, it also possesses a hydroxyl group at position 3.[135] This specific flavonol additionally displays hydroxyl groups positioned at carbons 3, 5, 7, 3' and 4' (Figure 4), and is very common in various fruits and vegetables.[135,136] Other examples of common flavonols found in nature include Kaempferol and Myricetin, which all display a wide array of diverse biological effects, that can be explored as potential therapeutic strategies in various health conditions.[137–139]

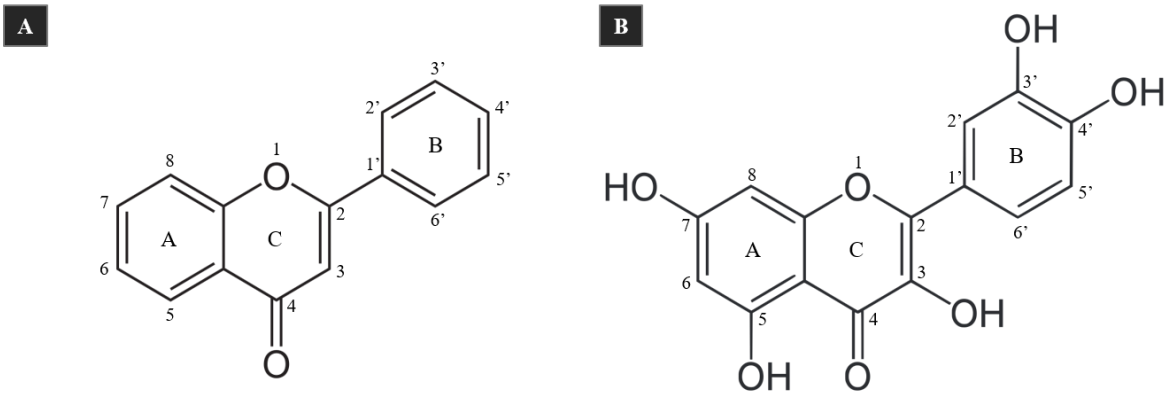

Figure 4: A – Schematic representation and numbering system of a generic flavonoid structure, with the B ring linked to the C ring in the position 2; **B** – Schematic representation and numbering system of the flavonol Quercetin. Adapted from[132,135].

Other compounds selected for this study include the flavanone Naringenin and its O-glycosylated form, Naringin, which contains two rhamnose molecules linked to the aglycone at the carbon 7 of the A ring (figure 5).[140] Structurally, flavanones have a distinct complete saturation of the C ring but are otherwise similar to flavones.[135] Other common flavanones with potential health benefits includes Hesperetin and its glycosylated form, Hesperidin. These compounds are very common in citrus fruits and are known for their properties regarding free-radical scavenging, anti-inflammatory effects and cholesterol lowering effects.[135,141]

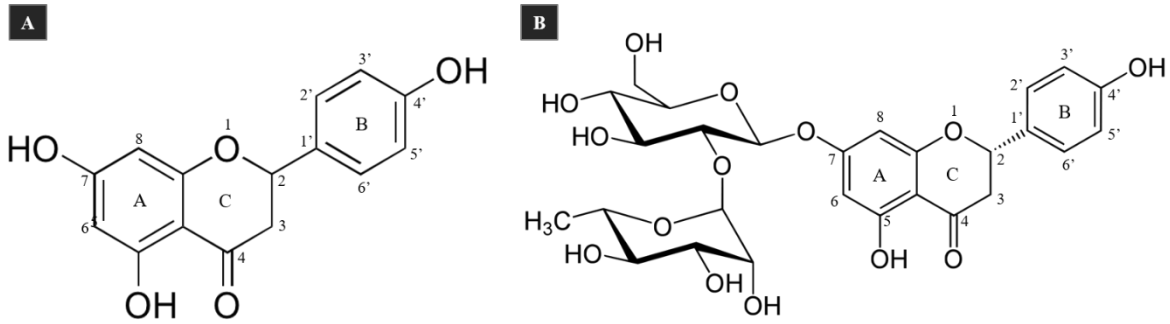

Figure 5: A – Schematic representation and numbering system of flavanone aglycone Naringenin; **B** – Schematic representation and numbering system of the Naringenin 7-O-glycoside, Naringin. Adapted from[135,140]

1.2.2. Effects of bioflavonoids on macrophage polarization

As mentioned earlier, one of the biological effects commonly described for flavonoids is immunomodulation, with particular interest in their anti-inflammatory potential.[142] The assessment of the modulation of M1/M2 polarization by these compounds is therefore a promising strategy to evaluate the therapeutic potential of bioflavonoids.[143] This modulation can be observed through different cellular alterations, including changes in signaling pathways, cytokine profile, gene expression and metabolism.[142]

One of the most common changes seen in inflammatory macrophages upon treatment with flavonoids is the reduction of key pro-inflammatory cytokines, indicating a certain level of suppression of the pro-inflammatory phenotype.[131,144,145] A study by Lee and colleagues showed that pre-treatment with Quercetin or Galangin of LPS-stimulated RAW 264.7 macrophages, led to a decrease in both IL-6 and NO levels, which are frequently associated with a pro-inflammatory phenotype and considered M1 polarization markers in some macrophage cell lines (e.g. RAW 246.7).[9,10,145] This indicates that pre-treatment with these flavonoids slightly hampers macrophage polarization towards the M1 phenotype, therefore displaying some anti-inflammatory activity.[145] NO suppression by Quercetin was also described in several other studies, both *in vitro*

and *in vivo*.[146–150] A study by Qureshi and colleagues showed that peritoneal macrophages stimulated with LPS had significantly lower levels of NO when mice were fed Quercetin and δ-tocotrienol before isolation, which further establishes the potential anti-inflammatory effects of Quercetin.[147] Additionally, a study by Raso and colleagues showed that among several flavonoids tested, Apigenin and Quercetin showed the most potent inhibitory effects on NO production.[149]

Another common M1 marker that seems to be susceptible to alterations in response to treatment with certain flavonoids is TNF-α. A study by Manjeet and colleagues showed that both NO and TNF-α levels were decreased in LPS-stimulated murine macrophages when co-cultured with Quercetin.[150] Additionally, Zhang and colleagues showed that treating LPS-stimulated human THP-1 and murine J774 macrophages with the flavone Apigenin led to a decrease not only in TNF-α levels, but also in the pro-inflammatory interleukins IL-6 and IL-1β.[151] Naringin has also been shown to be effective at decreasing several pro-inflammatory markers in LPS-stimulated macrophages. A study by Liu and colleagues showed a decrease in IL-8, MCP-1 and MIP-1α in RAW 264.7 murine macrophages pre-treated with Naringin, possibly by blocking the NF-kB signaling pathway.[152] Others have also shown a decrease in TNF-α and decreased sepsis-induced death in mice after treatment with Naringin, which clearly demonstrates its protective effects against inflammatory disorders.[153]

The anti-inflammatory effects of flavonoids can also be seen in several disease models that are coupled with dysregulation of the inflammatory process, with beneficial effects on wound healing, tissue regeneration and reducing fibrosis in the affected tissues.[143,154,155] Naringenin has been shown to reduce the severity of skin inflammation in mice with skin dermatitis, with several M1 markers being suppressed and an increase in IL-10, an M2 marker, being found in macrophages present in skin sections.[155] A study using mice with induced liver damage showed that orally administrated Quercetin was not only able to reduce inflammation, but also the extent of necrotic tissue.[154] This was accompanied by a marked decrease in several pro-inflammatory cytokines associated with macrophages present in the fibrotic tissue of the liver.[154] In a mouse model of kidney injury, Quercetin also showed protective action, reducing both inflammation and fibrosis, while

suppressing M1 polarization, thus protecting renal function.[143] Interestingly, in both liver and kidney damage models *in vivo* models, and in *in vitro* assays, Quercetin promoted a decrease in M2 macrophage populations.[143,154]

1.2.3. Effects of bioflavonoids on macrophage energy metabolism

Considering how different metabolic programs are involved in the establishment of the functional phenotypes of activated macrophages, targeting specific metabolic processes or signaling pathways involved in upstream regulatory mechanisms has been recognized as an interesting approach to modulate macrophage polarization.[156] Given the effects reported for several bioflavonoids on macrophage immunomodulation, and the key role of metabolism in macrophage polarization, investigating how flavonoids affect macrophage metabolism may shed light on their mechanisms of action and open new prospects regarding their therapeutic potential.

Most studies reported so far have focused on the modulation of signaling pathways that play an important role in metabolism regulation.[157–159] One of the signaling pathways that is frequently reported to be modulated by bioflavonoids is the adenosine monophosphate-activated protein kinase (AMPK) signaling pathway.[157,159–161] AMPK is a major regulator of glucose and lipid metabolism, acting as an energetic sensor that triggers the upregulation of energy-restoring catabolic pathways like FAO and OXPHOS, while downregulating glycolysis and switching off energy-consuming biosynthetic processes.[162,163] Several studies support an anti-inflammatory role for AMPK activation, which may be achieved by a variety of small-molecule compounds.[159–162] A study by Zhou and colleagues showed that administrating Eupatilin, a natural flavone, led to a decrease in several pro-inflammatory markers in THP-M human macrophages, partly via the activation of AMPK signaling pathway.[160] Additionally, a study by Dong and colleagues showed that Quercetin inhibited the polarization of BMDM macrophages by activation of AMPK.[159] This was confirmed by using an AMPK inhibitor, Compound C, which showed that one of the mechanisms through which Quercetin could abrogate the inflammatory response caused by LPS stimulation was indeed

through AMPK activation.[159] Another flavonoid that has been reported to activate AMPK is Naringenin,[157,160] both in murine RAW 264.7 macrophages[161] and human THP-1 macrophages,[157] contributing to the regulation of inflammation.[157,161]

Regulation of glucose metabolism has also been associated with other signaling pathways, such as the phosphoinositide 3-kinase (PI3K) pathway[164] and Mitogen-Activated Protein Kinase (MAPK) pathway.[165] Considering how these pathways have been shown to promote glycolysis,[165,166] and are associated with LPS stimulation,[91,166] their inhibition could potentially be a therapeutic strategy in regulating inflammation.[62] A study by Si and colleagues showed that Quercetin was able to reduce levels of several pro-inflammatory markers, such as NO, IL6, IL-1β and TNF-α, in LPS-stimulated murine RAW 264.7 macrophages, coupled with a significant decrease in phosphorylation of MAPK signaling proteins.[167] This indicates that Quercetin has a suppressing effect on the MAPK signaling pathway, which could contribute to the attenuation of the inflammatory phenotype in LPS-induced macrophages.[167] Another study by Endale and colleagues also showed this suppressing effect of Quercetin on the MAPK signaling pathway, which resulted in decreased levels of downstream pro-inflammatory mediators in LPS-stimulated murine RAW264.7 macrophages.[158] In this study, pre-treatment with Quercetin also suppressed the increase in PI3K and Akt that are commonly associated with LPS stimulation,[91] corroborating the potential of Quercetin to attenuate macrophage inflammatory response.[158]

Despite the suggested links between flavonoids anti-inflammatory action and their effects on cellular metabolism, little is known on the specific metabolites and metabolic pathways that are modulated upon flavonoid treatment. In this thesis, metabolomics was used as an advanced tool to further investigate this scientific question.

1.3. Metabolomics

1.3.1. Metabolomics strategies and tools

The comprehensive profiling of the inventory of small molecules (< 1 kDa) acting as substrates, intermediates or products of enzymatic reactions in mammalian cells, through metabolomics, has become an extensively applied methodology to seek for a better understanding of cell metabolism and function.[168] Metabolomic studies typically encompass identification and quantification of metabolites within tissues, biofluids or cells, and assessment of their variations in relation to a specific pathophysiological condition or external stimulus.[169,170] Unlike other conventional biochemical methods, which focus on a specific, pre-determined set of metabolites, metabolomics provides a broader, non-selective view of metabolic changes, potentially revealing unexpected effects and allowing for mechanistic hypothesis to be generated.[171,172]

The two analytical methods most commonly used in metabolomics are Nuclear Magnetic Resonance (NMR) spectroscopy and Mass Spectrometry (MS).[171] In the present work, ^{1}H-NMR was the profiling technique employed. In spite of its low sensitivity, which remains one of its biggest downsides, NMR does show important advantages, such as the possibility of acquiring data without requiring extensive sample treatment, the ability to identify metabolites of different chemical families in complex mixtures, high reproducibility and its non-destructive character.[173] Moreover, as the area of a signal is proportional to the number of protons giving rise to that signal, ^{1}H-NMR is inherently quantitative, enabling a straightforward assessment of quantitative variations in selected metabolites.[171,174,175]

^{1}H-NMR spectra of biological samples are usually complex, containing a very high number of signals which can be attributed to specific metabolites based on their chemical shifts (in ppm) and multiplicity, by comparing the information derived from 1D and 2D spectra with that available in spectral databases.[171,175]

To deal with such complexity and enable the multiparametric comparison of sample groups (e.g. control vs. treated) multivariate analysis (MVA) is commonly employed. This type of analysis considers the vast group of variables of each spectrum, allowing the user to assess the differences/similarities between spectra

of several samples.[171] The two most common MVA methods used in metabolomics are: (i) principal component analysis (PCA) and (ii) partial least squares discriminant analysis (PLS-DA). The first is a non-supervised method, which offers a general idea of separation patterns arising from the various sources of variability within the dataset, without any input regarding sample classes. The latter maximizes the separation between sample classes, allowing the variables (metabolites) responsible for class discrimination to be highlighted.[171,176]

1.3.2. Metabolomic studies of macrophage polarization

The metabolome of macrophages has been investigated in several previous studies, comprising the search for metabolic alterations upon different stimuli and in different macrophage cell lines (Table 2).[75,168,177–187] Some studies have addressed the characterization of metabolic alterations associated with canonical M1 macrophage polarization, using LPS alone or in co-incubation with IFN-γ.[75,168,177] In line with molecular studies, the main changes detected reflected glycolysis upregulation and TCA cycle disruption.[75,168,177] Others have investigated how macrophage metabolism and polarization were affected by direct exposure to pathogenic microorganisms (bacteria, parasites or viruses).[178–181] For instance, exposure of THP-1 macrophages to *Mycobacterium tuberculosis* was associated with changes in several biosynthetic pathways, including GSH, carbohydrate and lipid synthesis, while showing also decreased levels of amino acids and monoacylglycerols.[178,179] In another study, exposure of murine BMDMs to a parasite (*Leishmania major*) was found to cause increases in lactate and several amino acids, which was putatively explained by the upregulation of glycolysis, consistent with a pro-inflammatory stimuli.[180] Additionally, U1 macrophages chronically infected with HIV-1 virus showed changes in PPP metabolites and a reduced ability to generate NADPH, which could indicate a compromised capacity to generate *de novo* nucleotides and fatty acids.[181]

The metabolomic response of macrophages to pollutants and nanoparticles has also been addressed in a few studies.[184–186] Sapcariu and colleagues showed that exposing RAW 264.7 macrophages to HFO (heavy fuel oil) resulted in a shift

towards a more pro-inflammatory phenotype, with metabolic hallmarks like succinate and itaconate being elevated.[184] Similarly, a study conducted by Zhao and colleagues showed that the emerging pollutant bisphenol S (BPS) also had a pro-inflammatory polarizing effect in J774A.1 macrophages, with particular emphasis given to an increased glycolytic rate and GSH biosynthesis.[185] The effects of ultrasmall superparamagnetic iron oxide particles (USPIO), were assessed on LPS-induced M1 macrophages and comprised increases in succinate, pyruvate and lactate, consistent with increased glycolysis and aggravation of the pro-inflammatory phenotype.[186]

Regarding macrophage exposure to natural compounds, metabolomics studies have investigated the effects of Deoxynivalenol (DON), Helenalin (HEL), β-glucan and Glabridin (GB).[182,183,187,188] Incubation of ANA-1 murine macrophages with DON resulted in changes in several metabolic pathways, specifically regarding glucose and amino acid metabolism.[182] These changes included decreased levels of lactate and pyruvate, possibly indicating the downregulation of glycolysis.[182] Another study using THP-1 and PBMCs stimulated with HEL showed an increase in lactate production, accompanied by changes in several glycolytic and TCA cycle enzymes, together with an increase in ROS.[183] Additionally, a study by Liu and colleagues showed that a yeast-derived β-glucan could convert anti-inflammatory tumor associated macrophages (TAM) into a more pro-inflammatory phenotype, displaying immunosuppressive and anti-tumoral effects.[187] The metabolic changes accompanying this shift comprised of an upregulation of glycolysis, with increased levels of lactate, which would be consistent with a more pro-inflammatory phenotype. Other changes included increases in glutamine uptake and in GSH biosynthesis. As for the study involving the isoflavane Glabridin, it was shown that, in murine RAW264.7 macrophages, this flavonoid could revert some of the effects caused by LPS stimulation, particularly regarding pyruvate, alanine, aspartate and glutamate metabolism, as well as phenylalanine, tyrosine and tryptophan biosynthesis.[188]

The studies mentioned above illustrate the potential of metabolomics to characterize the changes in macrophage metabolism induced by various stimuli. However, to the best of our knowledge, comprehensive profiling of metabolic responses of human macrophages to bioflavonoids has not been reported before. In this thesis, NMR metabolomics is employed for the first time to assess macrophage metabolic reprogramming upon exposure to Quercetin, Naringin and Naringenin, three abundant bioflavonoids with well documented anti-inflammatory activity. This research is expected to advance current understanding of bioflavonoids mode of action, potentially supporting their future development as immunomodulatory drugs.

Table 2: Metabolomic studies of macrophage metabolism in response to different stimuli.

Cells	Stimuli	Profiling technique	Main findings	References
Canonical M1 polarization				
RAW 264.7	LPS	CE/TOF-MS	↑TCA cycle intermediates ↑Lactate	[168]
RAW 264.7	LPS	GC-MS	↑Itaconate ↑Succinate ↑Lactate	[177]
THP-1	LPS+IFN-γ	CE/TOF-MS	↑Glycolytic metabolites ↑PPP metabolites ↓TCA cycle metabolites	[75]
Infectious microorganisms				
THP-1	*Mycobacterium tuberculosis*	GC/TOF-MS	↓GSH anabolic metabolism ↑Carbohydrate biosynthesis ↓Lipid biosynthesis	[178]
THP-1	*Mycobacterium tuberculosis*	MS	↑Monoacyl glycerols ↓Amino acids	[179]
BMDM	*Leishmania major*	NMR	↑Lactate ↑Amino acids ↑Choline and derivatives	[180]
U1	HIV-1	LC-MS	↑Pyruvate ↑CTP and UTP ↓6-P-gluconate	[181]

Table 2 (continuation): Metabolomic studies of macrophage metabolism in response to different stimuli.

Cells	Stimuli	Profiling technique	Main findings	References
Pollutants				
RAW 264.7	Heavy Fuel Oil **(HFO)**	GC/FTICR-MS	↑Lactate ↑Succinate ↑Itaconate	[184]
J774A.1	Bisphenol S (BPS)	LC-MS	↑Glycolysis ↑GSH biosynthesis	[185]
Nanoparticles				
RAW 264.7	Ultrasmall superparamagnetic Iron Oxides (USPIO)	NMR	↑Succinate ↑Citrate ↑Lactate ↑Pyruvate	[186]
Natural compounds				
ANA-1	Deoxynivalenol (DON)	GC/TOF-MS	↓Lactate ↓Pyruvate ↑Glycerol ↑Linoleic acid methyl ester	[182]
THP-1 **PBMC**	Helenalin (HEL)	2D gel electrophoresis TOF-MS NMR	↓Serine ↑Lactate ↑ROS	[183]
BMDM **TAM**	β-glucan	GC-MS	↑Glutamine uptake ↑Glycolysis ↑Lactate ↑GSH biosynthesis	[187]
RAW 264.7	Glabridin (GB)	GC-MS	↓Pyruvate ↓Aspartate ↓Tyrosine ↑Lactate ↑Tryptophan	[188]

1.4. Objectives

The main goal of this thesis is to assess how different bioflavonoids (Quercetin, Naringin and Naringenin) modulate the metabolism of human macrophages, with a view to better understand their mode of action, specifically regarding macrophage-mediated anti-inflammatory activity.

Specific aims are:

- To characterize the metabolome of THP-1-derived macrophages in uncommitted (M0), pro-inflammatory (M1) and anti-inflammatory (M2) activation states.

- To assess the metabolic changes induced by Quercetin, Naringin and Naringenin and their dependence on: i) treatment time, ii) phenotype of treated macrophages (M0 vs. M1).

- To propose hypotheses on metabolic pathways affected by flavonoid treatments and their role in the cells inflammatory state.

- To advance current understanding of the metabolism-mediated immunomodulatory activity of bioflavonoids on human macrophages, envisaging their future application in the context of anti-inflammatory therapies.

CHAPTER 2

MATERIALS AND METHODS

2. Materials and Methods

2.1. Preparation of stock solutions

All flavonoid stock solutions were prepared with 99.5% DMSO at a concentration of 80 mM. The flavonoids used were Quercetin (Alfa Aesar), Naringenin (Sigma Aldrich) and Naringin (Sigma Aldrich). These solutions were protected from light and kept at -20ºC for a maximum of two weeks. A stock solution of phorbol 12-myristate 13-acetate (PMA, Sigma Aldrich) was also prepared in 99.5% of DMSO at a concentration of 100 µg/mL and protected from light at -20ºC. Considering the known cytotoxicity of DMSO to cells, all subsequent dilutions used in the various assays were prepared to have a maximum DMSO concentration of 0.5% (v/v). Additionally, cellular viability assays showed that a DMSO concentration of 0.6% (v/v) did not significantly decrease cellular viability in this cell line.

Powdered LPS (Sigma Aldrich) was dissolved in Gibco® Water for Injection (WFI) at a concentration of 1 mg/mL. Solutions of IFN-γ (BioLegend), IL-4 (BioLegend) and IL-13 (BioLegend) were kept in the original formulation at a concentration of 0.1 mg/mL for IFN-γ and 0.2 mg/mL for IL-4 and IL-13. These solutions were also kept at -20ºC. Subsequent dilutions were prepared either with the appropriate cell culture media or with sterile PBS.

2.2. Cell culture maintenance

Human monocytic THP-1 cells were obtained from the American Type Culture Collection (ATCC) and were cultured in suspension at 37ºC and a 5% CO_2 atmosphere, in RPMI 1640 (Roswell Park Memorial Institute Medium, Gibco) culture medium supplemented with 2.5 g/L of sodium bicarbonate (Sigma Aldrich) and containing 10% of heat inactivated FBS (fetal bovine serum) and 1 % of an antibiotic solution (penicillin and streptomycin).

The cells were maintained in suspension in 100 mm non-adherent petri-dishes. When cells reached a high confluency (about 80%), the cell culture media containing the cells was split into two new petri-dishes, to which fresh culture media was added. All experiments were performed with cells from passages 10 to 17.

2.3. Cell viability assay

The toxicity of the three flavonoids (Quercetin, Naringin and Naringenin) towards THP-1 derived macrophages was measured using an Alamar Blue® reduction assay. The active compound is resazurin (IUPAC name: 7-hydroxy-10-oxidophenoxazin-10-ium-3-one), which is water-soluble, cell-permeable and non-toxic to cells, thus being suitable for testing cell viability. In the presence of healthy cells, resazurin (a non-fluorescent blue die) works as an electron acceptor in the electron transport chain, where it is reduced to resorufin, which is highly fluorescent and pink-colored (Figure 6). The percentage of viable, metabolically active cells can then be estimated by measuring the emitted fluorescence.[189]

To perform this assay, THP-1 monocytes were seeded in 96-well plates with 5 x 10^4 cells per well in 200 µL of appropriate culture medium and differentiated into macrophages with 50 ng/mL PMA for 24h. Afterwards, cell media was removed and replaced with new media containing different concentrations of the test compounds (20, 40, 60, 80, 100, 150 and 200 µM). After different incubation times (6, 24 and 48h), cell media was removed again, and cells were incubated with 110 µL of a 10% Alamar Blue® solution in cell media for approximately 24h. A microplate reader Sinergy HTX was then used to measure fluorescence (λ_{Ex} = 540nm; λ_{Em} = 600nm).

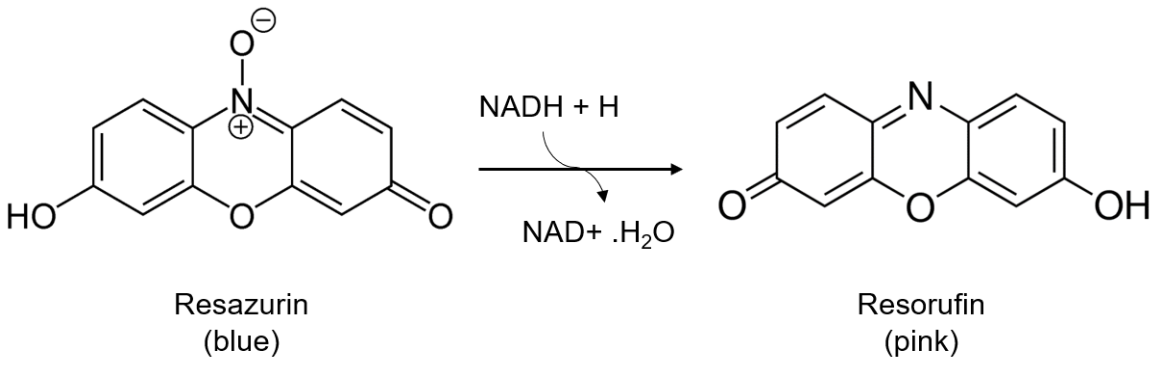

Figure 6: Schematic representation of the reduction of resazurin, the active compound in an Alamar Blue® reduction assay, to resorufin, a highly fluorescent pink compound, in the presence of a highly reductive cellular environment. Adapted from[190].

2.4. Immunofluorescence staining of M1 and M2 macrophages

THP-1 monocytes were seeded in IBIDI adherent plates at a density of 3×10^5 cells/mL and differentiated with 50 ng/mL of PMA for 24h, followed by 24h with fresh media. Macrophages were then stimulated with 100 ng/mL of LPS + 20 ng/mL of IFN-γ for 24h or with 20 ng/mL of IL-4 + 20 ng/mL of IL-13 for 48h, to obtain M1 and M2 polarized macrophages, respectively.

After the appropriate incubation time, the cells were fixated with 4% formalin and washed with cold PBS (pH 7.4). Subsequently, 70 µL/well of BSA were added to the cells for 30 min. BSA worked as a blocking agent to prevent non-specific binding of antigens and antibodies. After this step, cells were washed three times with PBS and then incubated for 1h with the appropriate antibodies. For assessing M1 markers, cells were incubated with 50 µL/well of mouse anti-human CD80 (clone 2D10, conjugated with Alexa Fluor® 488) and mouse anti-human CD64 (clone 10.1, conjugated with PE). M2 markers were assessed by incubating cells with 50 µL/well of mouse anti-human CD36 (clone 5-771, conjugated with PE) and mouse anti-human CD209 (clone 9E9A8, conjugated with FITC).

The next step involved washing the cells three times with PBS (pH=7.4), followed by incubation with DAPI (4′,6-diamidino-2-phenylindole) for 15 min, at room temperature (RT), which is a blue-fluorescent die that stains cells nuclei. The cells were then washed five times with PBS at RT and stored at 4ºC until visualization in 150 µL of PBS. When the cells were ready for visualization, the PBS was removed and replaced by mounting medium (DAKOTM), after which the cells could be observed in a fluorescence microscope (ZEISS AxioImager M2, equipped with a 10x/0.25 objective – Carl Zeiss, Germany).

2.5. Cytokine quantification assay (LEGENDplex™ array)

The production of several pro-inflammatory and anti-inflammatory cytokines was measured in the supernatants of THP-1 derived macrophages by a bead-based multiplex assay LEGENDplex™ (BioLegend). The multiplex assay used was the Human M1/M2 Macrophage Panel (10-plex) with V-bottom Plate and allowed the quantification of 10 cytokines, including IL-12p70, TNF-α, IL-6, IL-10, IL-1β, TARC, IL-1RA, IL-12p40, IL-23 and IP-10.

2.5.1. Reagent preparation

Each vial of individual analyte beads was sonicated for 1 min and vortexed for 30 seconds. Then, aliquots of the 10 vials were mixed at equal volumes and the resulting mixture diluted 13 times with Assay Buffer (provided by the supplier).

To prepare the standards, the lyophilized cytokine Standard Cocktail (provided by the supplier) was reconstituted in 250 µL of Assay Buffer, allowed to equilibrate at RT and transferred to a labeled polypropylene centrifuge tube. From this standard, serial dilutions (1:4) were performed to obtain different standard concentrations in the calibration curve.

2.5.2. Assay procedure

In each well of a 96-well V-bottom plate, 25 µL of Assay Buffer were mixed with 25 µL of standard or 25 µL of sample (cell culture medium supernatants). Then, 25 µL of the beads mixture was added to each well, giving a total volume of 75 µL per well. The plate was subsequently covered with a plate sealer and aluminum foil to protect it from light exposure, and placed in a plate shaker at 750 rpm for 2h at RT. Next, the plate was centrifuged at 250g for 5 min, after which the supernatants were carefully discarded using a multi-channel pipette. After removing the supernatant, each well was washed with 200 µL of Wash Buffer (provided by the supplier). This was followed by a second centrifugation, after which the supernatant was again discarded.

The next step involved incubating each well with 25 µL of Detection Antibodies for 1h, having the plate covered with a plate sealer and aluminum foil, while shaking at 800 rpm at RT. After 1h, without washing the plate, 25 µL of streptavidin-phycoerythrin (SA-PE) was added to each well. The plate was again sealed, covered with aluminum foil, and placed in the plate shaker for another 30 min, at RT. Afterwards, the plate was centrifuged in the same conditions as mentioned earlier, and the supernatant removed. This was followed by washing each well with 200 µL of Wash Buffer and a final centrifugation step. After removing the supernatant, 150 µL of Wash Buffer was added to each well and the beads were resuspended by pipetting.

The samples were then analyzed in a flow cytometer (BD Accuri™ C6 plus (BD Biosciences), configured to acquire 4000 events in the region of interest (ROI) corresponding to the different beads and corresponding analytes. Data was gated and treated in LegendPlex software.

2.6. NMR metabolomics assays

2.6.1. THP-1 differentiation into macrophages

The cell culture media containing the cells was transferred to 15 mL Falcon tubes and centrifuged at 300 xg for 5 min. The supernatant was then discarded and the pellet resuspended in 1 mL of fresh cell culture medium. The number of cells was counted using a Neubauer chamber, after adding 5 µL of the cell suspension to 45 µL of fresh medium and 50 µL of a trypan blue solution.

THP-1 monocytes were then seeded in adherent petri-dishes (10 cm diameter) at a density of 10×10^6 cells/mL and differentiated into macrophages through a 24-hour incubation with 50 ng/mL of phorbol 12-myristate 13-acetate (PMA). The cell media was then discarded and cells incubated with fresh media for another 24h, after which the monocytes were considered to have fully differentiated into adherent M0 macrophages.

Macrophage M1 and M2 polarization was performed based on information found in literature,[12,21] via a 24-hour incubation with 100 ng/mL of LPS and 20 ng/mL of IFN-γ, and a 48-hour incubation with 20 ng/mL of IL-4 and 20 ng/mL of IL-13, respectively.

2.6.2. Incubation of M0 and M1 macrophages with bioflavonoids

Uncommitted THP-1 derived macrophages (M0) were incubated with each of the three flavonoids for 6, 24 and 48h, at the highest non-toxic concentration found for each compound: Quercetin 60 µM, Naringenin 100 µM and Naringin 200 µM. These concentrations were determined through an Alamar Blue® cell viability assay, as described in section 2.3. Untreated M0 macrophages incubated for the same time periods were used as controls.

To evaluate the effects of these compounds on pro-inflammatory M1 macrophages, the same concentrations were used to treat M1 macrophages. After a 24h incubation with 100 ng/mL LPS and 20 ng/mL IFN-γ, the medium was replaced by fresh medium containing each of the three flavonoids and cells incubated for additional 24h. M1-polarized macrophages cultured in fresh medium for 24h were used as controls.

2.6.3. Sample collection and preparation

2.6.3.1. Cell culture supernatants

Medium aliquots were collected from each petri-dish (including medium without cells incubated under the same conditions) and centrifuged at 1000 xg for 10 min. The supernatants were then collected and stored at -80ºC. To remove interfering proteins, thawed supernatants were then subjected to a protein-precipitation protocol described by Kostidis and colleagues.[191] Briefly, 600 µL of cold methanol 100% (v/v) at -80ºC were added to 300 µL of supernatant (1:3 proportion). The aliquots were then kept at -20ºC for 30 min, after which they were centrifuged at 13000 x g for 20 min. The supernatant was then transferred to another vial, vacuum dried (SpeedVac, Eppendorf) and stored at -80ºC until NMR acquisition.

At the time of analysis, the dried samples were resuspended in 600 µL of deuterated phosphate buffer (PBS 100 mM, pH 7) containing 0.1 mM 3-(trimethylsilyl) propanoic acid (TSP-d4), and 550 µL of each sample were then transferred to 5 mm NMR tubes.

2.6.3.2. Cell extracts

To collect cell samples, the remaining medium was discarded from each dish and the cells washed 4 times with 10 mL of cold PBS. The intracellular metabolites were then extracted using a biphasic extraction protocol with methanol:chloroform:water (1:1:0.7). After adding1 mL of cold methanol (80% v/v) to quench metabolic activity of the cells, cells were scraped off the dish, transferred to a glass vial with 150 mg of glass beads (to aid in cell disruption) and vortexed for 2 min. Next, 400 µL of cold chloroform (-20ºC) was added to the tube and vortexed (2 min), followed by addition of 400 µL of chloroform and 360 µL cold milli-Q water. The samples were vortexed, allowed to rest on ice for 20 min and centrifuged at 3000 xg for 10 min. The lower organic phase was transferred to an amber glass vial and the remaining sample subjected to another chloroform addition (400 µL) and centrifugation. The resulting organic phase was then added to the previous amber vial, while the top aqueous phase was transferred to a

microcentrifuge tube. Finally, the polar extracts were vacuum dried, and lipophilic extracts were dried under a nitrogen flow, after which they were stored at -80ºC.

At the time of NMR analysis, the dried samples of the polar phases were resuspended in 600 µL of deuterated phosphate buffer (PBS 100 mM, pH 7) containing 0.1 mM TSP-d4, and 550 µL of each sample were then transferred to 5 mm NMR tubes. The lipophilic phases were used in another Masters work addressing the lipidomic study of macrophages.

A summarized schematic representation of the experimental protocol used in the section 2.6 can be found in Figure 7.

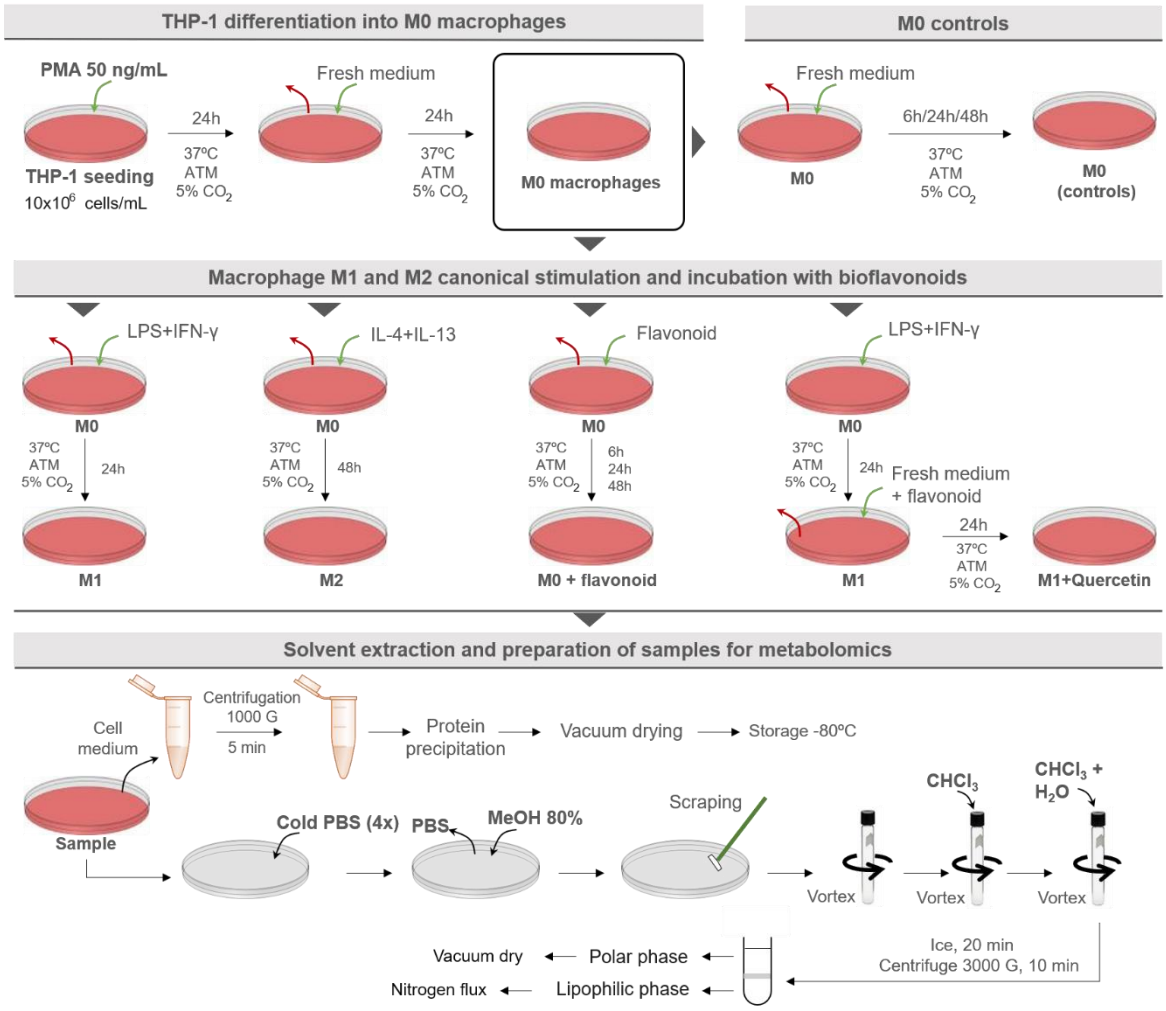

Figure 7: Schematic representation of the experimental protocol used to obtain the aqueous, lipophilic and cell media samples of the THP-1 derived macrophages in each condition, as described in section 2.6.

2.7. ^{1}H-NMR Spectroscopy

All samples were analyzed in a Bruker Avance III HD 500 NMR spectrometer (University of Aveiro, PT National NMR Network) operating at 500.13 MHz for 1H observation, at 298 K. Standard 1D 1H spectra with water presaturation (pulse program 'noesypr1d', Bruker library) were recorded with 32k points, 7002.801 Hz spectral width, a 2 s relaxation delay and 512/2048 scans (for media/ polar extracts, respectively). Two-dimensional NMR spectra were also recorded for selected samples to aid metabolite identification, namely ^{1}H-^{1}H TOCSY, J-resolved and ^{1}H-^{13}C HSQC spectra. Metabolite assignment was based on matching 1D and 2D spectral information to reference spectra available in Chenomx, BBIOREFCODE-2–0–0 (Bruker Biospin, Rheinstetten, Germany) and HMDB.[192,193]

Spectral processing was carried out using TopSpin 4.0.3 (Bruker Biospin, Rheinstetten, Germany). Each FID was multiplied by a cosine function (with an ssb value of 2), zero filled to 64k data points and Fourier-transformed. The resulting spectra were then manually phased, baseline corrected and calibrated to the TSP (δ 0 ppm) or the glucose (δ 5.235 ppm) signals, in media or polar extracts spectra, respectively.

2.8. Multivariate analysis of spectral data

After processing, the spectra were visualized and prepared for multivariate analysis in Amix-Viewer 3.9.15 (Bruker Biospin, Rheinstetten, Germany). Each spectrum was normalized by its total area, excluding the water-suppression region and some contaminant signals, such as chloroform, ethanol and methanol. The normalized data were then organized into matrices ('bucket tables'), containing the information on the signals intensity (variables) at each chemical shift in the different spectra (observations).

Data matrices were uploaded into SIMCA-P 11.5 (Umetrics, Umeå, Sweden), where PCA (Principal Component Analysis) and PLS-DA (Partial Least Squares-Discriminant Analysis) were applied. After testing different scaling types, unit-variance scaling (UV), in which each column (containing the intensities at a

particular chemical shift) is divided by its respective standard deviation, was chosen. This procedure gives equal variance to all variables, allowing for variations in less abundant metabolites to have the same weight in multivariate models as more intense signals. The results were then visualized through factorial coordinates ('scores') and factorial contributions ('loadings') colored according to variable importance to projection (VIP). For PLS-DA models, Q^2 and R^2 values, respectively reflecting predictive capability and explained variance, obtained from sevenfold internal cross validation, were used to assess the robustness of class discrimination.

2.9. Spectral integration and univariate analysis

Spectral integration of selected signals was carried out in Amix-Viewer 3.9.15 (Bruker Biospin, Rheinstetten, Germany), to provide a quantitative measurement of metabolic variations. Signals representative of each metabolite that were found to be relatively free of overlap were integrated and normalized by the total spectral area. For each metabolite, the percentage of variation in treated samples was calculated relative to respective controls, along with the effect size (ES)[194] and the statistical significance (p-value, as determined by the t-student test). The variations with medium-large magnitude (|ES|>0.5) were expressed in heatmaps colored as a function of % of variation, using the R-statistical software

2.10. Statistical analysis

The statistical analysis of both the metabolomics results and for the cytokine measurement of polarized M1 and M2 macrophages, were made via a t-student test, in which an approximation to normality was assumed, due to the small number of replicates.

The statistical significance of the results for cytokine quantification in flavonoid treated macrophages and for the cell viability assay were assessed through a one-way ANOVA, with a Sidak multiple comparisons test.

CHAPTER 3

RESULTS AND DISCUSSION

3. Results and Discussion

3.1. Macrophage responses to canonical M1 and M2 stimuli

3.1.1. Phenotypic characterization of M1 and M2 macrophages

Validation of M1 and M2 polarization states, induced, respectively, by a 24h-incubation with LPS/IFN-γ and a 48h-incubation with IL-4/IL-13, was carried out through assessment of cell surface markers and cytokine expression. Based on existing literature,[12,16,21] cell surface markers CD80 and CD64 were selected to assess M1 polarization, whereas CD36 and CD209 were used to evaluate M2 polarization. Figure 8 shows the fluorescence microscopy images obtained for macrophages stimulated with M1 and M2 canonical stimuli.

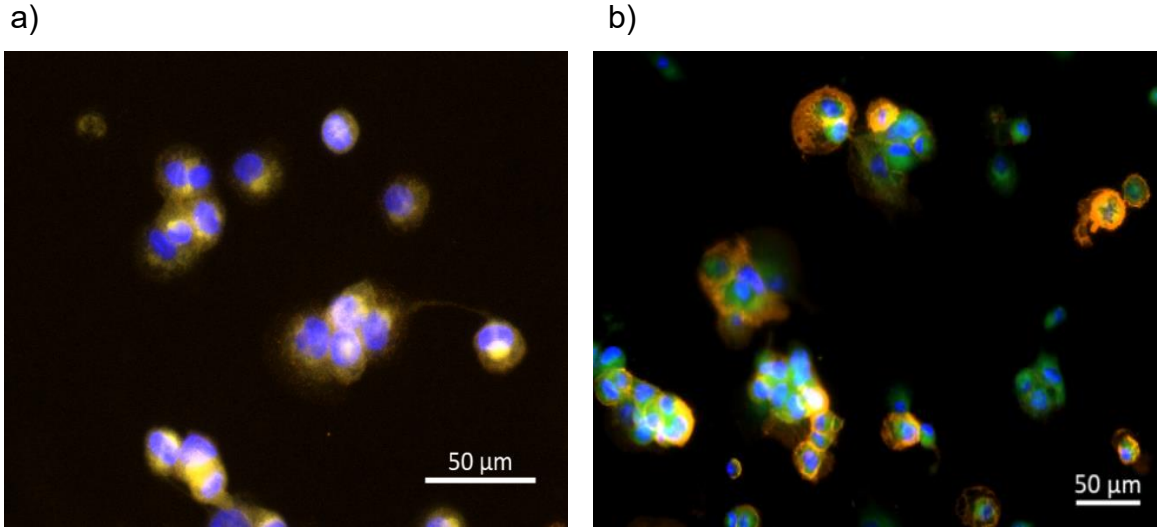

Figure 8: Fluorescence microscopy images of: a) LPS/IFN-γ–stimulated macrophages stained with CD64 (orange) - (CD80 no signal); b)IL4/IL-13-stimulated macrophages stained with CD209 (green) and CD36 (orange). Cell nuclei stained with DAPI (blue).

Macrophages stimulated with IL-4 and IL-13 for 48h were positive for both CD36 and CD209, confirming that the conditions employed appeared to be adequate for obtaining M2 macrophages. Macrophages stimulated with LPS and IFN-γ for 24h were positive for CD64, but not for CD80. To further characterize macrophage phenotype, cytokine expression was assessed after stimulation, using flow cytometry with a multiplex assay specific for macrophages. The concentrations of the 10 cytokines measured (TNF-α, IL-1β, CXCL10, IL-23, IL-12p40, IL-12p-70,

IL-6, IL-10, CCL17 and IL-1RA) in each condition (uncommitted, LPS/IFN-γ and IL4/IL13-stimulated) are shown in Figure 9.

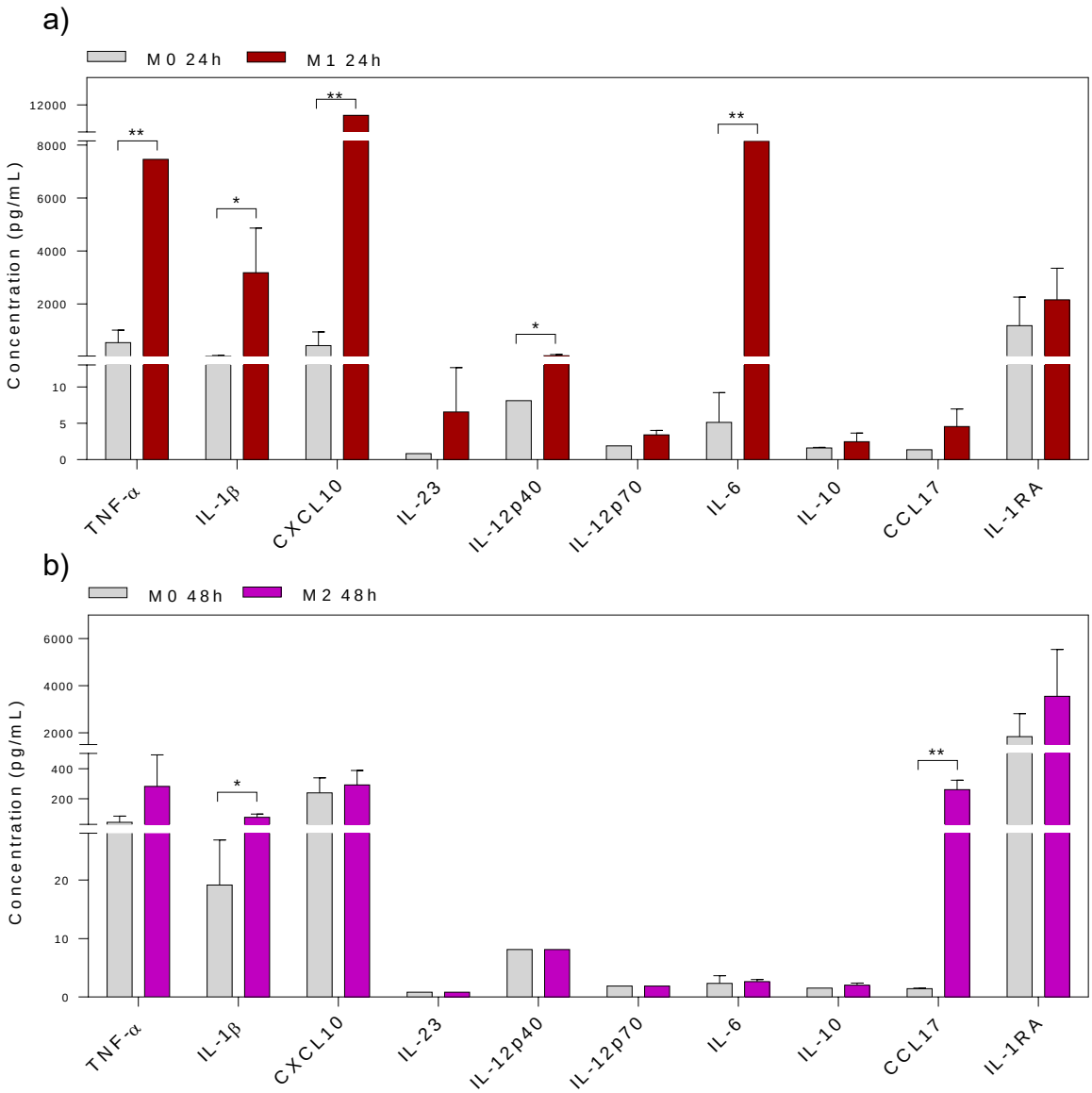

Figure 9: Concentrations of cytokines measured in the medium supernatants of polarized macrophages and their respective controls (n=3): a) M0 and M1 macrophages (24h) and b) M0 and M2 macrophages (48h).*p-value < 0.05; **p-value < 0.01.

These results clearly show distinct cytokine profiles for differentially stimulated macrophages. The main variations in cell culture supernatants of LPS/IFN-γ-stimulated macrophages included increased levels of TNF-α, IL-1β, CXCL10, IL-12p40 and IL-6. These can all be considered pro-inflammatory

cytokines,[10] although IL-6 has also been associated with alternative activation of macrophages, displaying a complex role in inflammation.[195] Here, IL-6 increased markedly in M1 macrophages, whereas no significant variation was found in M2 macrophages.

In IL-4/IL-13-stimulated macrophages, the most evident variation included a significant increase in CCL17 levels, an anti-inflammatory chemokine commonly described as a biomarker of M2 polarization.[16] Additionally, despite not being statistically significant, there appeared to be a tendency for an increase in IL-1RA, an IL-1 receptor agonist, which is also an established M2 polarization biomarker.[16] Other effects caused by M2 polarization included increased levels of IL-1β and of TNF-α, albeit to a much lesser extent when compared to M1 macrophages.

Based on these results, and for the sake of simplicity, macrophages stimulated with LPS/IFN-γ (24h) or with IL-4/IL-13 (48h) will be designated hereafter as M1 and M2 macrophages, respectively. Unstimulated macrophages are referred to as M0 macrophages.

3.1.2. Metabolic effects of canonical M1 and M2 stimuli

The metabolic profile of macrophages was assessed by ^{1}H-NMR spectroscopy. Figure 10 shows the ^{1}H-NMR spectra of macrophage polar extracts obtained under different conditions (M0, M1, M2). Based on the analysis of 2D spectra recorded for selected samples (Figure 11) and matching to spectral databases, 46 metabolites were identified (Table S1 in Supplementary Information). These include several amino acids, organic acids, choline compounds, sugars, nucleotides, among others. Most of these metabolites were present in all sample groups, although differing in quantitative levels. An exception was found for itaconate, which was only present at detectable levels in M1 macrophages, but not in M0 nor M2.

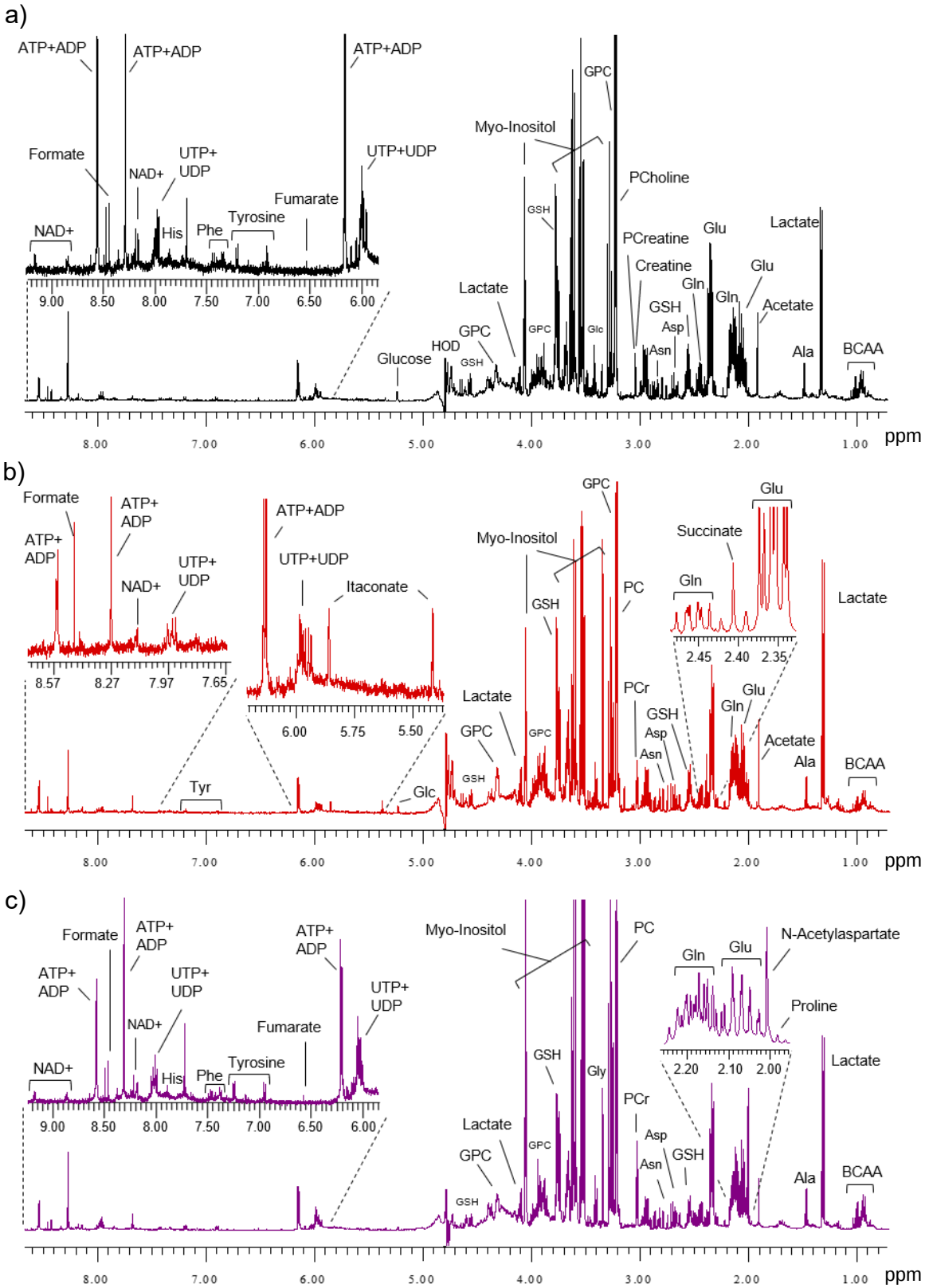

Figure 10: 500 MHz ^{1}H-NMR spectra of polar extracts from a) M0, b) M1 and c) M2 macrophages, with some metabolites assigned.

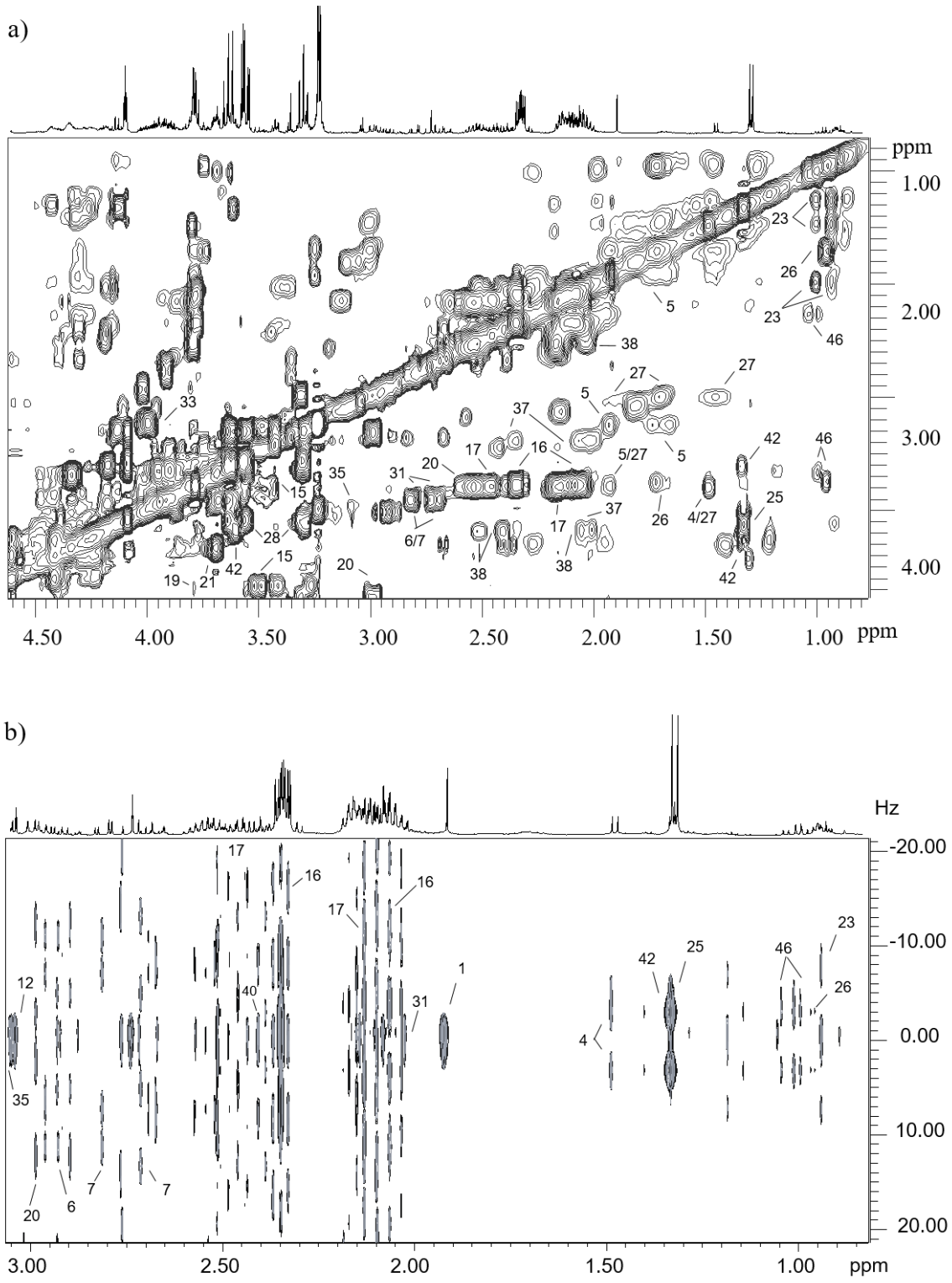

Figure 11: Expansions of a) ^{1}H-^{1}H TOCSY and b) *J*-resolved spectra of a polar extract from M0 macrophages. Signals are numbered in accordance to table S1 (Supplementary Information).

To assess the metabolic changes induced in M1 and M2 macrophages relative to uncommitted M0 macrophages, their metabolic profiles were compared using multivariate analysis. The PCA scores scatter plots (Figure 12, left) showed a reasonable separation between either M1 or M2 macrophages and their respective controls. Such discrimination was confirmed by PLS-DA (Figure 12, middle), where high Q^2 values were obtained.

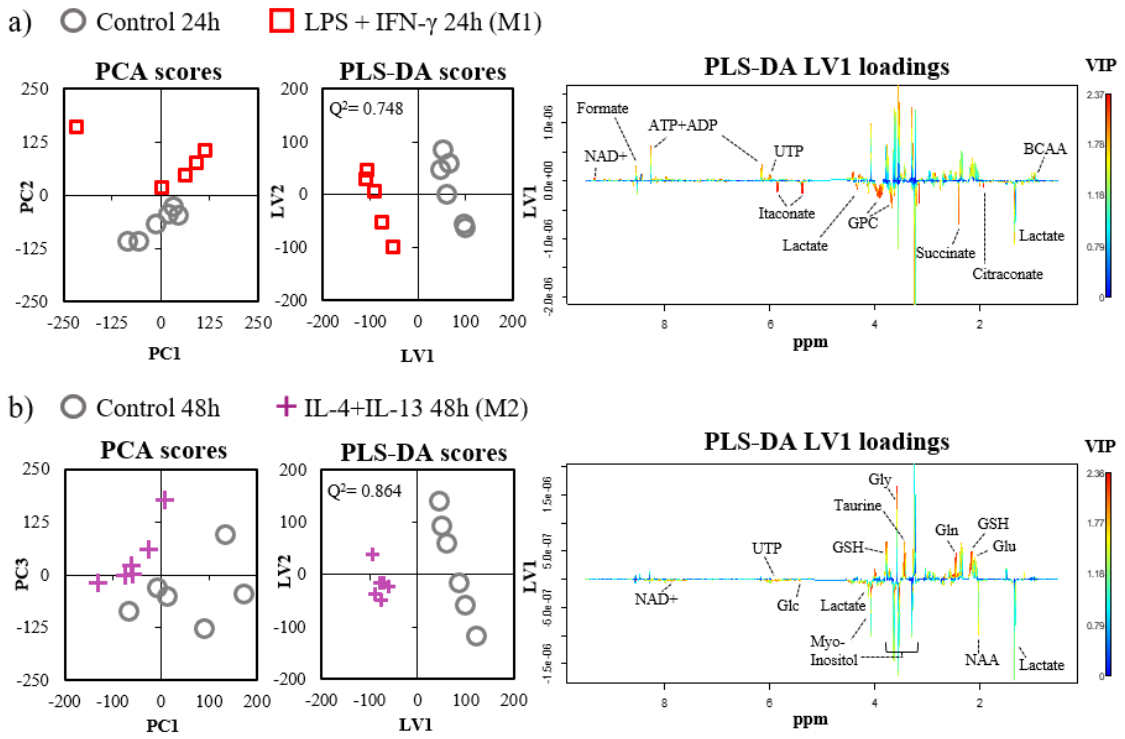

Figure 12: Multivariate analysis of ^{1}H-NMR spectra from polar extracts of a) M0 and M1 macrophages, b) M0 and M2 macrophages: PCA and PLS-DA scores scatter plots (left and center, respectively) and LV1 loadings *w* (right), colored according to variable importance to projection (VIP).

By inspecting the PLS-DA loadings (Figure 12, right), it is possible to get an immediate picture of the main metabolic effects induced by canonical stimulation of THP-1 derived macrophages. As in both PLS-DA scores plot M1 and M2 samples were grouped in the negative side of the LV1 axis, negative loadings correspond to metabolites increased in stimulated macrophages, whereas positive loadings correspond to metabolites elevated in controls. Then, based on spectral

integration, the magnitude and statistical significance in individual metabolite alterations highlighted in the PLS-DA loadings were further analyzed in more detail. These results are expressed in a heatmap (Figure 13) color-coded according to the percentage of variation of each metabolite in M1 and M2 macrophages relatively to their respective controls. Only variations with a medium-large magnitude (|ES|>0.5 according to Berben *et al.*[194]) were considered.

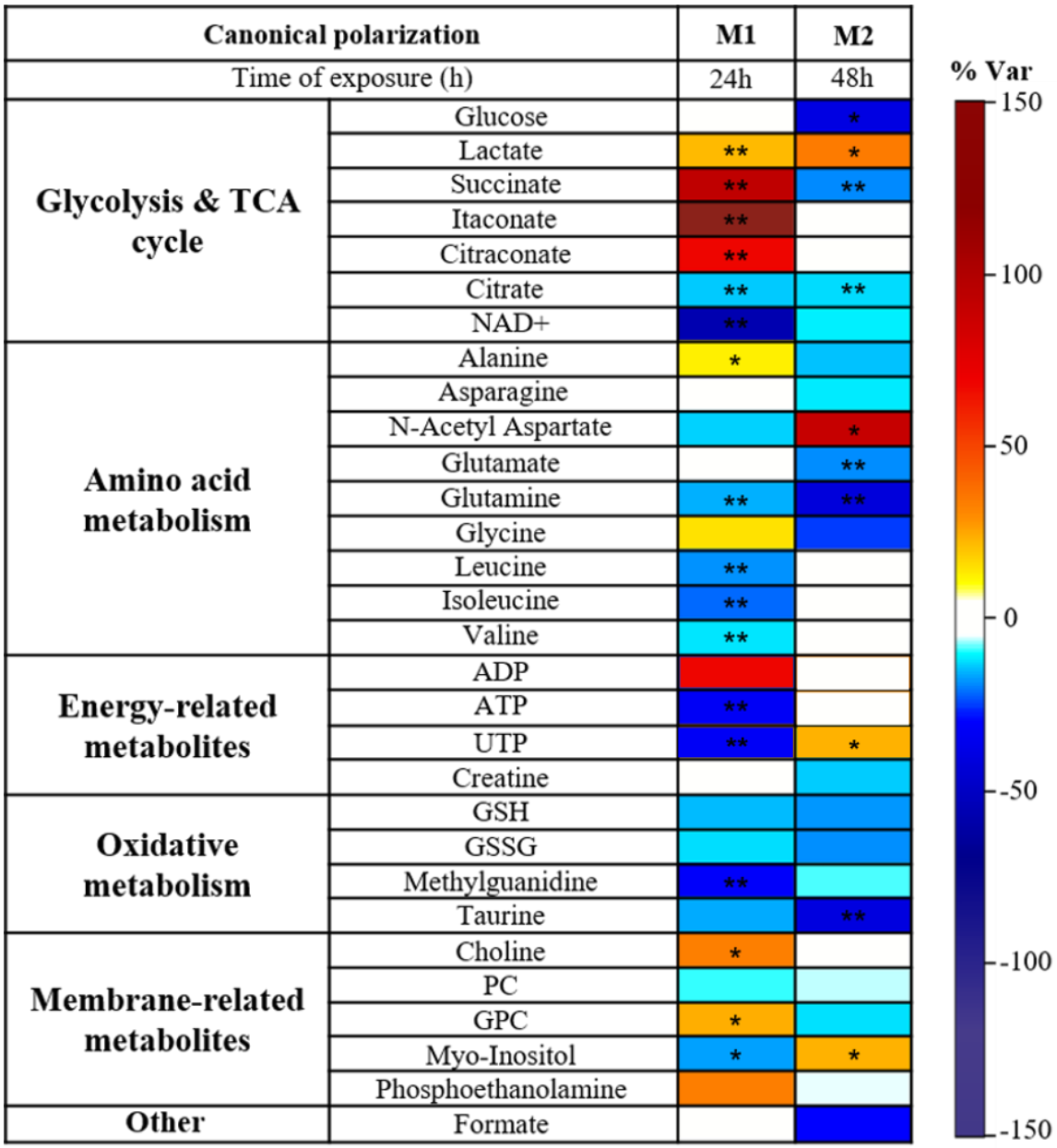

Figure 13: Heatmap of the main metabolite variations in the polar extracts of M1 and M2 macrophages. The color scale represents percentage of variation relative to respective controls (n=6). *p-value < 0.05; **p-value < 0.01.

The metabolites showing the most prominent (>20%) increases in M1 macrophages were itaconate, succinate, citraconate, phosphoethanolamine, choline, glycerophosphocholine (GPC), ADP and lactate. Glycine and alanine were also increased in M1 macrophages (<20%). On the other hand, these macrophages showed decreased levels of several other metabolites, including marked decreases in NAD+, ATP, UTP, methylguanidine and isoleucine, and milder decreases in leucine, valine, myo-inositol, taurine, glutamine, GSH, citrate, N-acetyl aspartate, GSSG and phosphocholine (PC).

In addition, M2 macrophage polarization was accompanied by a prominent increase in N-acetyl aspartate, lactate and myo-inositol, with UTP also showing a smaller increase. Moreover, glucose, taurine, succinate, GSSG, creatine and several amino acids (e.g. glutamine, glycine, alanine, asparagine) were decreased. Therefore, these results confirm that, as expected, M1 and M2 macrophages clearly differ in their intracellular metabolic composition.[60,62,63]

Analysis of the cell culture medium provided complementary information on cells metabolic activity, allowing for a better interpretation of the variations observed in polar extracts. By comparing the metabolite composition of cell-conditioned medium with that of acellular culture medium (incubated under the same conditions), the metabolites consumed and excreted by macrophages could be easily assessed.

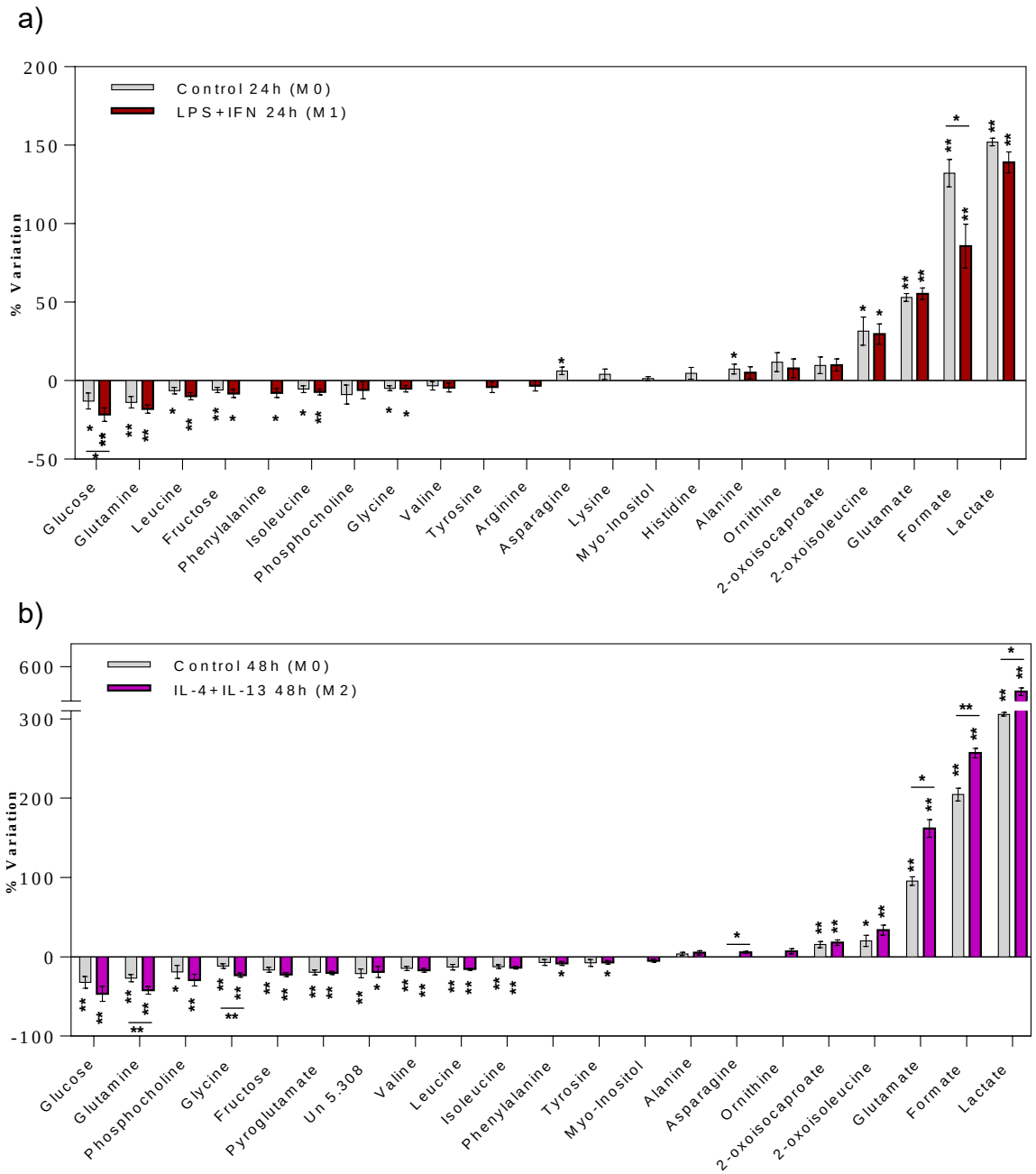

Figure 14: Variations in consumption (negative bars) and excretion (positive bars) of several metabolites in the cell culture supernatant of THP-1 derived macrophages incubated with: a) LPS+IFN-γ for 24h (M1 polarization) and b) IL-4+IL-13 for 48h (M2 polarization) when compared to acellular media (n=6). In both graphs, the red/purple bars represent the polarized macrophages and the grey bars correspond to uncommitted macrophages at the respective incubation times. *p-value < 0.05; **p-value < 0.01.

As shown in Figure 14, the main substrates consumed by cells (negative percentual variation) were glucose, glutamine, pyroglutamate, phosphocholine, fructose, valine, leucine, isoleucine and glycine, whereas the metabolites with a positive percentage of variation, like alanine, 2-oxoisocaproate, 2-oxoisoleucine, glutamate, formate and lactate, were excreted into the extracellular medium.

The graphs in Figure 14 also show the impact of M1 and M2 polarization on metabolite consumption/excretion patterns. Compared to M0 macrophages, M1 macrophages showed: i) significantly increased consumption of glucose, ii) non-significant trends for increased consumption of glutamine, branched chain amino acids and fructose, iii) significantly decreased excretion of formate, iv) non-significant decrease in lactate excretion.

On the other hand, relatively to their respective controls, M2 macrophages showed: i) non-significant trends for increased consumption of glucose, ii) significantly increased consumption of glutamine ang glycine, iii) significant increase in the excretion of asparagine, glutamate, formate and lactate, iv) non-significant trends for increased excretion of 2-oxoisoleucine.

3.2. Macrophage responses to bioflavonoids

3.2.1. Flavonoid effects on cell viability

To assess the effects of each bioflavonoid on cell viability and select appropriate concentrations for subsequent metabolomics experiments, THP-1 derived macrophages were exposed for 24h to Quercetin, Naringenin and Naringin at concentrations ranging from 20 to 200 µM. The results of the Alamar Blue® reduction assay are shown in Figure 15.

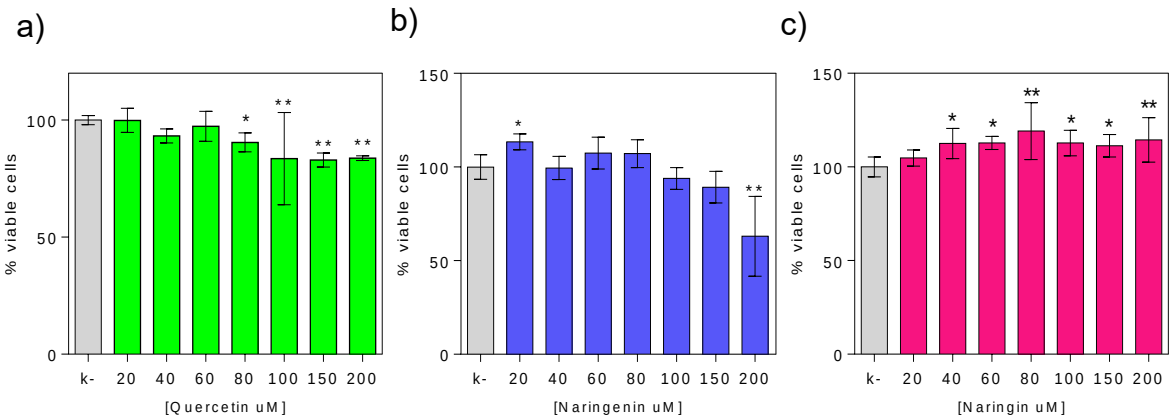

Figure 15: Cell viability of THP-1 derived macrophages exposed for 24h to: a) Quercetin; b) Naringenin; c) Naringin, at concentrations ranging from 20 µM to 200 µM, as assessed by the Alamar Blue® reduction assay. Statistical significance assessed in each concentration of the compound against the control (grey bar) via an ANOVA, with Sidak multiple comparisons test (n=5). *p-value < 0.05; **p-value < 0.01.

Naringin was the flavonoid that showed the least cytotoxic effects, as cell viability/metabolic activity was above that of the control even at the highest concentration tested (200 µM). This effect could be in line with findings that Naringin is capable of stimulating cell proliferation and differentiation of bone marrow stromal cells (BMSCs), possibly also applying to macrophages.[196] Naringenin lowered cell viability at concentrations ≥150 µM. This is consistent with data obtained in a study by Saenz and colleagues, where the chosen concentration of Naringenin was 100 µM, which did not show any decrease in cell viability in THP-1 derived macrophages.[157] Finally, Quercetin lowered cell viability at concentrations ≥80 µM. Therefore, for each flavonoid, a non-cytotoxic concentration was chosen for subsequent experiments: i) 60 µM of Quercetin; ii) 100 µM of Naringenin; iii) 200 µM of Naringin.

3.2.2. Phenotypic characterization of flavonoid-treated macrophages

Out of the ten cytokines measured in cell culture medium using a multiplex assay, only six showed changes in concentration upon flavonoid treatment. These were TNF-α, IL-1β, CXCL10, IL-6, CCL17 and IL-1RA (Figure 16). Although most differences between sample groups did not reach statistical significance, likely due to a small number of replicates (n=3) and large standard deviation values, there were some clear variation trends. The pro-inflammatory cytokine TNF-α decreased for all tested flavonoids, with Naringenin having the most marked effects in M0 macrophages. The levels of IL-1β were also affected, showing a decrease in the supernatants of treated pre-polarized M1 macrophages, with all three flavonoids having similar impact. In M0 macrophages, however, Quercetin treatment appeared to cause an increase in IL-1β, while no effects were caused by Naringenin or Naringin. The chemokine CXCL10, known as a pro-inflammatory mediator,[14,58] was also decreased in both Quercetin and Naringenin-treated M0 macrophages, while Naringin did not produce any noticeable effects. In pre-polarized M1 macrophages, the levels of CXCL10 were very high in comparison to M0 macrophages and did not seem to be particularly affected by flavonoid treatment. Flavonoid treatment was also associated with a decrease in IL-6, in almost all conditions, albeit to a much lesser extent in M0 macrophages, especially in the case of Naringin treatment. This IL-6 lowering effect has been described for some flavonoids (including Quercetin and Naringenin), tested in LPS-stimulated RAW 264.7 macrophages, indicating an attenuated inflammatory response.[197]

Regarding the anti-inflammatory chemokine CCL17, no changes were observed in flavonoid-treated M0 macrophages (the concentration was too low to be detected). In the case of pre-polarized M1 macrophages, CCL17 showed different variations depending on the flavonoid used. Quercetin and Naringin caused a decrease in CCL17 levels, whereas Naringenin led to an increase in this anti-inflammatory chemokine. Similarly, IL-1RA levels were also slightly increased in Naringenin-treated M0 macrophages, but decreased with Quercetin and Naringin treatment in both M0 and M1-like macrophages.

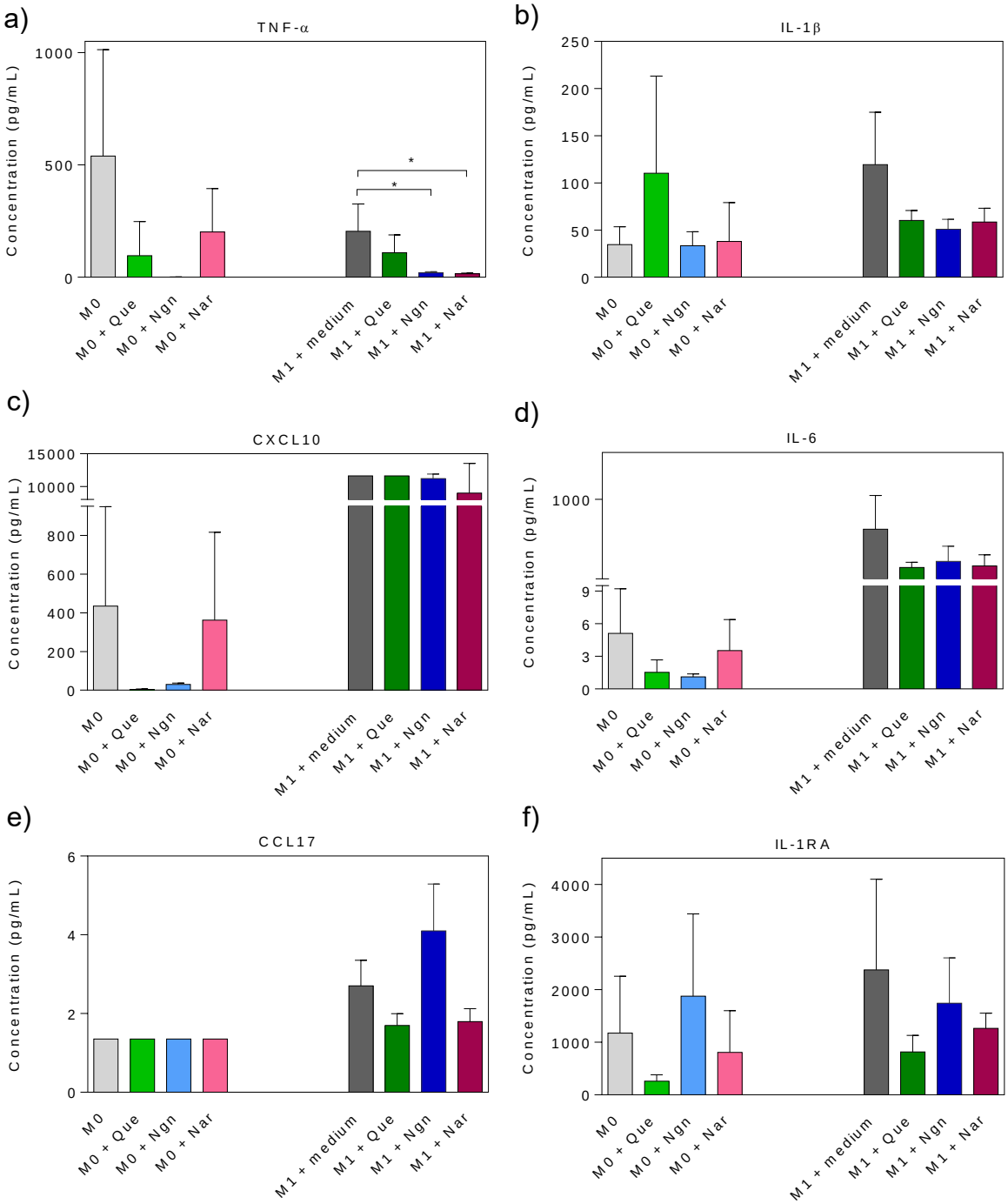

Figure 16: Concentration of pro- and anti-inflammatory cytokines in the medium supernatant of M0 macrophages and pre-polarized M1 macrophages upon 24h exposure to each flavonoid: a) TNF-α, b) IL-1β, c) CXCL10, d) IL-6, e) CCL17 and f) IL-1RA. Statistical significance was assessed using a one-way ANOVA, with a Sidak multiple comparisons test (n=3). **p*-value < 0.5.

The results described above indicate that: i) all flavonoids tested induced decreased production of pro-inflammatory cytokines, corroborating their substantial reported activity in attenuating inflammation, ii) Naringenin could additionally act by increasing the expression of anti-inflammatory cytokines (as shown here for CCL17).

3.2.3. Metabolic effects of Quercetin on M0 and M1 macrophages

The effects of Quercetin on the intracellular metabolome of THP-1 derived macrophages were assessed through ^{1}H-NMR analysis of cell polar extracts, followed by multivariate analysis and spectral integration. The PCA and PLS-DA results obtained for the comparison between untreated M0 macrophages and 24h Quercetin-treated M0 macrophages are shown in Figure 17. The two sample groups were clearly separated in the scores plots, with a very high Q2 value (reflecting model robustness) being obtained for the PLS-DA model. Also, PLS-DA LV1 loadings (Figure 17, right) showed intense coloring of many variables, indicating the marked impact of Quercetin on macrophages metabolic profile. Positive loadings correspond to metabolites increased in samples grouping in positive LV1, i.e. the controls (e.g. lactate, GSH), whereas negative loadings arise from metabolites increased in samples with negative LV1 scores, i.e. Quercetin-treated macrophages (e.g. glucose, citrate). Equally good MVA discriminations were also obtained for 6 and 48h treatments (Figure S1, Supplementary Information).

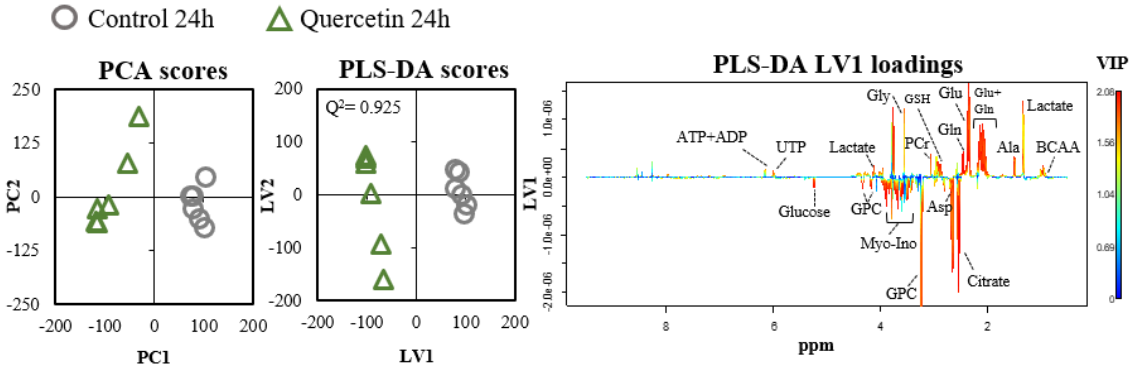

Figure 17: Multivariate analysis of ^{1}H-NMR spectra from the polar extracts of THP-1 derived macrophages comparing unstimulated M0 macrophages (grey) and Quercetin-treated macrophages (green) , incubated for 24h. PCA and PLS-DA scores scatter plots (left and center, respectively) and LV1 loadings *w* (right), colored according to variable importance to projection (VIP).

In order to analyze in more detail the metabolic changes induced by Quercetin, spectral signals representing individual metabolites were integrated and the percentage of variation in each treatment group calculated relative to respective controls. The results obtained for Quercetin treatment of M0 macrophages during 6, 24 and 48h are summarized in the heatmap shown in Figure 18. Additionally, Quercetin effects on pre-polarized M1 macrophages (incubated with LPS + IFN-γ for 24h and then stimulated with Quercetin for another 24h, after removing the medium containing the pro-inflammatory stimuli) is also shown in the heatmap. Overall, a 24h incubation with Quercetin appeared to have a more pronounced effect on the metabolic profile of THP-1 derived macrophages, and the effects seen in pre-polarized macrophages were, to some extent, similar to those observed in Quercetin-treated uncommitted macrophages.

Regarding the effects of Quercetin on M0 macrophages, most changes were common to all time points, albeit in different extents. In particular, the metabolites found to be consistently increased in treated macrophages were glucose, citrate, GSSG, methylguanidine, taurine, choline compounds and phosphoethanolamine, whereas lactate, succinate, several amino acids, phosphocreatine and GSH were decreased. Several of these changes were especially prominent in the 24h treatment. On the other hand, some variations were clearly time-dependent, namely those in aspartate (increased in macrophages treated for 6/24h, but decreased at 48h), ATP, UTP, valine, myo-inositol and formate.

When macrophages were polarized to a pro-inflammatory (M1) state before Quercetin treatment, there were also a significant number of changes in the intracellular metabolome (Figure 18, column on the far right). Many of these changes were common to those produced by Quercetin in M0 macrophages, including the increases in citrate, (glycero)phosphocholine and phosphoethanolamine, together with decreases in lactate, succinate, amino acids and phosphocreatine. On the other hand, unlike Quercetin-treated M0 macrophages, M1 macrophages showed no alteration in glucose, aspartate or GSSG intracellular levels upon Quercetin treatment. Additionally, an increase in itaconate (accompanied by a decrease in its predecessor citraconate) was detected in M1 Quercetin-treated macrophages. The results also indicate that the

variations in antioxidant metabolites and choline were opposite to those obtained for M0 treated macrophages.

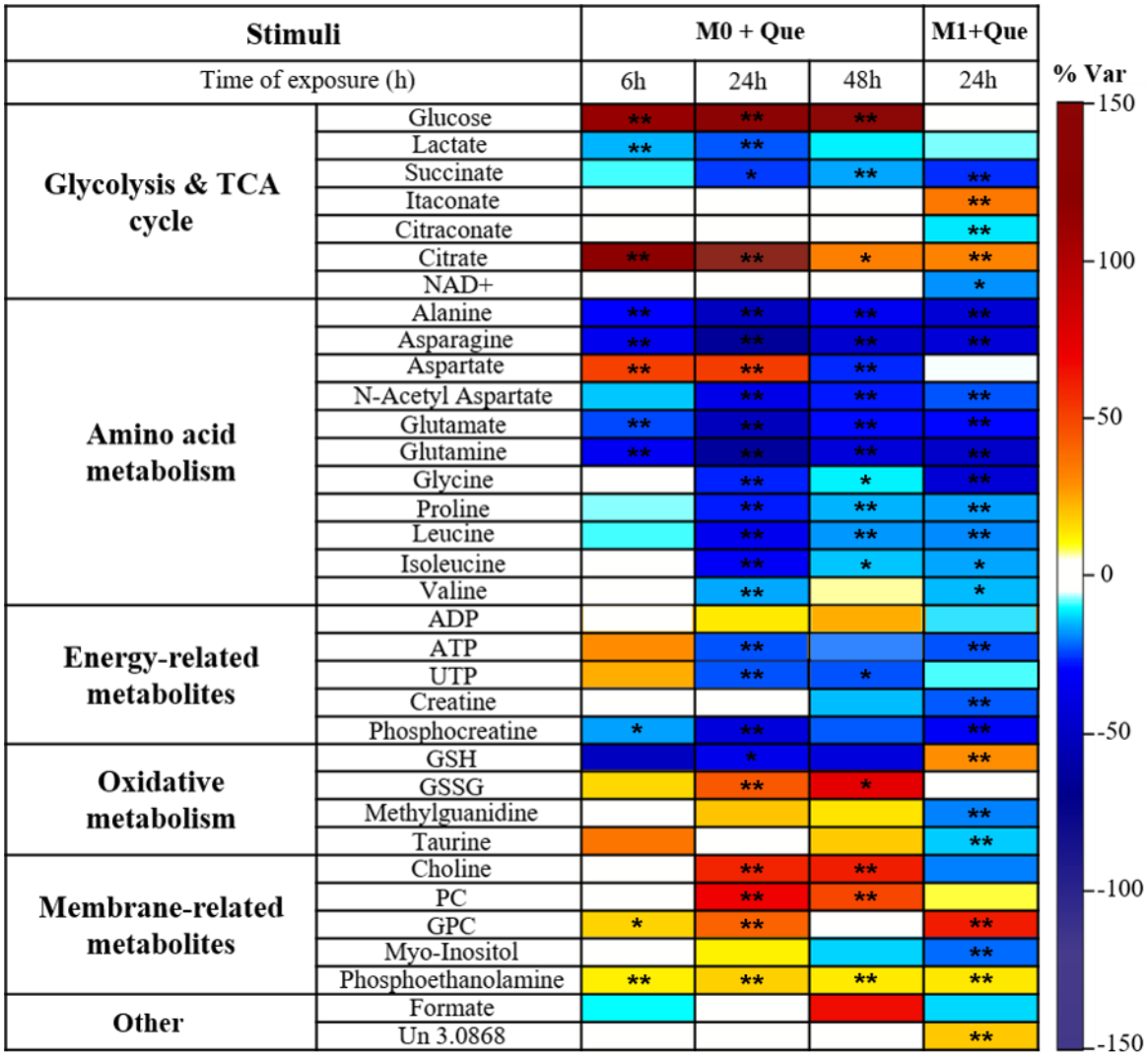

Figure 18: Heatmap of the main metabolite variations in the polar extracts of THP-1 derived macrophages upon treatment with Quercetin (60 µM): M0 macrophages incubated with the flavonoid for 6, 24 or 48h; M1 pre-polarized macrophages incubated with the flavonoid for 24h. The color scale represents percentage of variation relative to respective controls (n=6). *p-value < 0.05; **p-value < 0.01.

The variations in cell culture medium composition (exometabolome) in response to Quercetin treatment of both uncommitted and pre-polarized M1 macrophages are summarized in Figure 19. Overall, a higher number of significant changes were detected in 48h culture media samples. When exposed to Quercetin, uncommitted macrophages were found to excrete less lactate and formate ubiquitously in all incubation times, although reaching statistical significance only at 24 and 48h (Figures 19b and 19c, respectively). This effect was not present in Quercetin-treated M1 macrophages (Figure 19d), which actually showed a slight tendency of increased excretion of lactate. Similarly, glutamate excretion was decreased in Quercetin treated M0 macrophages, while pre-polarized macrophages showed increased excretion of glutamate upon incubation with Quercetin. Other differences in excreted metabolites include the reduced or ceased excretion of 2-oxoisoleucine in all groups, except for the 6h treated M0 macrophages (Figure 19a), and the increased excretion of valine in the 24h Quercetin-treated groups (both M0 and M1).

Interestingly, glucose consumption was affected in all conditions except in the cells treated for 6h, showing a tendency to decrease in 24h treated macrophages, a statistically significant decrease at 48h and a complete arrest of glucose consumption in pre-polarized M1 macrophages. A decrease in glutamine consumption could also be found in 48h treated macrophages and in pre-polarized macrophages. On the other hand, isoleucine was being less consumed in both 24h and 48h treated cells, whereas pre-polarized macrophages stopped consuming isoleucine and started excreting it to the extracellular media. Several other metabolites were found to be less consumed or not consumed at all, specifically in the 48h Quercetin treated macrophages, (e.g. glycine, leucine, valine, fructose, pyroglutamate, phosphocholine).

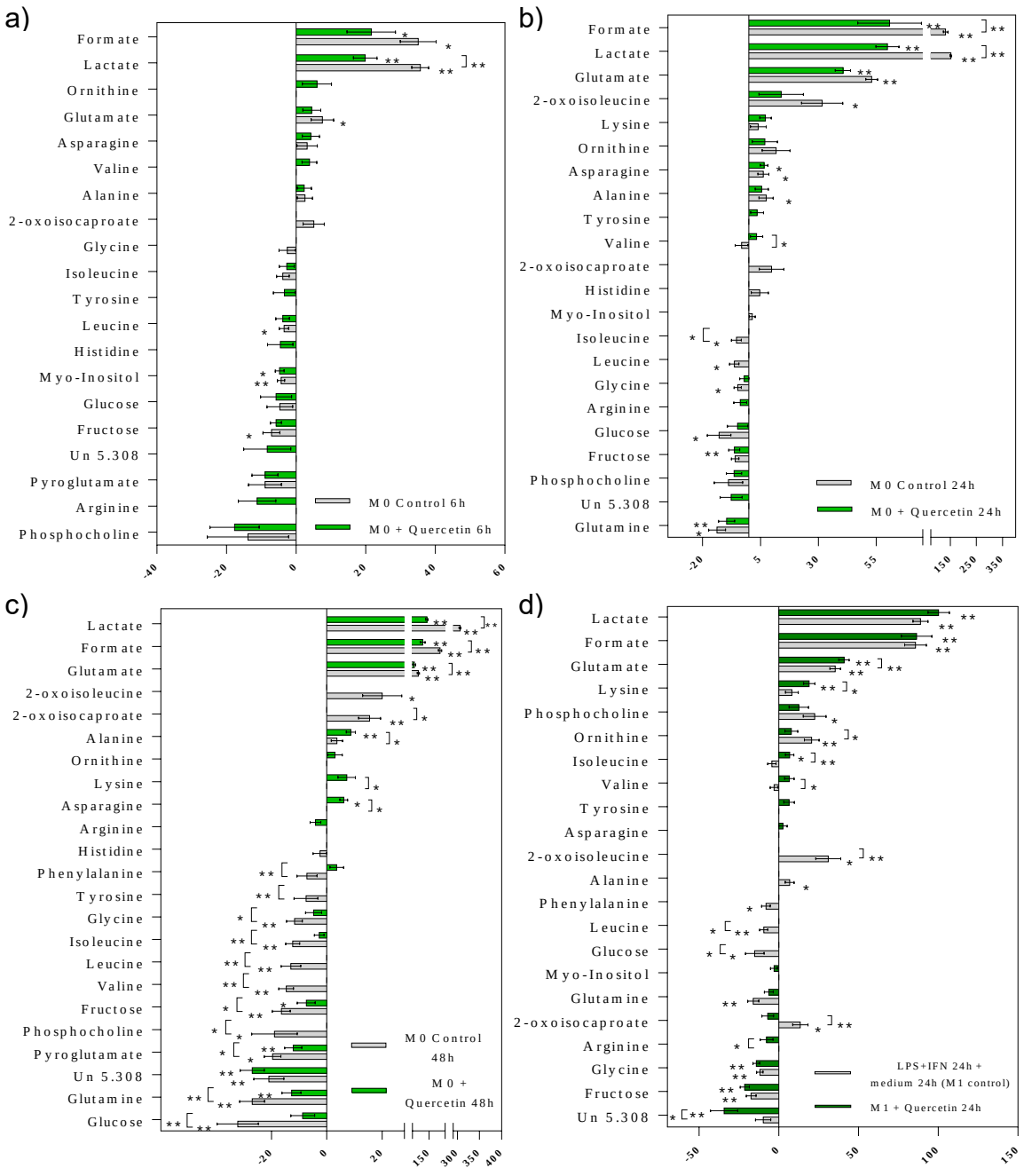

Figure 19: Variations in consumption (negative bars) and excretion (positive bars) of several metabolites in the cell culture supernatant of THP-1 derived macrophages incubated with 60 µM of Quercetin: a), b), c) M0 macrophages incubated with Quercetin for 6, 24 and 48h, respectively; d) Pre-polarized M1 macrophages incubated with Quercetin for 24h. Each Quercetin incubation (green bars) was compared to its respective control (grey bars). Statistical significance of variation was assessed via a t-student test (n=6): **p*-value < 0.05; ***p*-value < 0.01.

3.2.4. Metabolic effects of Naringenin on M0 and M1 macrophages

The metabolic effects of Naringenin treatment in THP-1 derived macrophages were assessed using the same strategy as that described for Quercetin.

Figure 20 shows the multivariate analysis performed on the ^{1}H-NMR spectra of polar extracts collected for 24h Naringenin-treated M0 macrophages and their respective controls (results for other time points shown in Figure S2, Supplementary Information). The separation between the control group and the Naringenin-treated group is visible in both PCA and PLS-DA scores scatter plots (Figure 20, left and middle). PLS-DA LV1 loadings (Figure 20, right) immediately revealed the most marked effects induced by Naringenin (e.g. increases in lactate and some amino acids, together with decreases in GSH and glycerophosphocholine).

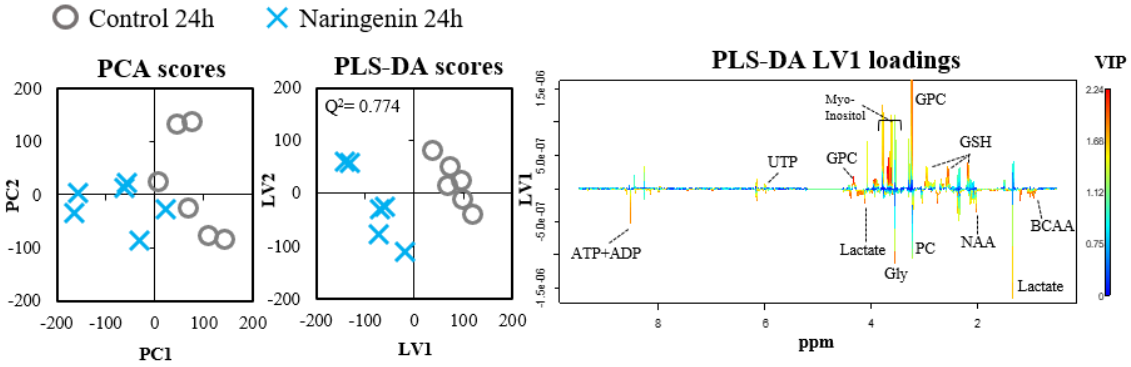

Figure 20: Multivariate analysis of ^{1}H-NMR spectra from the polar extracts of THP-1 derived macrophages comparing unstimulated M0 macrophages (grey) and Naringenin-treated macrophages (blue), incubated for 24h. PCA and PLS-DA scores scatter plots (left and center, respectively) and LV1 loadings w (right), colored according to variable importance to projection (VIP).

The quantitative analysis of individual metabolite variations in M0 macrophages treated with Naringenin for different time periods, as well as in 24h Naringenin-treated pre-polarized M1 macrophages is summarized in the heatmap shown in Figure 21. Several metabolic effects of Naringenin in M0 macrophages appeared to be time-dependent, generally intensifying with treatment duration. For instance, gradual increases were found in the intracellular levels of glucose, lactate, N-acetylaspartate, some amino acids and (phospho)choline. Additionally, succinate was increased only in 48h Naringenin-treated macrophages (relative to respective controls). On the other hand, Naringenin treatment caused decreases in the intracellular levels of citrate, asparagine, aspartate, glycerophosphocholine and myo-inositol. Moreover, a few metabolites even showed opposite variations depending on the incubation period with Naringenin. This was the case of GSH, which increased in 6h treated cells (where the oxidized form GSSG was decreased), but then decreased for 24 and 48h. Also, ATP levels were increased in both 6 and 48h but decreased in 24h treated M0 macrophages.

Interestingly, the metabolic signature of Naringenin in pre-polarized macrophages (Figure 21, column on the far right) showed several differences compared to the effects produced in M0 macrophages. In particular, opposite variations were found for glucose, lactate, succinate, (phospho)creatine, choline, asparagine and glutamine. Still, some Naringenin effects appeared to be independent of macrophage initial polarization state, namely the decreases in citrate, glycerophosphocholine and formate, together with the increases in NAD+ and glutamate.

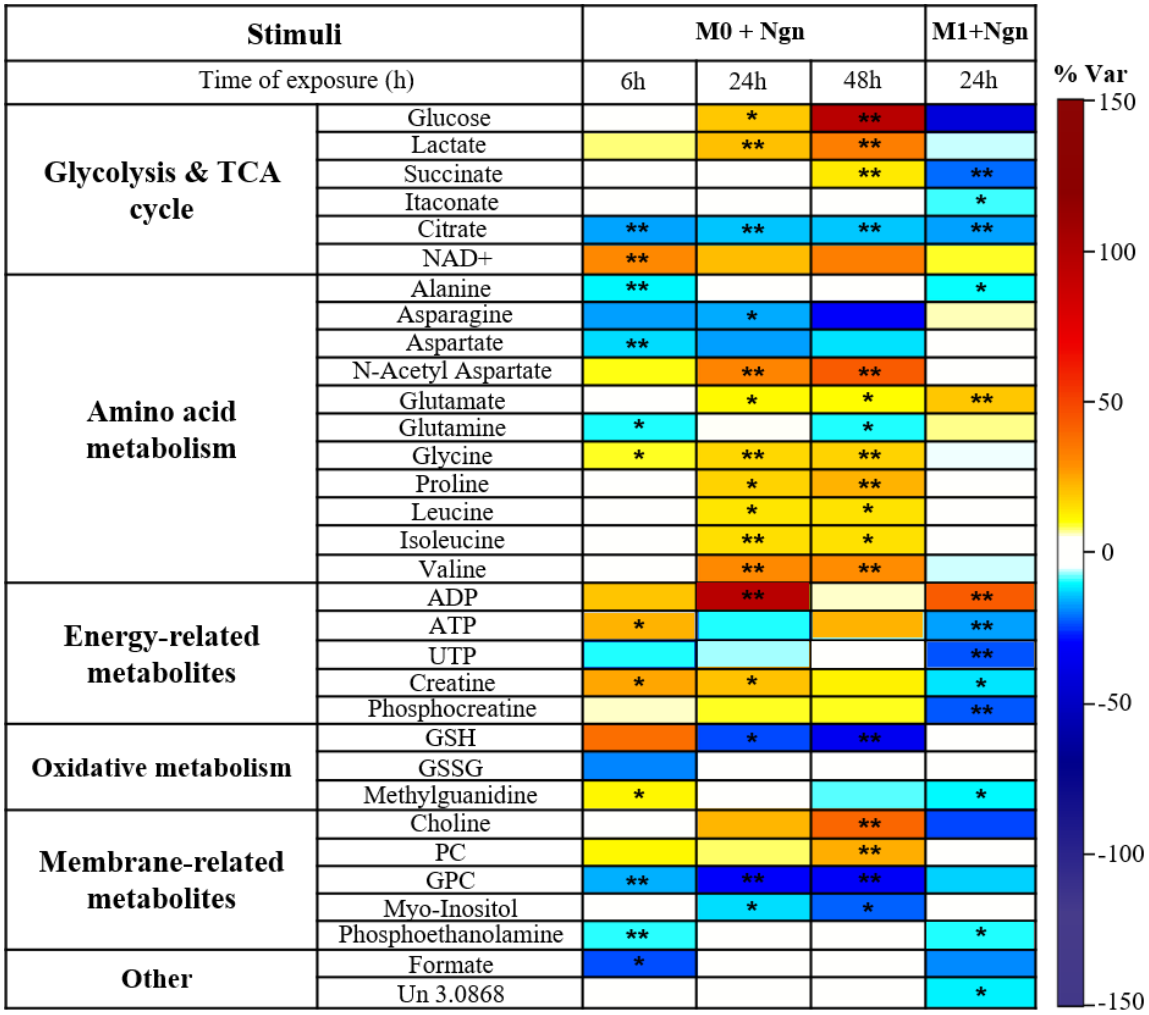

Figure 21: Heatmap of the main metabolite variations in the polar extracts of THP-1 derived macrophages upon treatment with Naringenin (100 µM): M0 macrophages incubated with the flavonoid for 6, 24 or 48h; M1 pre-polarized macrophages incubated with the flavonoid for 24h. The color scale represents percentage of variation relative to respective controls (n=6). *p-value < 0.05; **p-value < 0.01.

The variations in cell culture medium composition in response to Naringenin treatment of both uncommitted and pre-polarized M1 macrophages can be consulted in Figure 22. Similarly to the endometabolome, the differences induced by Naringenin in the exometabolome of M0 macrophages intensified over exposure time. Compared to untreated control macrophages, 48h Naringenin-treated macrophages consumed less phosphocholine, pyroglutamate and glutamine, while showing a non-significant trend to consume more glucose and/or fructose. Also, treated cells excrete less formate and glutamate, together with more alanine.

Interestingly, the variations in cells nutrients consumption and metabolites excretion patterns upon Naringenin treatment were exacerbated when macrophages were pre-polarized to a pro-inflammatory M1 state (Figure 22d). Compared to respective controls (24h in fresh medium after LPS/IFN-γ stimulation), Naringenin-treated M1 macrophages displayed increased consumption of fructose, myo-inositol and some amino acids, accompanied by reduced use of glutamine and glucose. Notably, while M0 macrophages showed a trend for consuming more glucose in the presence of Naringenin, M1 macrophages arrested glucose consumption upon Naringenin treatment. Regarding the excretion pattern, Naringenin-treated M1 macrophages excreted more lactate and formate, but lower amounts of alanine and metabolites resulting from branched chain amino acids catabolism (2-oxoisoleucine and 2-oxoisocaproate).

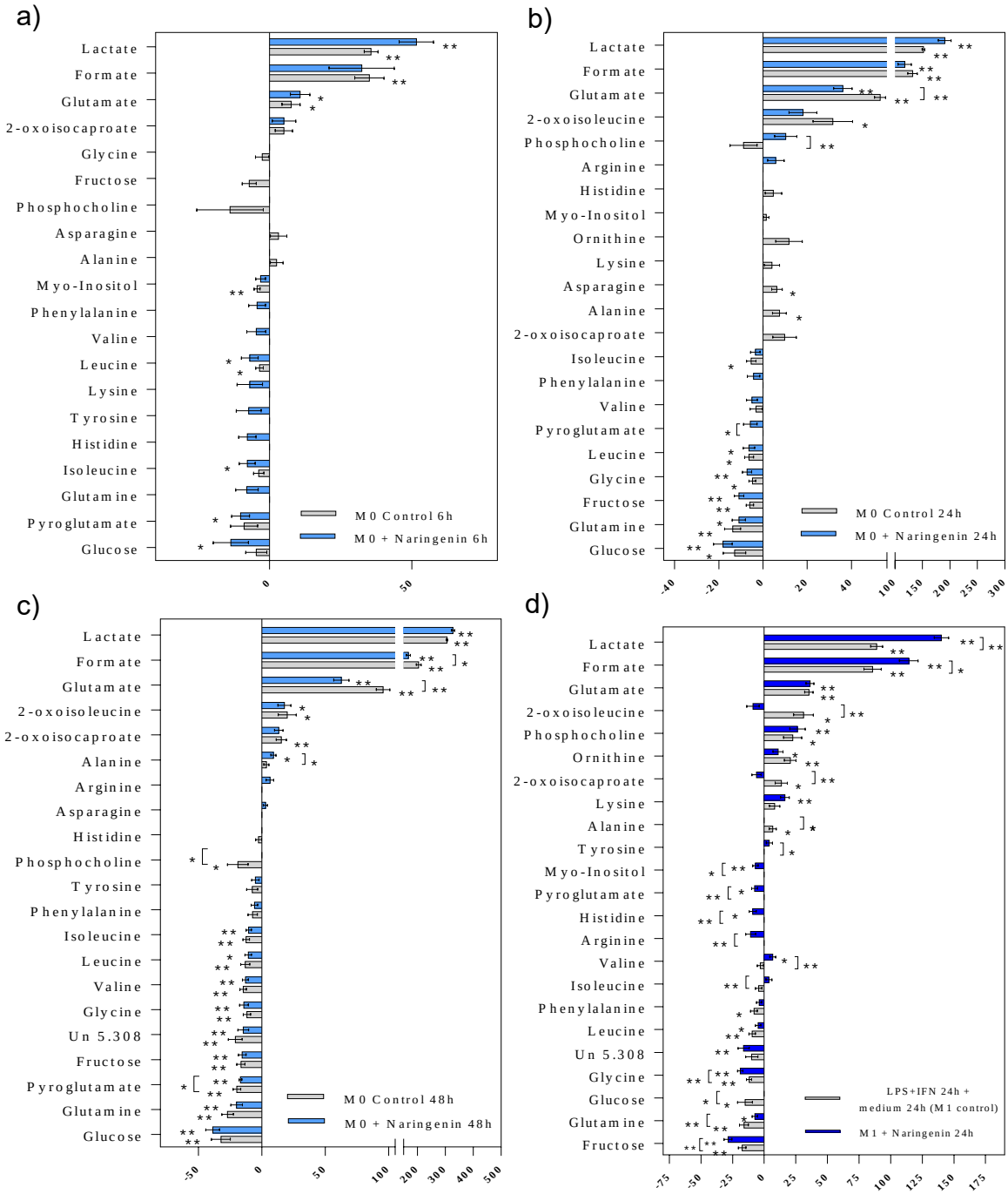

Figure 22: Variations in consumption (negative bars) and excretion (positive bars) of several metabolites in the cell culture supernatant of THP-1 derived macrophages incubated with 100 µM of Naringenin: a), b), c) M0 macrophages incubated with Naringenin for 6, 24 and 48h, respectively; d) Pre-polarized M1 macrophages incubated with Naringenin for 24h. Each Naringenin incubation (blue bars) was compared to its respective control (grey bars). Statistical significance of variation was assessed via a t-student test (n=6): **p*-value < 0.05; ***p*-value < 0.01

3.2.5. Metabolic effects of Naringin on M0 and M1 macrophages

Among the three flavonoids tested, Naringin was found to have the lowest impact on the endometabolome of THP-1 derived macrophages, despite the higher concentration used (200 µM). This can be clearly seen in Figure 23 showing the multivariate comparison of control and 24h Naringin-treated M0 macrophages. The two groups were not separated in the PCA scores scatter plot, and PLS-DA model robustness, as assessed by the Q2 value (0.582), was relatively lower. Also, few variables showed high VIP (importance to the projection), as demonstrated by the less intense colouring of LV1 loadings. Similar MVA results were obtained for 6 and 48h exposures (Figure S3, Supplementary Information). Still, the spectra were integrated and the variations with larger magnitude (|ES| > 0.5) were represented in the heatmap shown in Figure 24.

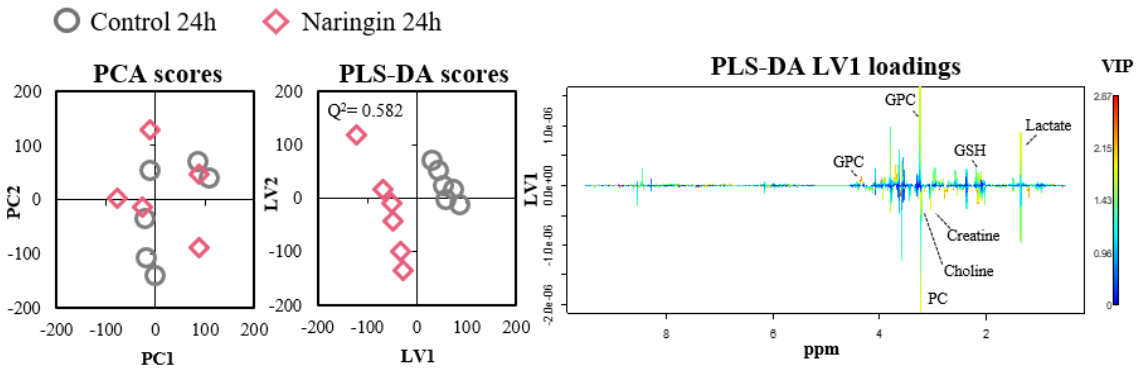

Figure 23: Multivariate analysis of ^{1}H-NMR spectra from the polar extracts of THP-1 derived macrophages comparing unstimulated M0 macrophages (grey) and Naringin-treated macrophages (pink), incubated for 24h. PCA and PLS-DA scores scatter plots (left and center, respectively) and LV1 loadings w (right), colored according to variable importance to projection (VIP).

In agreement with the MVA results, the number of metabolites varying consistently with Naringin treatment was smaller when compared to the other bioflavonoids. Also, the magnitude of most variations was relatively lower and differed according to the incubation time. In general, the longer the exposure of M0 macrophages to Naringin, the more noticeable its effects were.

Focusing on the changes detected at 24h of treatment, Naringin caused mild increases in NAD+, N-acetylaspartate, valine, ADP, creatine, GSSG, taurine and (phospho)choline, while decreasing the levels of aspartate, ATP and UTP, GSH, methylguanidine and glycerophosphocholine. Interestingly, some of these changes were also seen upon Naringin treatment of pre-polarized M1 macrophages (e.g. variations in creatine, GSH/GSSG and taurine), while others were absent or in the opposite direction. For example, glucose decreased in Naringin-treated M1 macrophages, contrarily to the variation induced in M0 macrophages (at 6 and 48h incubations). Also, lactate and phosphocreatine, which did not vary in treated M0 macrophages, decreased in M1 treated macrophage.

At the extracellular level, the changes induced by Naringin are summarized in Figure 25. Most significant changes were found when Naringin was given to pre-polarized M1 macrophages (Figure 25d), comprising: decreased consumption of glucose (also seen in 48h Naringin-treated M0 macrophages), as well as glutamine and other amino acids; increased consumption of fructose; increased excretion of myo-inositol and ceased excretion of alanine, 2-oxoisocaproate and 2-oxoisoleucine.

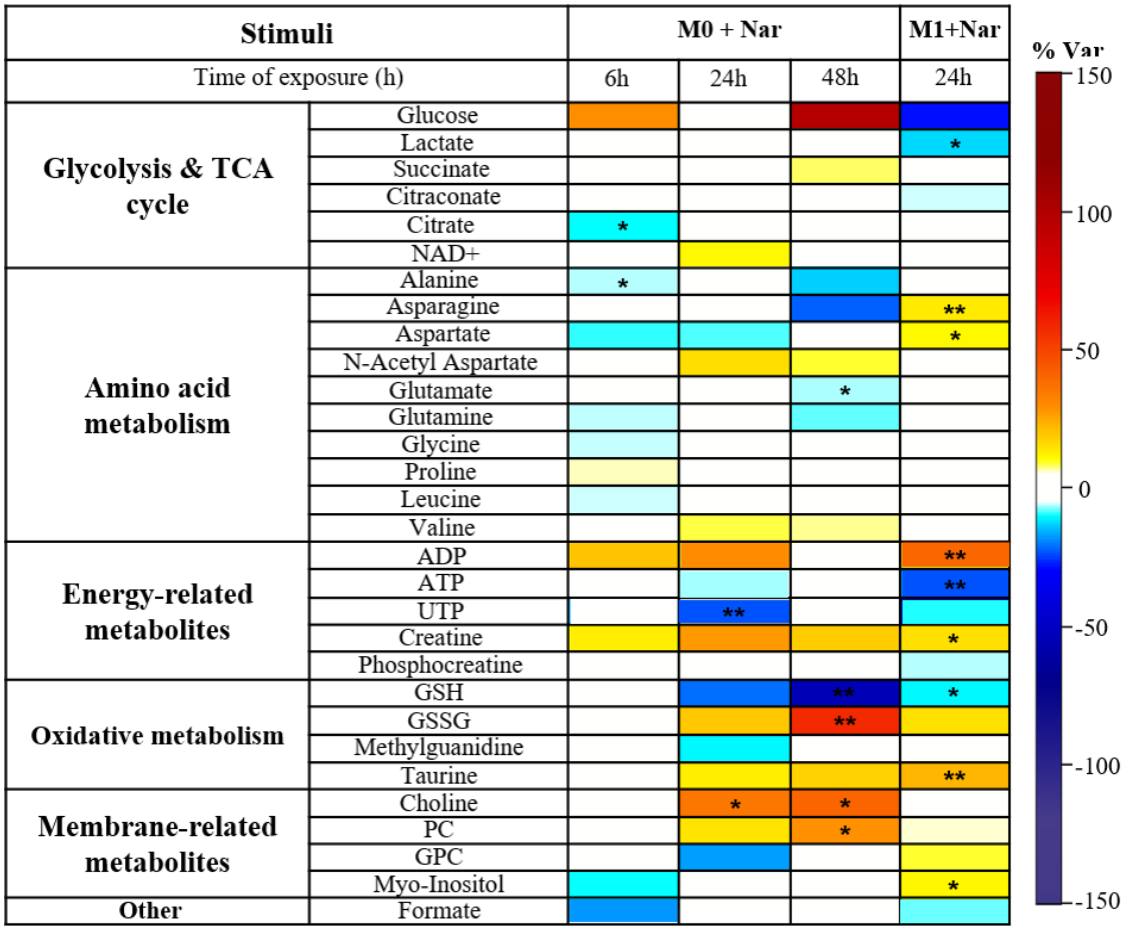

Figure 24: Heatmap of the main metabolite variations in the polar extracts of THP-1 derived macrophages upon treatment with Naringin (200 µM): M0 macrophages incubated with the flavonoid for 6, 24 or 48h; M1 pre-polarized macrophages incubated with the flavonoid for 24h. The color scale represents percentage of variation relative to respective controls (n=6). *p-value < 0.05; **p-value < 0.01.

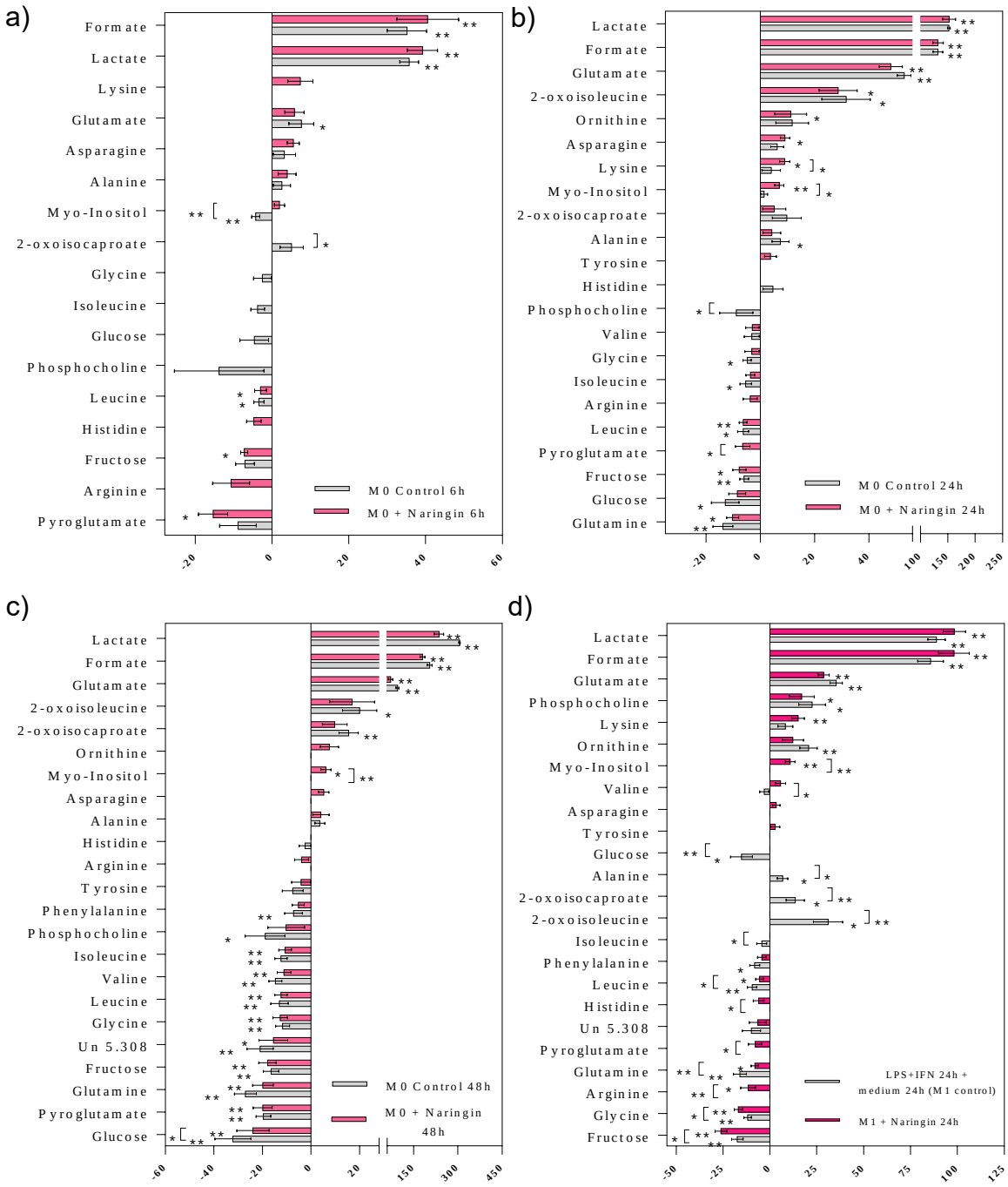

Figure 25: Variations in consumption (negative bars) and excretion (positive bars) of several metabolites in the cell culture supernatant of THP-1 derived macrophages incubated with 200 µM of Naringin: a), b), c) M0 macrophages incubated with Naringin for 6, 24 and 48h, respectively; d) Pre-polarized M1 macrophages incubated with Naringin for 24h. Each Naringin incubation (pink bars) was compared to its respective control (grey bars). Statistical significance of variation was assessed via a t-student test (n=6): *p-value < 0.05; **p-value < 0.01

3.3. Integration and discussion of macrophage metabolic changes

The ^{1}H-NMR metabolomics approach employed in this thesis enabled the detection of multiple changes in the metabolic profile of human THP-1-derived macrophages in response to different stimuli, including treatment with three bioflavonoids (Quercetin, Naringenin and Naringin). This section is now aimed at comparing and discussing those variations in the context of some major metabolic pathways operating in cells.

3.3.1. Effects on glucose uptake and glycolysis

The impact of the different treatments on cells glycolytic activity can be inferred from changes in glucose and lactate levels (Figures 26 and 27, respectively). Glucose consumption increased in both M1 and M2 macrophages, with M2 additionally showing decreased intracellular glucose levels (Figure 26d). Moreover, compared to their respective controls, M1 and M2 macrophages displayed considerably higher levels of intracellular lactate (Figure 27d), and in the case of M2, increased lactate excretion (Figure 27a). These results are consistent with the high glucose uptake and glycolytic activity reported for activated macrophages.[60–63] Interestingly, though, we found no evidence of glycolytic upregulation being more extensive in M1 than in M2 macrophages.

Quercetin treatment lowered glucose consumption in M0 macrophages but was accompanied by a marked increase in intracellular glucose levels (Figures 26b and 26d). Moreover, Quercetin-treated M0 macrophages displayed reduced extracellular and intracellular levels of lactate (Figures 27b and 27d). These alterations suggest that: i) glucose was less taken up by treated cells, ii) its glycolytic conversion into lactate was downregulated, leading to intracellular glucose accumulation. In the case of Quercetin-treated M1 macrophages, glucose uptake was completely inhibited (Figure 26c), which is possibly related to slightly decreased intracellular lactate levels (Figure 27d). Overall, these results are in line with the inhibitory effects of Quercetin towards the glucose transporter GLUT1, reported for different tumor cells.[198]

The effects of Naringenin on glucose uptake and metabolism greatly depended on the initial polarization state of macrophages (M0 or M1). Naringenin-treated M0 macrophages showed a trend for increased glucose consumption and intracellular glucose levels (Figures 26b and 26d), together with increased extracellular and intracellular lactate levels (Figures 27b and 27d). This suggests upregulated glucose uptake and subsequent glycolytic conversion into lactate. On the other hand, when Naringenin was given to pre-polarized M1 macrophages, the main effect appeared to be inhibition of glucose uptake (accompanied by decreased intracellular glucose and lactate levels). Similarly, Naringin also decreases glucose uptake, especially in pre-polarized M1 macrophages (Figure 26c), where decreased intracellular glucose and lactate were also visible (Figures 26d and 27d).

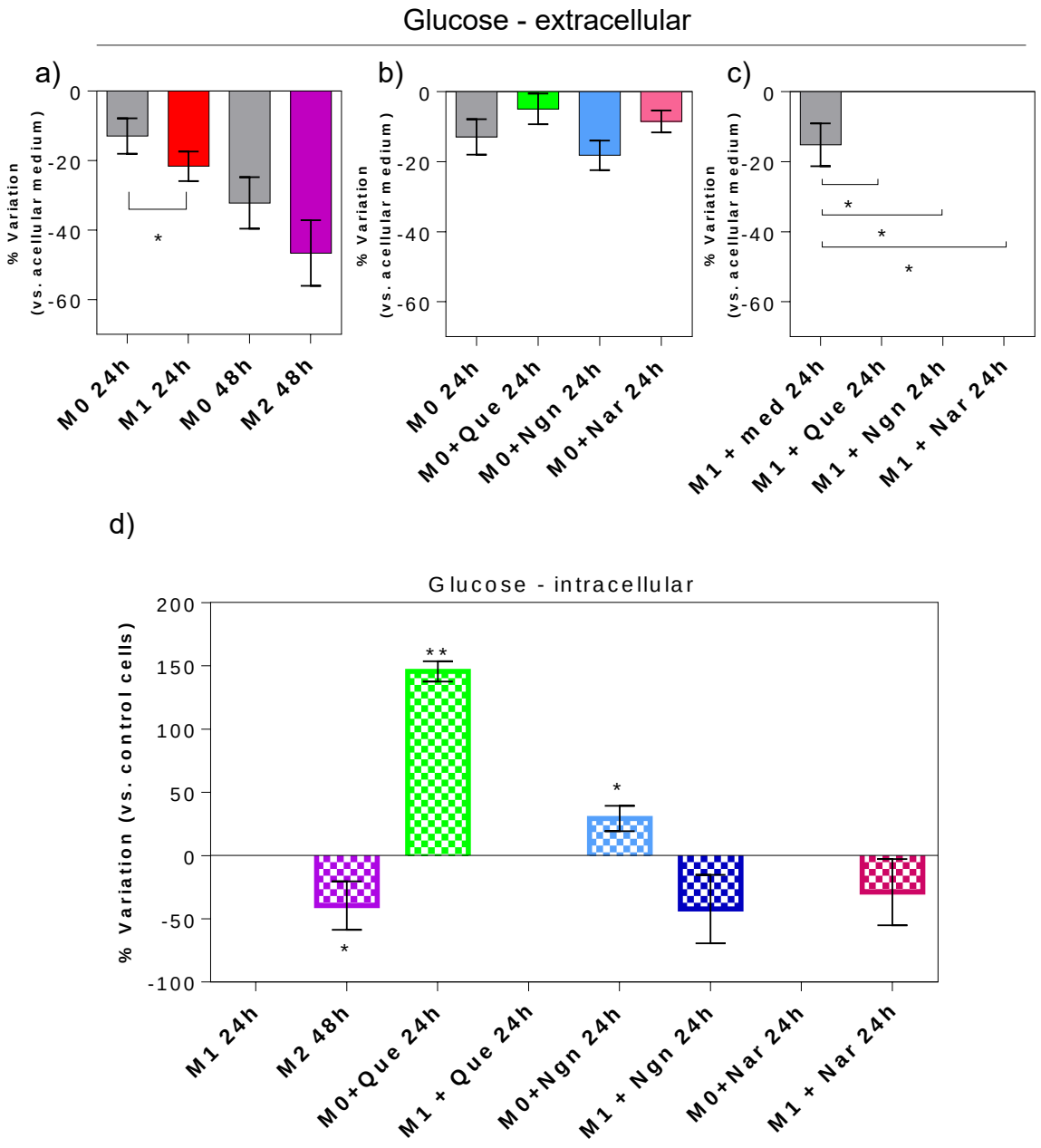

Figure 26: Extracellular (a-c) and intracellular (d) variations of glucose levels in macrophages incubated under different conditions, relative to respective controls (n=6). **p*-value < 0.05; ***p*-value < 0.01.

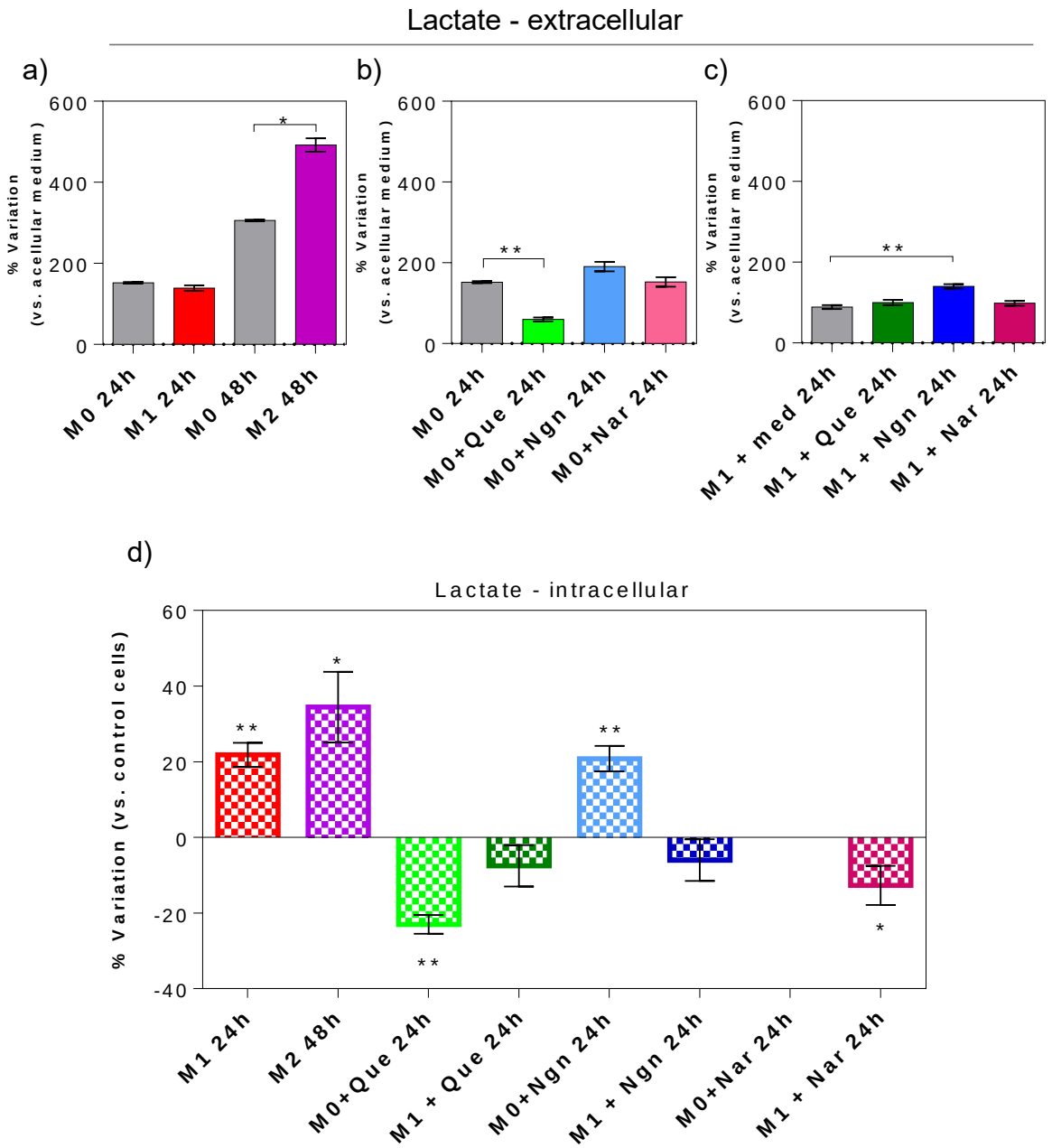

Figure 27: Extracellular (a-c) and intracellular (d) variations of lactate levels in macrophages incubated under different conditions, relative to respective controls (n=6). *p-value < 0.05; **p-value < 0.01.

3.3.2. Effects on the TCA cycle

One of the metabolic effects most commonly reported for different macrophage cells lines when subjected to a pro-inflammatory stimulus consists of increased levels of itaconate and succinate, which have been associated with a truncated TCA cycle.[62] Such increases were indeed verified in the present study upon stimulation of THP-1 derived macrophages with LPS/IFN-γ (Figure 28). Other TCA cycle intermediates that varied in M1 macrophages were citraconate, which is a structural isomer of itaconate,[199] and citrate (decreased in M1 vs. M0 macrophages). In M2 macrophages, neither itaconate nor citraconate levels were altered, but there was a decrease in both citrate and succinate. This is consistent with a functional TCA cycle, corroborating existing evidence that M2 macrophages rely not only on glycolysis, but also on the TCA cycle and oxidative phosphorylation for energy production,[60,62] delineating one of the differences between the metabolic profiles of M1 and M2 macrophages.

Quercetin treatment of M0 macrophages resulted in decreased levels of succinate, which is a TCA cycle intermediate with an established pro-inflammatory role.[97] Hence, attenuation of succinate by Quercetin in both M0 and M1 macrophages could be a good indicator of Quercetin's ability to attenuate macrophage-mediated inflammation. Additionally, Quercetin-treated M0 macrophages showed a huge increase of intracellular citrate, which was not channeled into itaconate production as reported for M1 macrophages.[122,177] Instead, citrate accumulation could possibly reflect its impaired use in fatty acid synthesis,[117] an hypothesis that requires proper testing in the future. In Quercetin-treated M1 macrophages, citrate increased to a lesser extent and itaconate levels were higher compared to M1 control cells (incubated for 24h in fresh medium after LPS/IFN-γ stimulation). Given that itaconate is currently recognized as an anti-inflammatory metabolite,[116,122] this variation corroborates the role of Quercetin in reducing inflammation via metabolic reprogramming.

In Naringenin-treated macrophages, succinate only decreased after M1 pre-polarization (no change in 24h treated M0 macrophages). Moreover, the variations in citrate, citraconate and itaconate were opposite to those observed for Quercetin,

suggesting different modulation of the TCA cycle by those flavonoids. Assessment of TCA cycle enzymes expression by using molecular biology tools would be useful to further understand this difference.

Finally, no significant variations were found for Naringin-treated macrophages regarding TCA cycle metabolites.

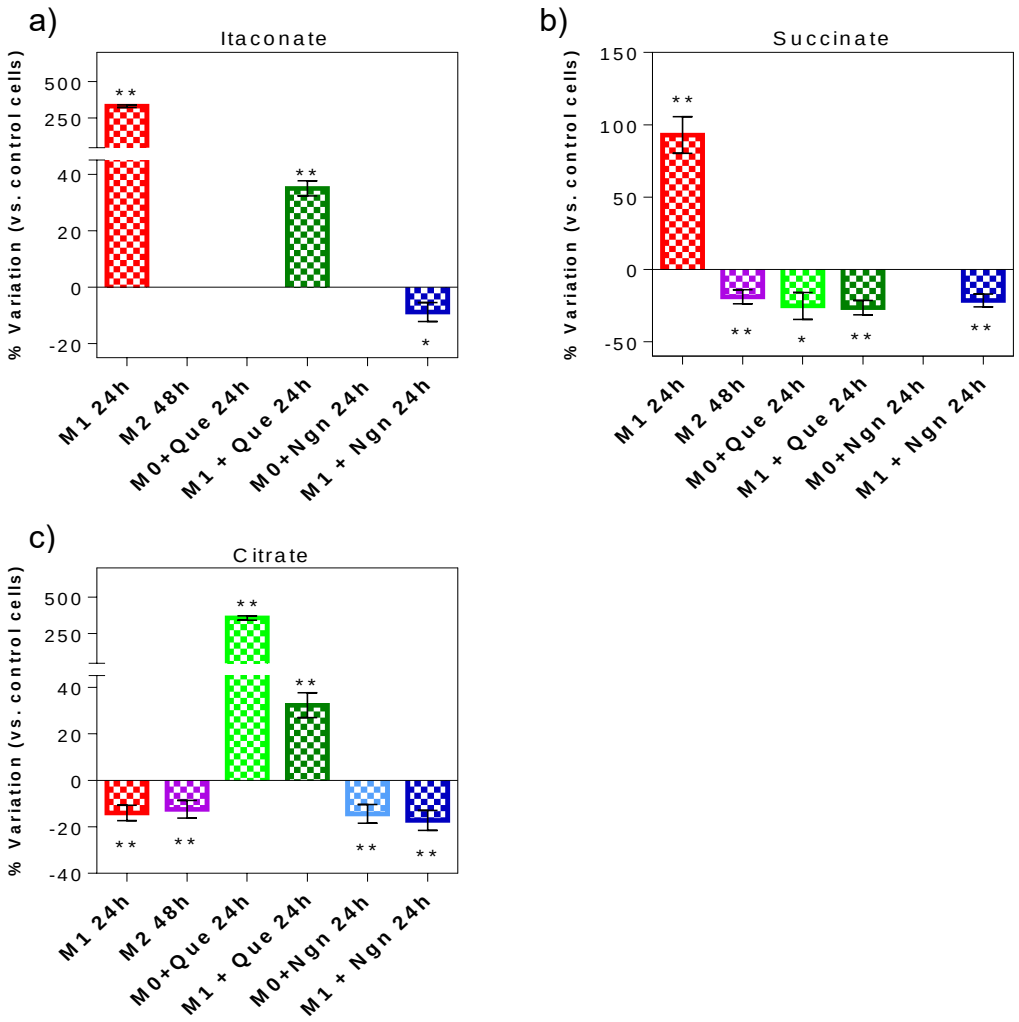

Figure 28: Intracellular variations of metabolites related to the TCA cycle in macrophages incubated under different conditions, relative to respective controls.: a) itaconate; b) succinate and c) citrate (n=6). *p-value < 0.05; **p-value < 0.01.

3.3.3. Effects on amino acid metabolism

Glutamine is another major fuel for macrophages, having been implied in macrophages phagocytic capacity,[200] as well as in M2-polarization.[102] Here, significant changes were observed on intracellular and extracellular levels of glutamine and glutamate, as shown in Figure 29.

Regarding macrophage activation with canonical M1 and M2 stimuli, M2 macrophages displayed considerably higher glutamine consumption and intracellular use (Figure 29 a,d). Glutamate was also decreased intracellularly in M2 macrophages. This could indicate that M2 macrophages took up more glutamine to fuel the TCA cycle through glutaminolysis, where glutamine is converted to glutamate and then to α-ketoglutarate, which has indeed been reported to be an important contributing factor to the alternative activation of macrophages.[62,112]

Quercetin treatment of either M0 or pre-polarized M1 macrophages caused decreased intracellular levels of both glutamine and glutamate (Figure 29 d,e). Although in this case glutamine uptake from the cell culture medium was not increased, these changes could indicate intensification of glutaminolysis, as a means to fuel the TCA cycle.[62] Indeed, this is consistent with the anaplerotic maintenance of this cycle, to cope with reduced glucose uptake and glycolytic conversion found for Quercetin treatment.

Interestingly, contrarily to Quercetin, Naringenin treatment induced higher intracellular levels of glutamate in both M0 and M1 macrophages and of glutamine in treated pre-polarized M1 macrophages (Figure 29 d,e). This suggests that glutaminolysis was not upregulated in Naringenin-treated macrophages. This difference adds up to the distinct TCA cycle modulation found for the two flavonoids.

As for Naringin, it did not cause any significant changes in glutamine metabolism.

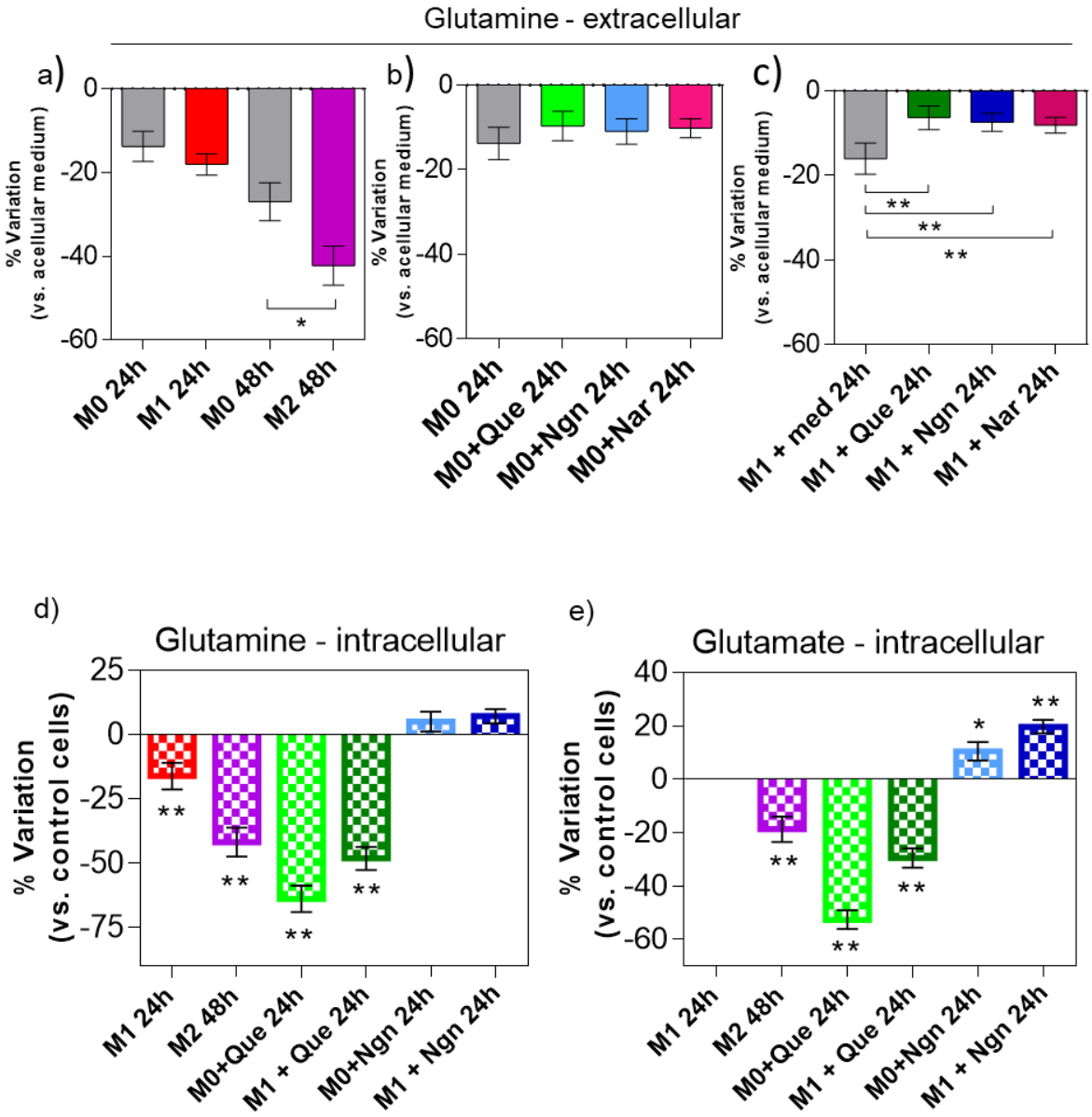

Figure 29: Variations in extracellular glutamine (a-c), intracellular glutamine (d), and intracellular glutamate (e) in macrophages incubated under different conditions, relative to respective controls (n=6). *p-value < 0.05; **p-value < 0.01.

The changes in intracellular levels of other amino acids, found to vary significantly with at least one of the stimuli tested, are shown in Figure 30. Again, M1 and M2 macrophages were found to respond differently in what concerns amino acids composition. In particular, compared to unstimulated macrophages, M1 cells showed decreased levels of branched chain amino acids (which did not vary in M2 macrophages) and of N-acetylaspartate (which significantly increased upon M2 activation). On the other hand, glycine and alanine were higher in M1 macrophages and decreased in M2 cells.

With Quercetin treatment, the levels of most amino acids assessed decreased in both M0 and pre-polarized M1 macrophages. Such variation is consistent with the anaplerotic fueling of the TCA cycle.[102,201] For example, alanine and glycine can be converted into pyruvate, isoleucine into succinyl-CoA or acetyl-CoA, proline into glutamate and then α-ketoglutarate, asparagine and aspartate to oxaloacetate. Interestingly, the variation in aspartate upon Quercetin treatment was dependent on macrophage initial activation, increasing in Quercetin-treated M0 macrophages. This could be associated with the conversion of glutamate and oxaloacetate into α-ketoglutarate to fuel the TCA cycle, with aspartate being the other product in this metabolic reaction.[202] This is consistent with increased glutaminolysis caused by Quercetin treatment, as suggested earlier.

Again, the effects of Naringenin on most amino acids were different to those of Quercetin. Moreover, several variations were dependent on macrophage activation state. For instance, asparagine decreased in Naringenin-treated M0 macrophages but increased in pre-polarized M1 macrophages, whereas an opposite variation was found for glycine and valine.

As for Naringin, it only caused mild variations in a few amino acids (Figure 27).

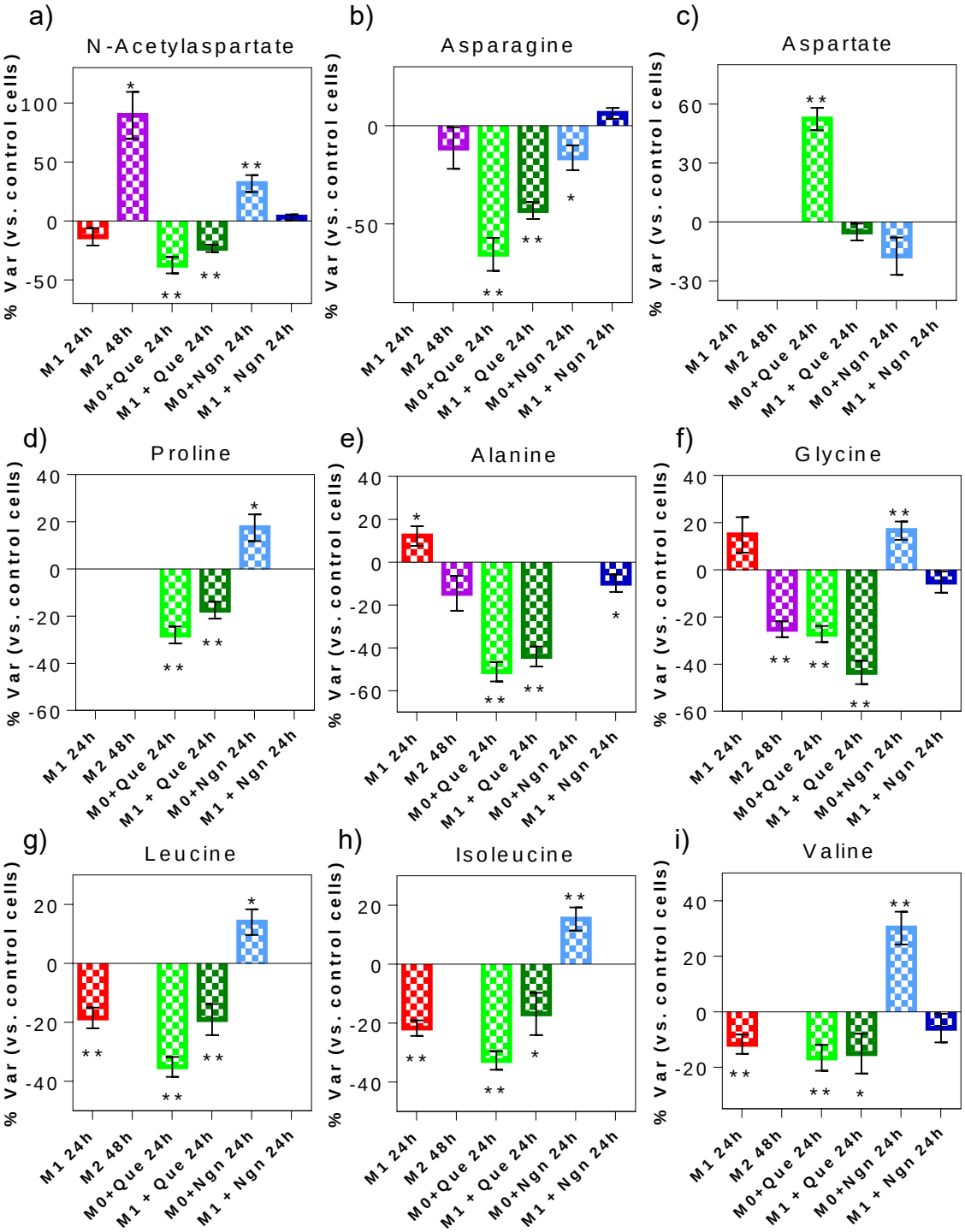

Figure 30: Intracellular variations of some amino acids in macrophages incubated under different conditions, relative to respective controls (n=6). *p-value < 0.05; **p-value < 0.01.

3.3.4. Effects on glutathione metabolism

The reduced form of the tripeptide glutathione (GSH, Glu-Cys-Gly) is an important scavenger of ROS and its ratio to the oxidized form (GSSG) is regarded as a marker of oxidative stress.[203] Figure 31 compiles the variations in GSH and GSSG found in this work. In M1 and M2 cells, GSH and GSSG levels did not vary significantly, and their ratio remained unaltered. Quercetin treatment, however, significantly affected glutathione levels. Compared to respective controls, Quercetin-treated M0 macrophages showed lower GSH and higher GSSG (i.e. decreased GSH:GSSG ratio), which suggests induction of ROS. Indeed, in agreement with inhibited glycolysis and an active TCA cycle, it is possible that Quercetin intensified mitochondrial oxidative metabolism and, consequently, ROS generation. In this scenario, GSH would be extensively converted to GSSG in order to neutralize ROS, an hypothesis which requires further confirmation, e.g. through measurement of oxygen consumption and intracellular ROS.

Interestingly, these changes in Quercetin-treated M0 macrophages were also accompanied by a significant increase in methylguanidine (Figure 21), which is a product of protein catabolism found to inhibit iNOS and hence the production of the pro-inflammatory mediator NO, as well as TNF-α.[204] Therefore, this variation could represent a countermeasure to cope with reactive species and reflect the anti-inflammatory action of Quercetin.

On the other hand, pre-polarized M1 macrophages showed a different response, whereby GSH increased upon Quercetin treatment. Two hypotheses can be drawn. One is that after an expected increase in ROS caused by LPS/IFN,[205] Quercetin could be able to decrease ROS levels, as reported in other studies.[206,207] This would imply a lesser use of GSH, thus explaining its increase compared to control M1 macrophages. The other possibility is that cells increased *de novo* GSH synthesis, which is consistent with decreased levels of two precursor amino acids (glycine and glutamate).[203] Again, further assays are required to verify these hypotheses.

Naringenin treatment also induced a decrease in GSH in M0 macrophages, which could either mean ROS neutralization (as suggested for Quercetin), or

inhibited synthesis, agreeing with the accumulation of precursor amino acids glycine and glutamate.

Regarding the effects of Naringin on glutathione metabolism, the results point to GSH conversion to GSSG, probably to neutralize ROS, as suggested for the other flavonoids.

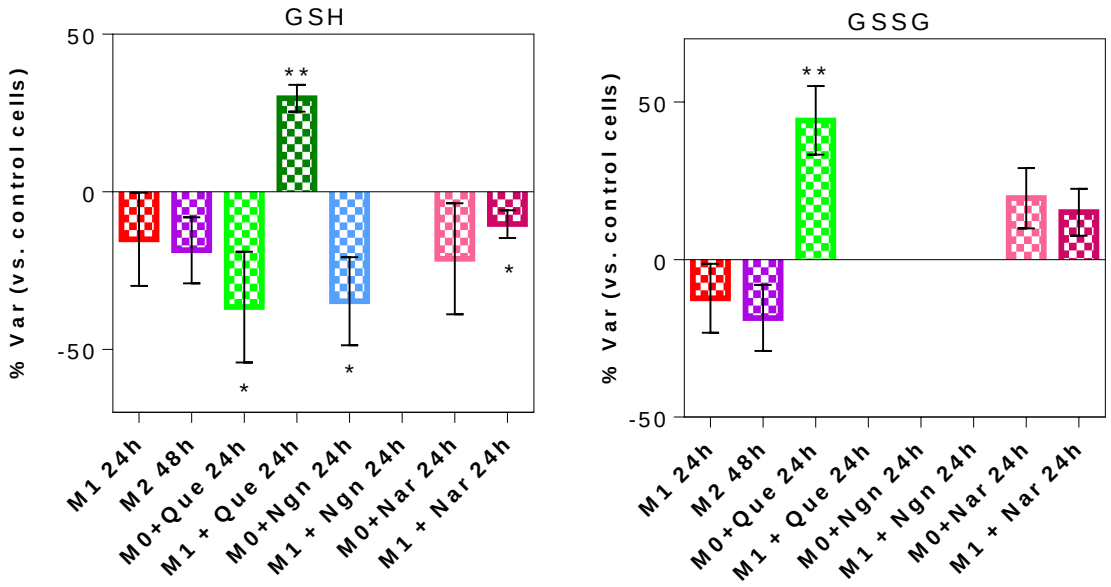

Figure 31: Intracellular variations of GSH and GSSG in macrophages incubated under different conditions, relative to respective controls (n=6). *p-value < 0.05; **p-value < 0.01.

Figure 32 shows an integrated view of the metabolic changes described above.

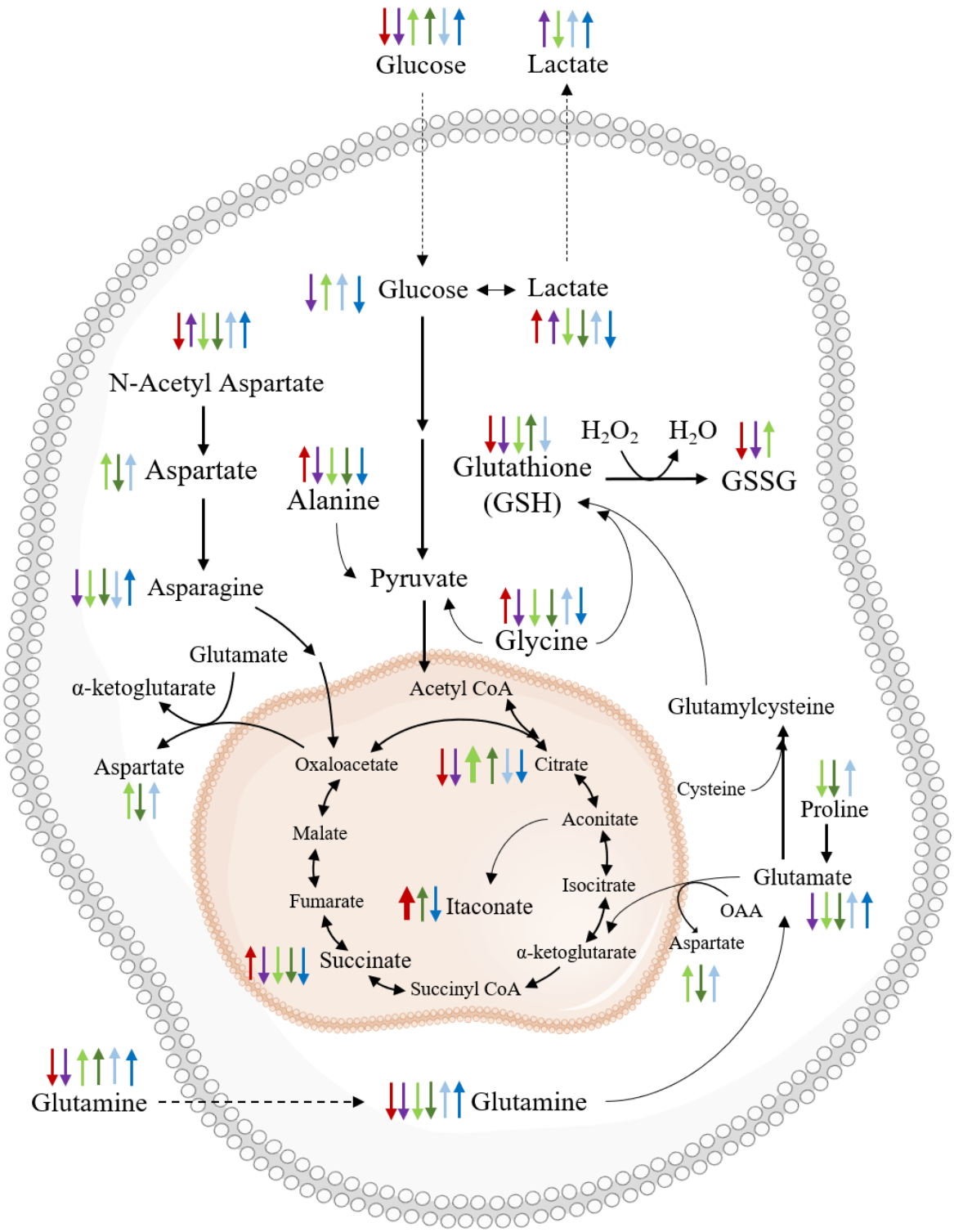

Figure 32: Schematic diagram of main metabolic effects in THP-1 derived macrophages incubated under different conditions: LPS+IFN-γ (red arrows), IL-4+IL-13 (purple arrows), Quercetin (light green arrows), Quercetin on pre-polarized macrophages (dark green arrows), Naringenin (light blue arrows), Naringenin on pre-polarized macrophages (dark blue arrows). Naringin effects not included due to their low magnitude/significance. Thick arrows indicate |% variation| > 300%.

3.3.5. Other metabolic effects

Interestingly, the three flavonoids tested also affected cells energy reserves. In most conditions, ATP decreased and ADP increased, possibly reflecting ATP hydrolysis and the release of free energy to perform cellular work. Exceptions regarded increases in ATP seen in M0 macrophages treated with Quercetin for 6h or with Naringenin for 6/48h. Interestingly, the levels of creatine and phosphocreatine also showed large variations. While phosphocreatine is recognised as an important energy transducer in muscle, heart and brain tissues,[208,209] its role on macrophages is less well established. Still, early works found that monocyte to macrophage differentiation was accompanied by the development of a phosphocreatine pool and that macrophages expressed creatine kinase, the enzyme responsible for the interconversion of these metabolites to replenish ATP in situations of high metabolic demand.[210] In the present study, phosphocreatine decreased upon treatment of pre-polarized M1 macrophages with each flavonoid. Therefore, it would be interesting to assess if the expression and/or activity of creatine kinase are modulated by these compounds.

Finally, there were also noticeable effects on choline-containing compounds, which are associated with the structural components of membranes, namely phosphatidylcholines. Choline and phosphocholine increased in all M0 flavonoid-treated macrophages, while glycerophosphocholine increased in the presence of Quercetin but decrease for the other two flavonoids. In pre-polarized M1 macrophages, the effects on these compounds were more variable.

CHAPTER 4

CONCLUSIONS AND FUTURE PERSPECTIVES

In this thesis, ^{1}H-NMR based metabolomics proved to be a very useful tool for characterizing the metabolic profiles of human THP-1 derived macrophages. Near 50 intracellular metabolites were detected in the cells polar extracts (endometabolome), whereas analysis of cells-conditioned culture medium (exometabolome) was useful to assess the consumption/excretion of several substrates/products. Multivariate analysis and discrete quantitative assessments of metabolic profiles revealed consistent variations upon exposure of macrophages to different stimuli, namely LPS/IFN-γ (M1 polarization), IL-4/IL-13 (M2 polarization) and three flavonoids (Quercetin, Naringenin and Naringin).

As expected, M1 and M2 polarization states were associated with considerably different metabolic profiles. Some of the main differences included changes in TCA cycle intermediates. In particular, M1 macrophages showed marked increases in succinate, citraconate and itaconate, in agreement with the well documented remodeling of this pathway in pro-inflammatory macrophages. On the other hand, M2 macrophages appeared to display increased glutaminolysis and showed decreased levels of succinate, a metabolite currently viewed as an important pro-inflammatory mediator. Also, while M2 macrophages showed unaltered intracellular ATP and increased UTP levels, ATP/UTP energy reserves decreased significantly in M1 macrophages, possibly in association with the predominance of oxidative pathways in M2 cells when compared with M1 macrophages. Furthermore, other less known differences between M1 and M2 cells were revealed, particularly in amino acids (alanine, glycine, N-acetylaspartate) and membrane-related metabolites (choline compounds and myo-inositol). Finally, it should be noted that M1 and M2 macrophages also shared some common features, namely concerning upregulated glucose uptake and glycolysis, and variations in antioxidant metabolites.

The effects of Quercetin, Naringenin and Naringin on macrophage metabolome were, to our knowledge, newly reported in this thesis. These compounds have well known anti-inflammatory activity, as corroborated by our results on cytokine production. Indeed, they attenuated the levels of several pro-inflammatory cytokines in the medium supernatants of treated macrophages. Additionally, Naringenin treatment caused an increase in the anti-inflammatory cytokine CCL17,

suggesting potential pro-resolving activity. At the metabolic level, the three flavonoids produced multiple effects, with the strongest impact being observed for Quercetin and the mildest for Naringin (Figure 33).

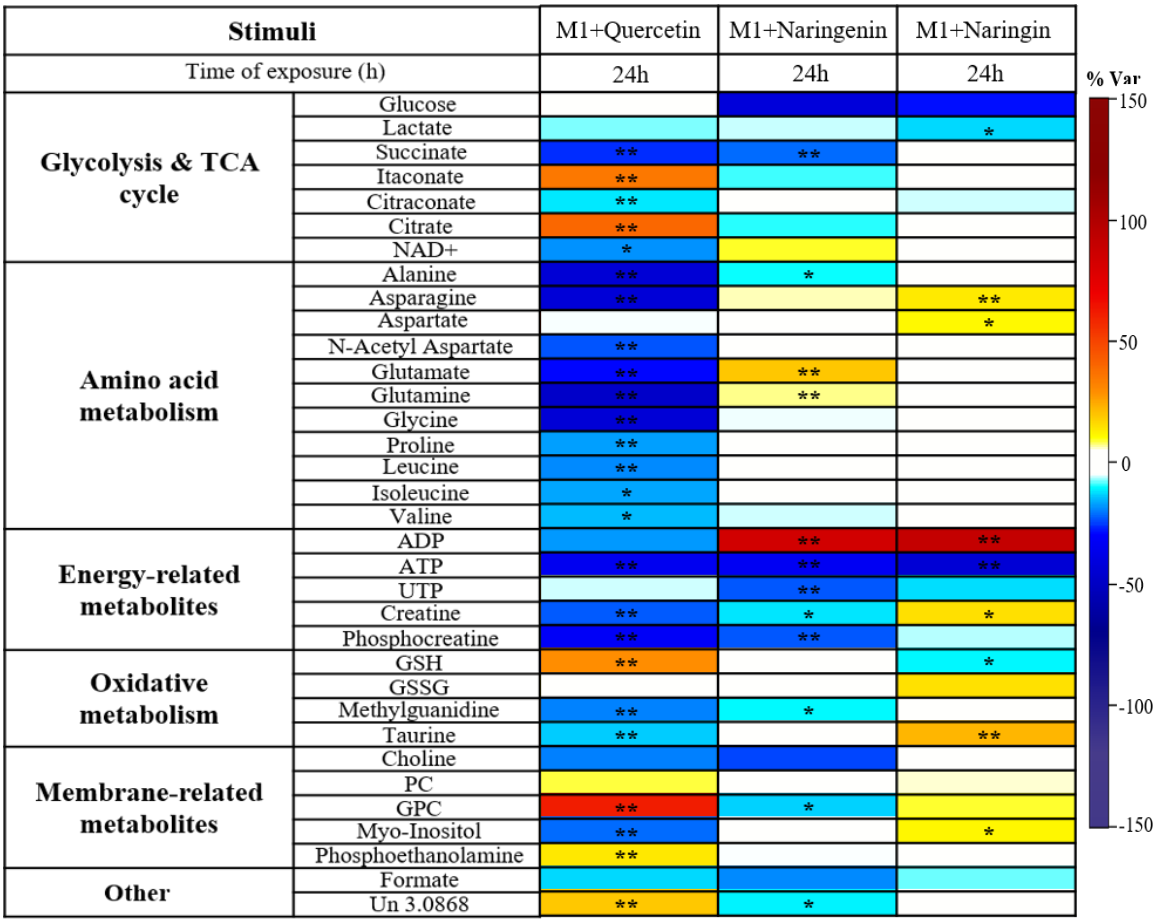

Figure 33: Heatmap of the main metabolite variations in the polar extracts of pre-polarized M1 macrophages upon a 24h treatment with: i) Quercetin (60 µM), ii) Naringenin (100 µM) and ii) Naringin (200 µM). The color scale represents percentage of variation relative to respective controls (M1 + medium) (n=6). *p-value < 0.05; **p-value < 0.01

Quercetin-induced metabolic variations suggested the following main effects: i) downregulation of glucose uptake (and possibly glycolysis); ii) downregulation of the pro-inflammatory TCA cycle metabolite succinate, accompanied, in flavonoid-treated M1 pre-polarized macrophages, by increased production of the anti-inflammatory metabolite itaconate; iii) intensification of anaplerotic reactions (including glutaminolysis) to fuel the TCA cycle; iv) accumulation of citrate, possibly

due to impairment of fatty acid synthesis; v) alteration of cells redox state, found to be highly dependent on macrophage initial polarization state; vi) alteration of energy reserves and involvement of the phosphocreatine - creatine kinase system; vii) membrane modification. Most of these effects were common to all incubation times tested in M0 macrophages (6, 24 and 48h). Still, oscillation in the magnitude of changes, together with a few time-dependent alterations (e.g. seen for aspartate, a vital amino acid in TCA cycle replenishment, and for the energetic molecules ATP and UTP), underscored the dynamic nature of metabolic adaptations.

In the case of Naringenin, metabolic changes appeared to be greatly dependent on both the incubation time and initial macrophage polarization state. Focusing on the 24h incubations, the main Naringenin effects were suggested to be: i) upregulated/downregulated glucose uptake in Naringenin-treated M0/M1 macrophages, respectively; ii) TCA cycle modulation involving decreased citrate levels (contrarily to Quercetin) and, in M1 macrophages, decreased succinate and itaconate levels; iii) very low impact on amino acids in M0 macrophages, and changes in M1 macrophages mostly contrary to those found for Quercetin; iv) antioxidant response; v) alteration in ATP, UTP and phosphocreatine pools, dependent on macrophage initial polarization; vi) membrane modification.

The impact of Naringin on the cells metabolome was much lower than that observed for the other flavonoids. The main effects were suggested to include: i) impaired glucose uptake in Naringin-treated M1 pre-polarized macrophages; ii) antioxidant response (mainly GSH to GSSG conversion); iii) altered pool of energy-related metabolites; iv) membrane modification. TCA cycle and amino acids metabolism appeared to remain practically unaltered. Given the high hydrophilicity of Naringin, it is expectable that this flavonoid is less cell-permeable than the other compounds tested. Indeed, in colorectal adenocarcinoma Caco-2 cells, Naringin showed much lower permeability than Naringenin, and so did other flavonoid glycosides.[211] This lower internalization could justify the less pronounced effects on the intracellular metabolome. Further studies are warranted to evaluate flavonoids uptake.

Overall, this work has shown that, although sharing similar ability to attenuate anti-inflammatory activity of macrophages, the three flavonoids modulate macrophage metabolism in distinct ways, underlying the need for an in depth study of their modes of action. This is especially interesting considering that both Naringenin and Quercetin have been reported to influence some signaling pathways in a similar manner (e.g. activation of AMPK, inhibition of MAPK, inhibition of NF-kB).[161,212] In the future, it would be important to assess the expression and/or activity of key enzymes involved in glycolysis, TCA cycle, glutaminolysis and FA synthesis, to verify the hypotheses generated based on the metabolomics results. Moreover, measurements of oxygen consumption rate, mitochondrial membrane potential and production of reactive oxygen species would nicely complement this work and help to further advance current understanding on flavonoid-mediated modulation of macrophage metabolism. This knowledge is expected to support the development of flavonoids as immunomodulatory drugs, especially aimed at attenuating and/or resolving inflammation, for instance, in the context of chronic inflammatory diseases or the rejection of implantable biomaterials.

REFERENCES

References

1. Varol, C., Mildner, A. & Jung, S. Macrophages: Development and Tissue Specialization. *Annu. Rev. Immunol.* **33,** 643–675 (2015).

2. Fujiwara, N. & Kobayashi, K. Macrophages in inflammation. *Curr. Drug Targets-Inflamm. Allergy* **4,** 281–286 (2005).

3. Epelman, S., Lavine, K. J. & Randolph, G. J. Origin and Functions of Tissue Macrophages. *Immunity* **41,** 21–35 (2014).

4. Koh, T. J. & DiPietro, L. A. Inflammation and wound healing: the role of the macrophage. *Expert Rev. Mol. Med.* **13,** (2011).

5. Mosser, D. M. & Edwards, J. P. Exploring the full spectrum of macrophage activation. *Nat. Rev. Immunol.* **8,** 958–969 (2008).

6. Elliott, M. R. & Ravichandran, K. S. The Dynamics of Apoptotic Cell Clearance. *Dev. Cell* **38,** 147–160 (2016).

7. Neumann, H., Kotter, M. R. & Franklin, R. J. M. Debris clearance by microglia: an essential link between degeneration and regeneration. *Brain* **132,** 288–295 (2008).

8. Koziel, J., Maciag-Gudowska, A., Mikolajczyk, T., Bzowska, M., Sturdevant, D. E., Whitney, A. R., Shaw, L. N., DeLeo, F. R. & Potempa, J. Phagocytosis of Staphylococcus aureus by Macrophages Exerts Cytoprotective Effects Manifested by the Upregulation of Antiapoptotic Factors. *PLoS ONE* **4,** (2009).

9. Davies, L. C., Jenkins, S. J., Allen, J. E. & Taylor, P. R. Tissue-resident macrophages. *Nat. Immunol.* **14,** 986–995 (2013).

10. Arango Duque, G. & Descoteaux, A. Macrophage Cytokines: Involvement in Immunity and Infectious Diseases. *Front. Immunol.* **5,** (2014).

11. Raggi, F., Pelassa, S., Pierobon, D., Penco, F., Gattorno, M., Novelli, F., Eva, A., Varesio, L., Giovarelli, M. & Bosco, M. C. Regulation of Human

Macrophage M1–M2 Polarization Balance by Hypoxia and the Triggering Receptor Expressed on Myeloid Cells-1. *Front. Immunol.* **8,** (2017).

12. Tarique, A. A., Logan, J., Thomas, E., Holt, P. G., Sly, P. D. & Fantino, E. Phenotypic, Functional, and Plasticity Features of Classical and Alternatively Activated Human Macrophages. *Am. J. Respir. Cell Mol. Biol.* **53,** 676–688 (2015).

13. Wynn, T. A. & Vannella, K. M. Macrophages in Tissue Repair, Regeneration, and Fibrosis. *Immunity* **44,** 450–462 (2016).

14. Mantovani, A., Sica, A., Sozzani, S., Allavena, P., Vecchi, A. & Locati, M. The chemokine system in diverse forms of macrophage activation and polarization. *Trends Immunol.* **25,** 677–686 (2004).

15. Meshkani, R. & Vakili, S. Tissue resident macrophages: Key players in the pathogenesis of type 2 diabetes and its complications. *Clin. Chim. Acta* **462,** 77–89 (2016).

16. Rőszer, T. Understanding the Mysterious M2 Macrophage through Activation Markers and Effector Mechanisms. *Mediators Inflamm.* **2015,** 1–16 (2015).

17. Ferrante, C. J. & Leibovich, S. J. Regulation of Macrophage Polarization and Wound Healing. *Adv. Wound Care* **1,** 10–16 (2012).

18. Li, Q. & Cherayil, B. J. Role of Toll-Like Receptor 4 in Macrophage Activation and Tolerance during Salmonella enterica Serovar Typhimurium Infection. *Infect. Immun.* **71,** 4873–4882 (2003).

19. Du, X., Poltorak, A., and Silva, M. & Beutler, B. Analysis of Tlr4-Mediated LPS Signal Transduction in Macrophages by Mutational Modification of the Receptor. *Blood Cells. Mol. Dis.* **25,** 328–38 (2000).

20. Xie, C., Liu, C., Wu, B., Lin, Y., Ma, T., Xiong, H., Wang, Q., Li, Z., Ma, C. & Tu, Z. Effects of IRF1 and IFN-β interaction on the M1 polarization of macrophages and its antitumor function. *Int. J. Mol. Med.* **38,** 148–160 (2016).

21. Genin, M., Clement, F., Fattaccioli, A., Raes, M. & Michiels, C. M1 and M2 macrophages derived from THP-1 cells differentially modulate the response of cancer cells to etoposide. *BMC Cancer* **15,** (2015).

22. Chimal-Ramírez, G. K., Espinoza-Sánchez, N. A., Chávez-Sánchez, L., Arriaga-Pizano, L. & Fuentes-Pananá, E. M. Monocyte Differentiation towards Protumor Activity Does Not Correlate with M1 or M2 Phenotypes. *J. Immunol. Res.* **2016,** 1–16 (2016).

23. Littlefield, M. J. Polarization of Human THP-1 Macrophages: Link between Adenosine Receptors, Inflammation and Lipid Accumulation. *Int. J. Immunol. Immunother.* **1,** (2014).

24. Vasandan, A. B., Jahnavi, S., Shashank, C., Prasad, P., Kumar, A. & Prasanna, S. J. Human Mesenchymal stem cells program macrophage plasticity by altering their metabolic status via a PGE2-dependent mechanism. *Sci. Rep.* **6,** 38308 (2016).

25. Zhang, F., Liu, H., Jiang, G., Wang, H., Wang, X., Wang, H., Fang, R., Cai, S. & Du, J. Changes in the proteomic profile during the differential polarization status of the human monocyte-derived macrophage THP-1 cell line. *Proteomics* **15,** 773–786 (2015).

26. Tang, L., Zhang, H., Wang, C., Li, H., Zhang, Q. & Bai, J. M2A and M2C Macrophage Subsets Ameliorate Inflammation and Fibroproliferation in Acute Lung Injury Through Interleukin 10 Pathway: *SHOCK* **48,** 119–129 (2017).

27. Heller, N. M., Qi, X., Junttila, I. S., Shirey, K. A., Vogel, S. N., Paul, W. E. & Keegan, A. D. Type I IL-4Rs Selectively Activate IRS-2 to Induce Target Gene Expression in Macrophages. *Sci. Signal.* **1,** ra17–ra17 (2008).

28. Obiri, N. I., Debinski, W., Leonard, W. J. & Puri, R. K. Receptor for Interleukin 13 interaction with interleukin 4 by a mechanism that does not involve the common chain shared by receptors for interleukins 2, 4, 7, 9, and 15. *J. Biol. Chem.* **270,** 8797–8804 (1995).

29. Minty, A., Chalon, P., Derocq, J.-M., Dumont, X., Guillemot, J.-C., Kaghad, M., Labit, C., Leplatois, P., Liauzun, P., Miloux, B., Minty, C., Casellas, P., Loison, G., Lupker, J., Shire, D., Ferrara, P. & Caput, D. Interleukin-13 is a new human lymphokine regulating inflammatory and immune responses. *Nature* **362,** 248–250 (1993).

30. Zhang, M.-Z., Wang, X., Wang, Y., Niu, A., Wang, S., Zou, C. & Harris, R. C. IL-4/IL-13–mediated polarization of renal macrophages/dendritic cells to an M2a phenotype is essential for recovery from acute kidney injury. *Kidney Int.* **91,** 375–386 (2017).

31. Multhoff, G., Molls, M. & Radons, J. Chronic Inflammation in Cancer Development. *Front. Immunol.* **2,** (2012).

32. Kinne, R. W., Bräuer, R., Stuhlmüller, B., Palombo-Kinne, E. & Burmester, G.-R. Macrophages in rheumatoid arthritis. *Arthritis Res. Ther.* **2,** 189 (2000).

33. Vogel, D. Y., Vereyken, E. J., Glim, J. E., Heijnen, P. D., Moeton, M., van der Valk, P., Amor, S., Teunissen, C. E., van Horssen, J. & Dijkstra, C. D. Macrophages in inflammatory multiple sclerosis lesions have an intermediate activation status. *J. Neuroinflammation* **10,** 809 (2013).

34. Anderson, J. M., Rodriguez, A. & Chang, D. T. Foreign body reaction to biomaterials. in *Semin. Immunol.* **20,** 86–100 (2008).

35. Momiyama, Y., Ishizaka, N., Adachi, H., Saita, E. & Fairweather, D. Inflammation, Atherosclerosis and Coronary Artery Disease. C*lin Med Insights Cardiol*. **8,** 67-70 (2016)

36. Klopfleisch, R. Macrophage reaction against biomaterials in the mouse model – Phenotypes, functions and markers. *Acta Biomater.* **43,** 3–13 (2016).

37. Barros, M. H. M., Hauck, F., Dreyer, J. H., Kempkes, B. & Niedobitek, G. Macrophage Polarisation: an Immunohistochemical Approach for Identifying M1 and M2 Macrophages. *PLoS ONE* **8,** e80908 (2013).

38. Duluc, D., Delneste, Y., Tan, F., Moles, M.-P., Grimaud, L., Lenoir, J., Preisser, L., Anegon, I., Catala, L., Ifrah, N., Descamps, P., Gamelin, E., Gascan, H., Hebbar, M. & Jeannin, P. Tumor-associated leukemia inhibitory factor and IL-6 skew monocyte differentiation into tumor-associated macrophage-like cells. *Blood* **110,** 4319–4330 (2007).

39. Ying, W., Cheruku, P. S., Bazer, F. W., Safe, S. H. & Zhou, B. Investigation of Macrophage Polarization Using Bone Marrow Derived Macrophages. *J. Vis. Exp.* **76,** (2013)

40. Jablonski, K. A., Amici, S. A., Webb, L. M., Ruiz-Rosado, J. de D., Popovich, P. G., Partida-Sanchez, S. & Guerau-de-Arellano, M. Novel Markers to Delineate Murine M1 and M2 Macrophages. *PLOS ONE* **10,** e0145342 (2015).

41. Guo, F. H., De Raeve, H. R., Rice, T. W., Stuehr, D. J., Thunnissen, F. B. & Erzurum, S. C. Continuous nitric oxide synthesis by inducible nitric oxide synthase in normal human airway epithelium in vivo. *Proc. Natl. Acad. Sci.* **92,** 7809–7813 (1995).

42. Mestas, J. & Hughes, C. C. W. Of Mice and Not Men: Differences between Mouse and Human Immunology. *J. Immunol.* **172,** 2731–2738 (2004).

43. Thomas, A. C. & Mattila, J. T. “Of Mice and Men”: Arginine Metabolism in Macrophages. *Front. Immunol.* **5,** (2014).

44. Martinez, F. O., Gordon, S., Locati, M. & Mantovani, A. Transcriptional Profiling of the Human Monocyte-to-Macrophage Differentiation and Polarization: New Molecules and Patterns of Gene Expression. *J. Immunol.* **177,** 7303–7311 (2006).

45. Raes, G., Van den Bergh, R., De Baetselier, P., Ghassabeh, G. H., Scotton, C., Locati, M., Mantovani, A. & Sozzani, S. Arginase-1 and Ym1 Are Markers for Murine, but Not Human, Alternatively Activated Myeloid Cells. *J. Immunol.* **174,** 6561–6562 (2005).

46. Ohashi, T., Aoki, M., Tomita, H., Akazawa, T., Sato, K., Kuze, B., Mizuta, K., Hara, A., Nagaoka, H., Inoue, N. & Ito, Y. M2-like macrophage polarization in high lactic acid-producing head and neck cancer. *Cancer Sci.* **108,** 1128–1134 (2017).

47. Singla, D. K., Wang, J. & Singla, R. Primary human monocytes differentiate into M2 macrophages and involve Notch-1 pathway. *Can. J. Physiol. Pharmacol.* **95,** 288–294 (2017).

48. Makita, N., Hizukuri, Y., Yamashiro, K., Murakawa, M. & Hayashi, Y. IL-10 enhances the phenotype of M2 macrophages induced by IL-4 and confers the ability to increase eosinophil migration. *Int. Immunol.* **27,** 131–141 (2015).

49. Lisi, L., Ciotti, G. M. P., Braun, D., Kalinin, S., Currò, D., Dello Russo, C., Coli, A., Mangiola, A., Anile, C., Feinstein, D. L. & Navarra, P. Expression of iNOS, CD163 and ARG-1 taken as M1 and M2 markers of microglial polarization in human glioblastoma and the surrounding normal parenchyma. *Neurosci. Lett.* **645,** 106–112 (2017).

50. Daigneault, M., Preston, J. A., Marriott, H. M., Whyte, M. K. B. & Dockrell, D. H. The Identification of Markers of Macrophage Differentiation in PMA-Stimulated THP-1 Cells and Monocyte-Derived Macrophages. *PLoS ONE* **5,** (2010).

51. Schutte, R. J., Parisi-Amon, A. & Reichert, W. M. Cytokine profiling using monocytes/macrophages cultured on common biomaterials with a range of surface chemistries. *J. Biomed. Mater. Res. A* **88A,** 128–139 (2009).

52. Edwards, J. P., Zhang, X., Frauwirth, K. A. & Mosser, D. M. Biochemical and functional characterization of three activated macrophage populations. *J. Leukoc. Biol.* **80,** 1298–1307 (2006).

53. Song, E., Ouyang, N., Hörbelt, M., Antus, B., Wang, M. & Exton, M. S. Influence of Alternatively and Classically Activated Macrophages on Fibrogenic Activities of Human Fibroblasts. *Cell. Immunol.* **204,** 19–28 (2000).

54. Sellon, R. K., Tonkonogy, S., Schultz, M., Dieleman, L. A., Grenther, W., Balish, E. D., Rennick, D. M. & Sartor, R. B. Resident enteric bacteria are necessary for development of spontaneous colitis and immune system activation in interleukin-10-deficient mice. *Infect. Immun.* **66,** 5224–5231 (1998).

55. Ejrnaes, M., Filippi, C. M., Martinic, M. M., Ling, E. M., Togher, L. M., Crotty, S. & von Herrath, M. G. Resolution of a chronic viral infection after interleukin-10 receptor blockade. *J. Exp. Med.* **203,** 2461–2472 (2006).

56. Xuan, W., Qu, Q., Zheng, B., Xiong, S. & Fan, G.-H. The chemotaxis of M1 and M2 macrophages is regulated by different chemokines. *J. Leukoc. Biol.* **97,** 61–69 (2015).

57. Vogel, D. Y., Heijnen, P. D., Breur, M., de Vries, H. E., Tool, A. T., Amor, S. & Dijkstra, C. D. Macrophages migrate in an activation-dependent manner to chemokines involved in neuroinflammation. *J. Neuroinflammation* **11,** 23 (2014).

58. Owen, J. L. & Mohamadzadeh, M. Macrophages and chemokines as mediators of angiogenesis. *Front. Physiol.* **4,** (2013).

59. Watanabe, K., Jose, P. J. & Rankin, S. M. Eotaxin-2 Generation Is Differentially Regulated by Lipopolysaccharide and IL-4 in Monocytes and Macrophages. *J. Immunol.* **168,** 1911–1918 (2002).

60. Langston, P. K., Shibata, M. & Horng, T. Metabolism Supports Macrophage Activation. *Front. Immunol.* **8,** (2017).

61. Mills, E. L. & O'Neill, L. A. Reprogramming mitochondrial metabolism in macrophages as an anti-inflammatory signal: HIGHLIGHTS. *Eur. J. Immunol.* **46,** 13–21 (2016).

62. Van den Bossche, J., O'Neill, L. A. & Menon, D. Macrophage Immunometabolism: Where Are We (Going)? *Trends Immunol.* **38,** 395–406 (2017).

63. Gleeson, L. E. & Sheedy, F. J. Metabolic reprogramming & inflammation: Fuelling the host response to pathogens. *Semin. Immunol.* **28,** 450–468 (2016).

64. Suzuki, H., Hisamatsu, T., Chiba, S., Mori, K., Kitazume, M. T., Shimamura, K., Nakamoto, N., Matsuoka, K., Ebinuma, H., Naganuma, M. & Kanai, T. Glycolytic pathway affects differentiation of human monocytes to regulatory macrophages. *Immunol. Lett.* **176,** 18–27 (2016).

65. Tan, Z., Xie, N., Cui, H., Moellering, D. R., Abraham, E., Thannickal, V. J. & Liu, G. Pyruvate Dehydrogenase Kinase 1 Participates in Macrophage Polarization via Regulating Glucose Metabolism. *J. Immunol.* **194,** 6082–6089 (2015).

66. Rodriguez, P. C., Zea, A. H., DeSalvo, J., Culotta, K. S., Zabaleta, J., Quiceno, D. G., Ochoa, J. B. & Ochoa, A. C. L-Arginine Consumption by Macrophages Modulates the Expression of CD3 Chain in T Lymphocytes. *J. Immunol.* **171,** 1232–1239 (2003).

67. Sanman, L. E., Qian, Y., Eisele, N. A., Ng, T. M., van der Linden, W. A., Monack, D. M., Weerapana, E. & Bogyo, M. Disruption of glycolytic flux is a signal for inflammasome signaling and pyroptotic cell death. *Elife* **5,** e13663 (2016).

68. Haschemi, A., Kosma, P., Gille, L., Evans, C. R., Burant, C. F., Starkl, P., Knapp, B., Haas, R., Schmid, J. A., Jandl, C., Amir, S., Lubec, G., Park, J., Esterbauer, H., Bilban, M., Brizuela, L., Pospisilik, J. A., Otterbein, L. E. & Wagner, O. The Sedoheptulose Kinase CARKL Directs Macrophage Polarization through Control of Glucose Metabolism. *Cell Metab.* **15,** 813–826 (2012).

69. Chan, K. L., Pillon, N. J., Sivaloganathan, D. M., Costford, S. R., Liu, Z., Théret, M., Chazaud, B. & Klip, A. Palmitoleate Reverses High Fat-induced Proinflammatory Macrophage Polarization via AMP-activated Protein Kinase (AMPK). *J. Biol. Chem.* **290,** 16979–16988 (2015).

70. Namgaladze, D. & Brüne, B. Macrophage fatty acid oxidation and its roles in macrophage polarization and fatty acid-induced inflammation. *Biochim. Biophys. Acta BBA - Mol. Cell Biol. Lipids* **1861,** 1796–1807 (2016).

71. Namgaladze, D. & Brüne, B. Fatty acid oxidation is dispensable for human macrophage IL-4-induced polarization. *Biochim. Biophys. Acta BBA - Mol. Cell Biol. Lipids* **1841,** 1329–1335 (2014).

72. O'Neill, L. A. J., Kishton, R. J. & Rathmell, J. A guide to immunometabolism for immunologists. *Nat. Rev. Immunol.* **16,** 553–565 (2016).

73. Berg, J. M., Tymoczko, J. L. & Stryer, L. Amino Acids Are Made from Intermediates of the Citric Acid Cycle and Other Major Pathways. (2002). at <https://www.ncbi.nlm.nih.gov/books/NBK22459/>

74. Chen, N., LaCrue, A. N., Teuscher, F., Waters, N. C., Gatton, M. L., Kyle, D. E. & Cheng, Q. Fatty Acid Synthesis and Pyruvate Metabolism Pathways Remain Active in Dihydroartemisinin-Induced Dormant Ring Stages of Plasmodium falciparum. *Antimicrob. Agents Chemother.* **58,** 4773–4781 (2014).

75. Yamashita, A., Zhao, Y., Matsuura, Y., Yamasaki, K., Moriguchi-Goto, S., Sugita, C., Iwakiri, T., Okuyama, N., Koshimoto, C., Kawai, K., Tamaki, N., Zhao, S., Kuge, Y. & Asada, Y. Increased Metabolite Levels of Glycolysis and Pentose Phosphate Pathway in Rabbit Atherosclerotic Arteries and Hypoxic Macrophage. *PLoS ONE* **9,** e86426 (2014).

76. Gleeson, L. E., Sheedy, F. J., Palsson-McDermott, E. M., Triglia, D., O'Leary, S. M., O'Sullivan, M. P., O'Neill, L. A. J. & Keane, J. Cutting Edge: Mycobacterium tuberculosis Induces Aerobic Glycolysis in Human Alveolar Macrophages That Is Required for Control of Intracellular Bacillary Replication. *J. Immunol.* **196,** 2444–2449 (2016).

77. Liu, L., Lu, Y., Martinez, J., Bi, Y., Lian, G., Wang, T., Milasta, S., Wang, J., Yang, M., Liu, G., Green, D. R. & Wang, R. Proinflammatory signal suppresses

proliferation and shifts macrophage metabolism from Myc-dependent to HIF1 **α** -dependent. *Proc. Natl. Acad. Sci.* **113,** 1564–1569 (2016).

78. Van den Bossche, J., Baardman, J., Otto, N. A., van der Velden, S., Neele, A. E., van den Berg, S. M., Luque-Martin, R., Chen, H.-J., Boshuizen, M. C. S., Ahmed, M., Hoeksema, M. A., de Vos, A. F. & de Winther, M. P. J. Mitochondrial Dysfunction Prevents Repolarization of Inflammatory Macrophages. *Cell Rep.* **17,** 684–696 (2016).

79. Venter, G., Oerlemans, F. T. J. J., Wijers, M., Willemse, M., Fransen, J. A. M. & Wieringa, B. Glucose Controls Morphodynamics of LPS-Stimulated Macrophages. *PLoS ONE* **9,** e96786 (2014).

80. Zhao, Q., Chu, Z., Zhu, L., Yang, T., Wang, P., Liu, F., Huang, Y., Zhang, F., Zhang, X., Ding, W. & Zhao, Y. 2-Deoxy-d-Glucose Treatment Decreases Anti-inflammatory M2 Macrophage Polarization in Mice with Tumor and Allergic Airway Inflammation. *Front. Immunol.* **8,** (2017).

81. Chiba, S., Hisamatsu, T., Suzuki, H., Mori, K., Kitazume, M. T., Shimamura, K., Mizuno, S., Nakamoto, N., Matsuoka, K., Naganuma, M. & Kanai, T. Glycolysis regulates LPS-induced cytokine production in M2 polarized human macrophages. *Immunol. Lett.* **183,** 17–23 (2017).

82. Xie, N., Cui, H., Ge, J., Banerjee, S., Guo, S., Dubey, S., Abraham, E., Liu, R.-M. & Liu, G. Metabolic characterization and RNA profiling reveal glycolytic dependence of pro-fibrotic phenotype of alveolar macrophages in lung fibrosis. *Am. J. Physiol. - Lung Cell. Mol. Physiol.* **313**, L834-L844 (2017)

83. Li, C., Ding, X. Y., Xiang, D. M., Xu, J., Huang, X. L., Hou, F. F. & Zhou, Q. G. Enhanced M1 and Impaired M2 Macrophage Polarization and Reduced Mitochondrial Biogenesis via Inhibition of AMP Kinase in Chronic Kidney Disease. *Cell. Physiol. Biochem.* **36,** 358–372 (2015).

84. Wolf, A. J., Reyes, C. N., Liang, W., Becker, C., Shimada, K., Wheeler, M. L., Cho, H. C., Popescu, N. I., Coggeshall, K. M., Arditi, M. & Underhill, D. M.

Hexokinase Is an Innate Immune Receptor for the Detection of Bacterial Peptidoglycan. *Cell* **166,** 624–636 (2016).

85. Jo, E.-K., Kim, J. K., Shin, D.-M. & Sasakawa, C. Molecular mechanisms regulating NLRP3 inflammasome activation. *Cell. Mol. Immunol.* **13,** 148–159 (2016).

86. Xie, M., Yu, Y., Kang, R., Zhu, S., Yang, L., Zeng, L., Sun, X., Yang, M., Billiar, T. R., Wang, H., Cao, L., Jiang, J. & Tang, D. PKM2-dependent glycolysis promotes NLRP3 and AIM2 inflammasome activation. *Nat. Commun.* **7,** 13280 (2016).

87. Palsson-McDermott, E. M., Curtis, A. M., Goel, G., Lauterbach, M. A., Sheedy, F. J., Gleeson, L. E., van den Bosch, M. W., Quinn, S. R., Domingo-Fernandez, R., Johnson, D. G., Jiang, J., Israelsen, W. J., Keane, J., Thomas, C., Clish, C., Heiden, M. V., Xavier, R. J. & O'Neill, L. A. J. Pyruvate Kinase M2 regulates Hif-1α activity and IL-1β induction, and is a critical determinant of the Warburg Effect in LPS-activated macrophages. *Cell Metab.* **21,** 65–80 (2015).

88. Alves-Filho, J. C. & Pålsson-McDermott, E. M. Pyruvate Kinase M2: A Potential Target for Regulating Inflammation. *Front. Immunol.* **7,** (2016).

89. Bae, S., Kim, H., Lee, N., Won, C., Kim, H.-R., Hwang, Y., Song, Y. W., Kang, J. S. & Lee, W. J. α-Enolase Expressed on the Surfaces of Monocytes and Macrophages Induces Robust Synovial Inflammation in Rheumatoid Arthritis. *J. Immunol.* **189,** 365–372 (2012).

90. Millet, P., Vachharajani, V., McPhail, L., Yoza, B. & McCall, C. GAPDH Binding to TNF-α mRNA Contributes to Post-Transcriptional Repression in Monocytes: A Novel Mechanism of Communication between Inflammation and Metabolism. *J. Immunol. Baltim. Md 1950* **196,** 2541–2551 (2016).

91. Guha, M. & Mackman, N. The PI3K-Akt pathway limits LPS activation of signaling pathways and expression of inflammatory mediators in human monocytic cells. *J. Biol. Chem.* **277** (2002).

92. Everts, B., Amiel, E., Huang, S. C.-C., Smith, A. M., Chang, C.-H., Lam, W. Y., Redmann, V., Freitas, T. C., Blagih, J., van der Windt, G. J. W., Artyomov, M. N., Jones, R. G., Pearce, E. L. & Pearce, E. J. TLR-driven early glycolytic reprogramming via the kinases TBK1-IKKε supports the anabolic demands of dendritic cell activation. *Nat. Immunol.* **15,** 323–332 (2014).

93. Byles, V., Covarrubias, A. J., Ben-Sahra, I., Lamming, D. W., Sabatini, D. M., Manning, B. D. & Horng, T. The TSC-mTOR pathway regulates macrophage polarization. *Nat. Commun.* **4,** (2013).

94. Covarrubias, A. J., Aksoylar, H. I., Yu, J., Snyder, N. W., Worth, A. J., Iyer, S. S., Wang, J., Ben-Sahra, I., Byles, V. & Polynne-Stapornkul, T. Akt-mTORC1 signaling regulates Acly to integrate metabolic input to control of macrophage activation. *Elife* **5,** e11612 (2016).

95. Huang, S. C.-C., Smith, A. M., Everts, B., Colonna, M., Pearce, E. L., Schilling, J. D. & Pearce, E. J. Metabolic Reprogramming Mediated by the mTORC2-IRF4 Signaling Axis Is Essential for Macrophage Alternative Activation. *Immunity* **45,** 817–830 (2016).

96. Ham, M., Lee, J.-W., Choi, A. H., Jang, H., Choi, G., Park, J., Kozuka, C., Sears, D. D., Masuzaki, H. & Kim, J. B. Macrophage Glucose-6-Phosphate Dehydrogenase Stimulates Proinflammatory Responses with Oxidative Stress. *Mol. Cell. Biol.* **33,** 2425–2435 (2013).

97. Jl, C. & A, B. The M1/M2 Pattern and the Oxidative Stress are Modulated by Low- Level Laser in Human Macrophage. *J. Clin. Cell. Immunol.* **07,** (2016).

98. Zhang, Y., Choksi, S., Chen, K., Pobezinskaya, Y., Linnoila, I. & Liu, Z.-G. ROS play a critical role in the differentiation of alternatively activated

macrophages and the occurrence of tumor-associated macrophages. *Cell Res.* **23,** 898–914 (2013).

99. Tannahill, G. M., Curtis, A. M., Adamik, J., Palsson-McDermott, E. M., McGettrick, A. F., Goel, G., Frezza, C., Bernard, N. J., Kelly, B., Foley, N. H., Zheng, L., Gardet, A., Tong, Z., Jany, S. S., Corr, S. C., Haneklaus, M., Caffrey, B. E., Pierce, K., Walmsley, S., Beasley, F. C., Cummins, E., Nizet, V., Whyte, M., Taylor, C. T., Lin, H., Masters, S. L., Gottlieb, E., Kelly, V. P., Clish, C., Auron, P. E., Xavier, R. J. & O'Neill, L. A. J. Succinate is an inflammatory signal that induces IL-1β through HIF-1α. *Nature* **496,** 238–242 (2013).

100. Mills, E. L., Kelly, B., Logan, A., Costa, A. S. H., Varma, M., Bryant, C. E., Tourlomousis, P., Däbritz, J. H. M., Gottlieb, E., Latorre, I., Corr, S. C., McManus, G., Ryan, D., Jacobs, H. T., Szibor, M., Xavier, R. J., Braun, T., Frezza, C., Murphy, M. P. & O'Neill, L. A. Succinate Dehydrogenase Supports Metabolic Repurposing of Mitochondria to Drive Inflammatory Macrophages. *Cell* **167,** 457-470 (2016).

101. Baseler, W. A., Davies, L. C., Quigley, L., Ridnour, L. A., Weiss, J. M., Hussain, S. P., Wink, D. A. & McVicar, D. W. Autocrine IL-10 functions as a rheostat for M1 macrophage glycolytic commitment by tuning nitric oxide production. *Redox Biol.* **10,** 12–23 (2016).

102. Jha, A. K., Huang, S. C.-C., Sergushichev, A., Lampropoulou, V., Ivanova, Y., Loginicheva, E., Chmielewski, K., Stewart, K. M., Ashall, J., Everts, B., Pearce, E. J., Driggers, E. M. & Artyomov, M. N. Network Integration of Parallel Metabolic and Transcriptional Data Reveals Metabolic Modules that Regulate Macrophage Polarization. *Immunity* **42,** 419–430 (2015).

103. England, R. M., Masiá, E., Giménez, V., Lucas, R. & Vicent, M. J. Polyacetal-stilbene conjugates — The first examples of polymer therapeutics for the inhibition of HIF-1 in the treatment of solid tumours. *J. Controlled Release* **164,** 314–322 (2012).

104. Selak, M. A., Armour, S. M., MacKenzie, E. D., Boulahbel, H., Watson, D. G., Mansfield, K. D., Pan, Y., Simon, M. C., Thompson, C. B. & Gottlieb, E. Succinate links TCA cycle dysfunction to oncogenesis by inhibiting HIF-α prolyl hydroxylase. *Cancer Cell* **7,** 77–85 (2005).

105. Ohh, M., Park, C. W., Ivan, M., Hoffman, M. A., Kim, T.-Y., Huang, L. E., Pavletich, N., Chau, V. & Kaelin, W. G. Ubiquitination of hypoxia-inducible factor requires direct binding to the β-domain of the von Hippel–Lindau protein. *Nat. Cell Biol.* **2,** 423–427 (2000).

106. Koivunen, P., Hirsilä, M., Remes, A. M., Hassinen, I. E., Kivirikko, K. I. & Myllyharju, J. Inhibition of Hypoxia-inducible Factor (HIF) Hydroxylases by Citric Acid Cycle Intermediates: possible links between cell metabolism and stabilization of HIF. *J. Biol. Chem.* **282,** 4524–4532 (2007).

107. Braverman, J., Sogi, K. M., Benjamin, D., Nomura, D. K. & Stanley, S. A. HIF-1α Is an Essential Mediator of IFN-γ–Dependent Immunity to *Mycobacterium tuberculosis*. *J. Immunol.* **197,** 1287–1297 (2016).

108. Papandreou, I., Cairns, R. A., Fontana, L., Lim, A. L. & Denko, N. C. HIF-1 mediates adaptation to hypoxia by actively downregulating mitochondrial oxygen consumption. *Cell Metab.* **3,** 187–197 (2006).

109. Quinlan, C. L., Orr, A. L., Perevoshchikova, I. V., Treberg, J. R., Ackrell, B. A. & Brand, M. D. Mitochondrial Complex II Can Generate Reactive Oxygen Species at High Rates in Both the Forward and Reverse Reactions. *J. Biol. Chem.* **287,** 27255–27264 (2012).

110. Garaude, J., Acín-Pérez, R., Martínez-Cano, S., Enamorado, M., Ugolini, M., Nistal-Villán, E., Hervás-Stubbs, S., Pelegrín, P., Sander, L. E., Enríquez, J. A. & Sancho, D. Mitochondrial respiratory-chain adaptations in macrophages contribute to antibacterial host defense. *Nat. Immunol.* **17,** 1037–1045 (2016).

111. Kelly, B., Tannahill, G. M., Murphy, M. P. & O'Neill, L. A. J. Metformin Inhibits the Production of Reactive Oxygen Species from NADH:Ubiquinone

Oxidoreductase to Limit Induction of Interleukin-1β (IL-1β) and Boosts Interleukin-10 (IL-10) in Lipopolysaccharide (LPS)-activated Macrophages. *J. Biol. Chem.* **290,** 20348–20359 (2015).

112. Liu, P.-S., Wang, H., Li, X., Chao, T., Teav, T., Christen, S., Di Conza, G., Cheng, W.-C., Chou, C.-H., Vavakova, M., Muret, C., Debackere, K., Mazzone, M., Huang, H.-D., Fendt, S.-M., Ivanisevic, J. & Ho, P.-C. α-ketoglutarate orchestrates macrophage activation through metabolic and epigenetic reprogramming. *Nat. Immunol.* **18,** 985-994. (2017).

113. Arts, R. J. W., Novakovic, B., ter Horst, R., Carvalho, A., Bekkering, S., Lachmandas, E., Rodrigues, F., Silvestre, R., Cheng, S.-C., Wang, S.-Y., Habibi, E., Gonçalves, L. G., Mesquita, I., Cunha, C., van Laarhoven, A., van de Veerdonk, F. L., Williams, D. L., van der Meer, J. W. M., Logie, C., O'Neill, L. A., Dinarello, C. A., Riksen, N. P., van Crevel, R., Clish, C., Notebaart, R. A., Joosten, L. A. B., Stunnenberg, H. G., Xavier, R. J. & Netea, M. G. Glutaminolysis and Fumarate Accumulation Integrate Immunometabolic and Epigenetic Programs in Trained Immunity. *Cell Metab.* **24,** 807–819 (2016).

114. Qualls, J. E., Subramanian, C., Rafi, W., Smith, A. M., Balouzian, L., DeFreitas, A. A., Shirey, K. A., Reutterer, B., Kernbauer, E., Stockinger, S., Decker, T., Miyairi, I., Vogel, S. N., Salgame, P., Rock, C. O. & Murray, P. J. Sustained Generation of Nitric Oxide and Control of Mycobacterial Infection Requires Argininosuccinate Synthase 1. *Cell Host Microbe* **12,** 313–323 (2012).

115. Munder, M., Eichmann, K., Morán, J. M., Centeno, F., Soler, G. & Modolell, M. Th1/Th2-regulated expression of arginase isoforms in murine macrophages and dendritic cells. *J. Immunol.* **163,** 3771–3777 (1999).

116. Lampropoulou, V., Sergushichev, A., Bambouskova, M., Nair, S., Vincent, E. E., Loginicheva, E., Cervantes-Barragan, L., Ma, X., Huang, S. C.-C., Griss, T., Weinheimer, C. J., Khader, S., Randolph, G. J., Pearce, E. J., Jones, R. G., Diwan, A., Diamond, M. S. & Artyomov, M. N. Itaconate Links Inhibition of

Succinate Dehydrogenase with Macrophage Metabolic Remodeling and Regulation of Inflammation. *Cell Metab.* **24,** 158–166 (2016).

117. Infantino, V., Convertini, P., Cucci, L., Panaro, M. A., Di Noia, M. A., Calvello, R., Palmieri, F. & Iacobazzi, V. The mitochondrial citrate carrier: a new player in inflammation. *Biochem. J.* **438,** 433–436 (2011).

118. Ashbrook, M. J., McDonough, K. L., Pituch, J. J., Christopherson, P. L., Cornell, T. T., Selewski, D. T., Shanley, T. P. & Blatt, N. B. Citrate modulates lipopolysaccharide-induced monocyte inflammatory responses: Citrate modulates monocyte inflammatory responses. *Clin. Exp. Immunol.* **180,** 520–530 (2015).

119. Infantino, V., Iacobazzi, V., Palmieri, F. & Menga, A. ATP-citrate lyase is essential for macrophage inflammatory response. *Biochem. Biophys. Res. Commun.* **440,** 105–111 (2013).

120. Tallam, A., Perumal, T. M., Antony, P. M., Jäger, C., Fritz, J. V., Vallar, L., Balling, R., del Sol, A. & Michelucci, A. Gene Regulatory Network Inference of Immunoresponsive Gene 1 (IRG1) Identifies Interferon Regulatory Factor 1 (IRF1) as Its Transcriptional Regulator in Mammalian Macrophages. *PLOS ONE* **11,** e0149050 (2016).

121. Michelucci, A., Cordes, T., Ghelfi, J., Pailot, A., Reiling, N., Goldmann, O., Binz, T., Wegner, A., Tallam, A., Rausell, A., Buttini, M., Linster, C. L., Medina, E., Balling, R. & Hiller, K. Immune-responsive gene 1 protein links metabolism to immunity by catalyzing itaconic acid production. *Proc. Natl. Acad. Sci.* **110,** 7820–7825 (2013).

122. Cordes, T., Wallace, M., Michelucci, A., Divakaruni, A. S., Sapcariu, S. C., Sousa, C., Koseki, H., Cabrales, P., Murphy, A. N., Hiller, K. & Metallo, C. M. Immunoresponsive Gene 1 and Itaconate Inhibit Succinate Dehydrogenase to Modulate Intracellular Succinate Levels. *J. Biol. Chem.* **291,** 14274–14284 (2016).

123. Mills, E. L., Ryan, D. G., Prag, H. A., Dikovskaya, D., Menon, D., Zaslona, Z., Jedrychowski, M. P., Costa, A. S. H., Higgins, M., Hams, E., Szpyt, J., Runtsch, M. C., King, M. S., McGouran, J. F., Fischer, R., Kessler, B. M., McGettrick, A. F., Hughes, M. M., Carroll, R. G., Booty, L. M., Knatko, E. V., Meakin, P. J., Ashford, M. L. J., Modis, L. K., Brunori, G., Sévin, D. C., Fallon, P. G., Caldwell, S. T., Kunji, E. R. S., Chouchani, E. T., Frezza, C., Dinkova-Kostova, A. T., Hartley, R. C., Murphy, M. P. & O'Neill, L. A. Itaconate is an anti-inflammatory metabolite that activates Nrf2 via alkylation of KEAP1. *Nature* **556,** 113–117 (2018).

124. Gonzalez-Hurtado, E., Lee, J., Choi, J., Selen Alpergin, E. S., Collins, S. L., Horton, M. R. & Wolfgang, M. J. Loss of macrophage fatty acid oxidation does not potentiate systemic metabolic dysfunction. *Am. J. Physiol.-Endocrinol. Metab.* **312,** E381–E393 (2017).

125. Moon, J.-S., Nakahira, K. & Choi, A. M. K. Fatty acid synthesis and NLRP3-inflammasome. *Oncotarget* **6,** 21765–21766 (2015).

126. Moon, J.-S., Nakahira, K., Chung, K.-P., DeNicola, G. M., Koo, M. J., Pabón, M. A., Rooney, K. T., Yoon, J.-H., Ryter, S. W., Stout-Delgado, H. & Choi, A. M. K. NOX4-dependent fatty acid oxidation promotes NLRP3 inflammasome activation in macrophages. *Nat. Med.* **22,** 1002–1012 (2016).

127. Yu, T., Tutwiler, V. J. & Spiller, K. in *Biomater. Regen. Med. Immune Syst.* (ed. Santambrogio, L.) 17–34 (Springer International Publishing, 2015).

128. Jantan, I., Ahmad, W. & Bukhari, S. N. A. Plant-derived immunomodulators: an insight on their preclinical evaluation and clinical trials. *Front. Plant Sci.* **6,** (2015).

129. Serafini, M., Peluso, I. & Raguzzini, A. Flavonoids as anti-inflammatory agents. *Proc. Nutr. Soc.* **69,** 273–278 (2010).

130. Narayana, K. R., Reddy, M. S., Chaluvadi, M. R. & Krishna, D. R. Bioflavonoids classification, pharmacological and therapeutic potential. *Indian J. Pharmacol.* **33,** 2–16 (2001).

131. Zeinali, M., Rezaee, S. A. & Hosseinzadeh, H. An overview on immunoregulatory and anti-inflammatory properties of chrysin and flavonoids substances. *Biomed. Pharmacother.* **92,** 998–1009 (2017).

132. Wang, T., Li, Q. & Bi, K. Bioactive flavonoids in medicinal plants: Structure, activity and biological fate. *Asian J. Pharm. Sci.* **13,** 12–23 (2018).

133. Annapurna, A., Reddy, C. S., Akondi, R. B. & Rao, S. R. C. Cardioprotective actions of two bioflavonoids, quercetin and rutin, in experimental myocardial infarction in both normal and streptozotocin-induced type I diabetic rats. *J. Pharm. Pharmacol.* **61,** 1365–1374 (2009).

134. Xiao, J. Dietary Flavonoid Aglycones and Their Glycosides: Which Show Better Biological Significance? *Crit. Rev. Food Sci. Nutr.* **7,** 1874-1905 (2015).

135. Panche, A. N., Diwan, A. D. & Chandra, S. R. Flavonoids: an overview. *J. Nutr. Sci.* **5,** (2016).

136. Li, Y., Yao, J., Han, C., Yang, J., Chaudhry, M., Wang, S., Liu, H. & Yin, Y. Quercetin, Inflammation and Immunity. *Nutrients* **8,** 167 (2016).

137. Chen, A. Y. & Chen, Y. C. A review of the dietary flavonoid, kaempferol on human health and cancer chemoprevention. *Food Chem.* **138,** 2099–2107 (2013).

138. Semwal, D., Semwal, R., Combrinck, S. & Viljoen, A. Myricetin: A Dietary Molecule with Diverse Biological Activities. *Nutrients* **8,** 90 (2016).

139. Nair, M. P., Mahajan, S., Reynolds, J. L., Aalinkeel, R., Nair, H., Schwartz, S. A. & Kandaswami, C. The Flavonoid Quercetin Inhibits Proinflammatory Cytokine (Tumor Necrosis Factor Alpha) Gene Expression in Normal

Peripheral Blood Mononuclear Cells via Modulation of the NF- System. *Clin. Vaccine Immunol.* **13,** 319–328 (2006).

140. Alam, M. A., Subhan, N., Rahman, M. M., Uddin, S. J., Reza, H. M. & Sarker, S. D. Effect of Citrus Flavonoids, Naringin and Naringenin, on Metabolic Syndrome and Their Mechanisms of Action. *Adv. Nutr.* **5,** 404–417 (2014).

141. Parhiz, H., Roohbakhsh, A., Soltani, F., Rezaee, R. & Iranshahi, M. Antioxidant and Anti-Inflammatory Properties of the Citrus Flavonoids Hesperidin and Hesperetin: An Updated Review of their Molecular Mechanisms and Experimental Models: Hesperidin and hesperetin as antioxidant and anti-inflammatory agents. *Phytother. Res.* **29,** 323–331 (2015).

142. Durga, M & Nathiya, S & Devasena, Thiyagarajan. (2014). Immunomodulatory and antioxidant actions of dietary flavonoids. *International Journal of Pharmacy and Pharmaceutical Sciences*. **6,** 50-56 (2014)

143. Lu, H., Wu, L., Liu, L., Ruan, Q., Zhang, X., Hong, W., Wu, S., Jin, G. & Bai, Y. Quercetin ameliorates kidney injury and fibrosis by modulating M1/M2 macrophage polarization. *Biochem. Pharmacol.* **154,** 203–212 (2018).

144. Lee, G. H., Lee, S. J., Jeong, S. W., Kim, H.-C., Choi, J. H. & Lee, S. G. Inhibitory Effects of an Antioxidant Coating on a Polylactic Acid Film on Inflammatory Cytokines from Macrophage. *Polym. Korea* **39,** 934 (2015).

145. Lee, H. N., Shin, S. A., Choo, G. S., Kim, H. J., Park, Y. S., Kim, B. S., Kim, S. K., Cho, S. D., Nam, J. S., Choi, C. S., Che, J. H., Park, B. K. & Jung, J. Y. Anti-inflammatory effect of quercetin and galangin in LPS-stimulated RAW264.7 macrophages and DNCB-induced atopic dermatitis animal models. *Int. J. Mol. Med.* (2017).

146. Cui, S., Wu, Q., Wang, J., Li, M., Qian, J. & Li, S. Quercetin inhibits LPS-induced macrophage migration by suppressing the iNOS/FAK/paxillin pathway and modulating the cytoskeleton. *Cell Adhes. Migr.* 1–12 (2018).

147. Qureshi, A. A., Tan, X., Reis, J. C., Badr, M. Z., Papasian, C. J., Morrison, D. C. & Qureshi, N. Inhibition of nitric oxide in LPS-stimulated macrophages of young and senescent mice by δ-tocotrienol and quercetin. *Lipids Health Dis.* **10,** 239 (2011).

148. Cho, Y.-J. & Kim, S.-J. Effect of quercetin on the production of nitric oxide in murine macrophages stimulated with lipopolysaccharide from *Prevotella intermedia*. *J. Periodontal Implant Sci.* **43,** 191 (2013).

149. Raso, G. M., Meli, R., Di Carlo, G., Pacilio, M. & Di Carlo, R. Inhibition of inducible nitric oxide synthase and cyclooxygenase-2 expression by flavonoids in macrophage J774A.1. *Life Sci.* **68,** 921–931 (2001).

150. Rao Manjeet K., B. Ghosh. Quercetin inhibits LPS-induced nitric oxide and tumor necrosis factor-α production in murine macrophages. International Journal of Immunopharmacology. 21, 435-443 (1999).

151. Zhang, X., Wang, G., Gurley, E. C. & Zhou, H. Flavonoid Apigenin Inhibits Lipopolysaccharide-Induced Inflammatory Response through Multiple Mechanisms in Macrophages. *PLoS ONE* **9,** e107072 (2014).

152. Liu, Y., Su, W.-W., Wang, S. & Li, P.-B. Naringin inhibits chemokine production in an LPS-induced RAW 264.7 macrophage cell line. *Mol. Med. Rep.* **6,** 1343–1350 (2012).

153. Gil, M., Kim, Y. K., Hong, S. B. & Lee, K. J. Naringin Decreases TNF-α and HMGB1 Release from LPS-Stimulated Macrophages and Improves Survival in a CLP-Induced Sepsis Mice. *PLOS ONE* **11,** e0164186 (2016).

154. Li, X., Jin, Q., Yao, Q., Xu, B., Li, L., Zhang, S. & Tu, C. The Flavonoid Quercetin Ameliorates Liver Inflammation and Fibrosis by Regulating Hepatic Macrophages Activation and Polarization in Mice. *Front. Pharmacol.* **9,** (2018).

155. Karuppagounder, V., Arumugam, S., Thandavarayan, R. A., Sreedhar, R., Giridharan, V. V., Pitchaimani, V., Afrin, R., Harima, M., Krishnamurthy, P., Suzuki, K., Nakamura, M., Ueno, K. & Watanabe, K. Naringenin ameliorates

skin inflammation and accelerates phenotypic reprogramming from M1 to M2 macrophage polarization in atopic dermatitis NC/Nga mouse model. *Exp. Dermatol.* **25,** 404–407 (2016).

156. Geeraerts, X., Bolli, E., Fendt, S.-M. & Van Ginderachter, J. A. Macrophage Metabolism As Therapeutic Target for Cancer, Atherosclerosis, and Obesity. *Front. Immunol.* **8,** (2017).

157. Saenz, J., Santa-María, C., Reyes-Quiroz, M. E., Geniz, I., Jiménez, J., Sobrino, F. & Alba, G. Grapefruit Flavonoid Naringenin Regulates the Expression of LXRα in THP-1 Macrophages by Modulating AMP-Activated Protein Kinase. *Mol. Pharm.* **15,** 1735–1745 (2018).

158. Endale, M., Park, S.-C., Kim, S., Kim, S.-H., Yang, Y., Cho, J. Y. & Rhee, M. H. Quercetin disrupts tyrosine-phosphorylated phosphatidylinositol 3-kinase and myeloid differentiation factor-88 association, and inhibits MAPK/AP-1 and IKK/NF-κB-induced inflammatory mediators production in RAW 264.7 cells. *Immunobiology* **218,** 1452–1467 (2013).

159. Dong, X., Lan, W., Yin, X., Yang, C., Wang, W. & Ni, J. Simultaneous Determination and Pharmacokinetic Study of Quercetin, Luteolin, and Apigenin in Rat Plasma after Oral Administration of *Matricaria chamomilla* L. Extract by HPLC-UV. *Evid. Based Complement. Alternat. Med.* **2017,** 1–7 (2017).

160. Zhou, K., Cheng, R., Liu, B., Wang, L., Xie, H. & Zhang, C. Eupatilin ameliorates dextran sulphate sodium-induced colitis in mice partly through promoting AMPK activation. *Phytomedicine* **46,** 46–56 (2018).

161. Liu, X., Wang, N., Fan, S., Zheng, X., Yang, Y., Zhu, Y., Lu, Y., Chen, Q., Zhou, H. & Zheng, J. The citrus flavonoid naringenin confers protection in a murine endotoxaemia model through AMPK-ATF3-dependent negative regulation of the TLR4 signalling pathway. *Sci. Rep.* **6,** (2016).

162. Srivastava, R. A. K., Pinkosky, S. L., Filippov, S., Hanselman, J. C., Cramer, C. T. & Newton, R. S. AMP-activated protein kinase: an emerging drug target to regulate imbalances in lipid and carbohydrate metabolism to treat cardio-metabolic diseases: Thematic Review Series: New Lipid and Lipoprotein Targets for the Treatment of Cardiometabolic Diseases. *J. Lipid Res.* **53,** 2490–2514 (2012).

163. O'Neill, H. M., Holloway, G. P. & Steinberg, G. R. AMPK regulation of fatty acid metabolism and mitochondrial biogenesis: Implications for obesity. *Mol. Cell. Endocrinol.* **366,** 135–151 (2013).

164. Hu, H., Juvekar, A., Lyssiotis, C. A., Lien, E. C., Albeck, J. G., Oh, D., Varma, G., Hung, Y. P., Ullas, S., Lauring, J., Seth, P., Lundquist, M. R., Tolan, D. R., Grant, A. K., Needleman, D. J., Asara, J. M., Cantley, L. C. & Wulf, G. M. Phosphoinositide 3-Kinase Regulates Glycolysis through Mobilization of Aldolase from the Actin Cytoskeleton. *Cell* **164,** 433–446 (2016).

165. Marko, A. J., Miller, R. A., Kelman, A. & Frauwirth, K. A. Induction of Glucose Metabolism in Stimulated T Lymphocytes Is Regulated by Mitogen-Activated Protein Kinase Signaling. *PLoS ONE* **5,** e15425 (2010).

166. Lloberas, J., Valverde-Estrella, L., Tur, J., Vico, T. & Celada, A. Mitogen-Activated Protein Kinases and Mitogen Kinase Phosphatase 1: A Critical Interplay in Macrophage Biology. *Front. Mol. Biosci.* **3,** (2016).

167. Si, T.-L., Liu, Q., Ren, Y.-F., Li, H., Xu, X.-Y., Li, E.-H., Pan, S.-Y., Zhang, J.-L. & Wang, K.-X. Enhanced anti-inflammatory effects of DHA and quercetin in lipopolysaccharide-induced RAW264.7 macrophages by inhibiting NF-κB and MAPK activation. *Mol. Med. Rep.* **14,** 499–508 (2016).

168. Sugimoto, M., Sakagami, H., Yokote, Y., Onuma, H., Kaneko, M., Mori, M., Sakaguchi, Y., Soga, T. & Tomita, M. Non-targeted metabolite profiling in activated macrophage secretion. *Metabolomics* **8,** 624–633 (2012).

169. Zhang, A., Sun, H., Xu, H., Qiu, S. & Wang, X. Cell Metabolomics. *OMICS J. Integr. Biol.* **17,** 495–501 (2013).

170. Duarte, I. F., Lamego, I., Rocha, C. & Gil, A. M. NMR metabonomics for mammalian cell metabolism studies. *Bioanalysis* **1,** 1597–1614 (2009).

171. Alonso, A., Marsal, S. & JuliÃ, A. Analytical Methods in Untargeted Metabolomics: State of the Art in 2015. *Front. Bioeng. Biotechnol.* **3,** (2015).

172. Patti, G. J., Yanes, O. & Siuzdak, G. Metabolomics: the apogee of the omics trilogy: Innovation. *Nat. Rev. Mol. Cell Biol.* **13,** 263–269 (2012).

173. Van, Q. N., Issaq, H. J., Jiang, Q., Li, Q., Muschik, G. M., Waybright, T. J., Lou, H., Dean, M., Uitto, J. & Veenstra, T. D. Comparison of 1D and 2D NMR Spectroscopy for Metabolic Profiling. *J. Proteome Res.* **7,** 630–639 (2008).

174. Dunn, W. B., Broadhurst, D. I., Atherton, H. J., Goodacre, R. & Griffin, J. L. Systems level studies of mammalian metabolomes: the roles of mass spectrometry and nuclear magnetic resonance spectroscopy. *Chem Soc Rev* **40,** 387–426 (2011).

175. Fan, T. W. M., & Lane, A. N. Structure-based profiling of metabolites and isotopomers by NMR. *Progress in Nuclear Magnetic Resonance Spectroscopy,* **52,** 69-117 (2007)

176. Xia, J., Broadhurst, D. I., Wilson, M. & Wishart, D. S. Translational biomarker discovery in clinical metabolomics: an introductory tutorial. *Metabolomics* **9,** 280–299 (2013).

177. Meiser, J., Krämer, L., Sapcariu, S. C., Battello, N., Ghelfi, J., D'Herouel, A. F., Skupin, A. & Hiller, K. Pro-inflammatory Macrophages Sustain Pyruvate Oxidation through Pyruvate Dehydrogenase for the Synthesis of Itaconate and to Enable Cytokine Expression. *J. Biol. Chem.* **291,** 3932–3946 (2016).

178. Cheng, J., Che, N., Li, H., Ma, K., Wu, S., Fang, J., Gao, R., Liu, J., Yan, X., Li, C. & Dong, F. Gas Chromatography Time-Of-Flight Mass Spectrometry-

Based Metabolomic Analysis of Human Macrophages Infected by *M. tuberculosis*. *Anal. Lett.* **46,** 1922–1936 (2013).

179. Zimmermann, M., Kogadeeva, M., Gengenbacher, M., McEwen, G., Mollenkopf, H.-J., Zamboni, N., Kaufmann, S. H. E. & Sauer, U. Integration of Metabolomics and Transcriptomics Reveals a Complex Diet of *Mycobacterium tuberculosis* during Early Macrophage Infection. *mSystems* **2,** e00057-17 (2017).

180. Lamour, S. D., Choi, B.-S., Keun, H. C., Müller, I. & Saric, J. Metabolic Characterization of Leishmania major Infection in Activated and Nonactivated Macrophages. *J. Proteome Res.* **11,** 4211–4222 (2012).

181. Hollenbaugh, J. A., Munger, J. & Kim, B. Metabolite profiles of human immunodeficiency virus infected CD4+ T cells and macrophages using LC–MS/MS analysis. *Virology* **415,** 153–159 (2011).

182. Ji, J., Sun, J., Pi, F., Zhang, S., Sun, C., Wang, X., Zhang, Y. & Sun, X. GC-TOF/MS-based metabolomics approach to study the cellular immunotoxicity of deoxynivalenol on murine macrophage ANA-1 cells. *Chem. Biol. Interact.* **256,** 94–101 (2016).

183. Zwicker, P., Schultze, N., Niehs, S., Albrecht, D., Methling, K., Wurster, M., Wachlin, G., Lalk, M., Lindequist, U. & Haertel, B. Differential effects of Helenalin, an anti-inflammatory sesquiterpene lactone, on the proteome, metabolome and the oxidative stress response in several immune cell types. *Toxicol. In Vitro* **40,** 45–54 (2017).

184. Sapcariu, S. C., Kanashova, T., Dilger, M., Diabaté, S., Oeder, S., Passig, J., Radischat, C., Buters, J., Sippula, O. & Streibel, T. Metabolic profiling as well as stable isotope assisted metabolic and proteomic analysis of RAW 264.7 macrophages exposed to ship engine aerosol emissions: different effects of heavy fuel oil and refined diesel fuel. *PloS One* **11,** e0157964 (2016).

185. Zhao, C., Tang, Z., Yan, J., Fang, J., Wang, H. & Cai, Z. Bisphenol S exposure modulate macrophage phenotype as defined by cytokines profiling, global metabolomics and lipidomics analysis. *Sci. Total Environ.* **592,** 357–365 (2017).

186. Feng, J., Zhao, J., Hao, F., Chen, C., Bhakoo, K. & Tang, H. NMR-based metabonomic analyses of the effects of ultrasmall superparamagnetic particles of iron oxide (USPIO) on macrophage metabolism. *J. Nanoparticle Res.* **13,** 2049–2062 (2011).

187. Liu, M., Luo, F., Ding, C., Albeituni, S., Hu, X., Ma, Y., Cai, Y., McNally, L., Sanders, M. A., Jain, D., Kloecker, G., Bousamra, M., Zhang, H., Higashi, R. M., Lane, A. N., Fan, T. W.-M. & Yan, J. Dectin-1 Activation by a Natural Product β-Glucan Converts Immunosuppressive Macrophages into an M1-like Phenotype. *J. Immunol.* **195,** 5055–5065 (2015).

188. Liu, K., Pi, F., Zhang, H., Ji, J., Xia, S., Cui, F., Sun, J. & Sun, X. Metabolomics Analysis To Evaluate the Anti-Inflammatory Effects of Polyphenols: Glabridin Reversed Metabolism Change Caused by LPS in RAW 264.7 Cells. *J. Agric. Food Chem.* **65,** 6070–6079 (2017).

189. Rampersad, S. N. Multiple Applications of Alamar Blue as an Indicator of Metabolic Function and Cellular Health in Cell Viability Bioassays. *Sensors* **12,** 12347–12360 (2012).

190. O'Brien, J., Wilson, I., Orton, T. & Pognan, F. Investigation of the Alamar Blue (resazurin) fluorescent dye for the assessment of mammalian cell cytotoxicity: Resazurin as a cytotoxicity assay. *Eur. J. Biochem.* **267,** 5421–5426 (2000).

191. Kostidis, S., Addie, R. D., Morreau, H., Mayboroda, O. A. & Giera, M. Quantitative NMR analysis of intra- and extracellular metabolism of mammalian cells: A tutorial. *Anal. Chim. Acta* **980,** 1–24 (2017).

192. Wishart, D. S., Feunang, Y. D., Marcu, A., Guo, A. C., Liang, K., Vázquez-Fresno, R., Sajed, T., Johnson, D., Li, C., Karu, N., Sayeeda, Z., Lo, E.,

Assempour, N., Berjanskii, M., Singhal, S., Arndt, D., Liang, Y., Badran, H., Grant, J., Serra-Cayuela, A., Liu, Y., Mandal, R., Neveu, V., Pon, A., Knox, C., Wilson, M., Manach, C. & Scalbert, A. HMDB 4.0: the human metabolome database for 2018. *Nucleic Acids Res.* **46,** D608–D617 (2018).

193. Weljie, A. M., Newton, J., Mercier, P., Carlson, E. & Slupsky, C. M. Targeted Profiling: Quantitative Analysis of ^{1}H NMR Metabolomics Data. *Anal. Chem.* **78,** 4430–4442 (2006).

194. Berben, L., Sereika, S. M. & Engberg, S. Effect size estimation: Methods and examples. *Int. J. Nurs. Stud.* **49,** 1039–1047 (2012).

195. Fuster, J. J. & Walsh, K. The good, the bad, and the ugly of interleukin-6 signaling. *EMBO J.* **33,** 1425-7.(2014).

196. Chen, R., Qi, Q.-L., Wang, M.-T. & Li, Q.-Y. Therapeutic potential of naringin: an overview. *Pharm. Biol.* **54,** 3203–3210 (2016).

197. Leyva-López, N., Gutierrez-Grijalva, E., Ambriz-Perez, D. & Heredia, J. Flavonoids as Cytokine Modulators: A Possible Therapy for Inflammation-Related Diseases. *Int. J. Mol. Sci.* **17,** 921 (2016).

198. Guerra, A. R., Duarte, M. F. & Duarte, I. F. Targeting Tumor Metabolism with Plant-Derived Natural Products: Emerging Trends in Cancer Therapy. *J. Agric. Food Chem.* **66,** 10663–10685 (2018).

199. Strelko, C. L., Lu, W., Dufort, F. J., Seyfried, T. N., Chiles, T. C., Rabinowitz, J. D. & Roberts, M. F. Itaconic Acid Is a Mammalian Metabolite Induced during Macrophage Activation. *J. Am. Chem. Soc.* **133,** 16386–16389 (2011).

200. Newsholme, P., Rosa, L. F. B. P. C., Newsholme, E. A. & Curi, R. The importance of fuel metabolism to macrophage function. *Cell Biochem. Funct.* **14,** 1–10 (1996).

201. Owen, O. E., Kalhan, S. C. & Hanson, R. W. The Key Role of Anaplerosis and Cataplerosis for Citric Acid Cycle Function. *J. Biol. Chem.* **277,** 30409–30412 (2002).

202. Jin, L., Alesi, G. N. & Kang, S. Glutaminolysis as a target for cancer therapy. *Oncogene* **35,** 3619–3625 (2016).

203. Lu, S. C. Regulation of glutathione synthesis. *Mol. Aspects Med.* **30,** 42–59 (2009).

204. Marzocco, S., Di Paola, R., Serraino, I., Sorrentino, R., Meli, R., Mattaceraso, G., Cuzzocrea, S., Pinto, A. & Autore, G. Effect of methylguanidine in carrageenan-induced acute inflammation in the rats. *Eur. J. Pharmacol.* **484,** 341–350 (2004).

205. Tan, H.-Y., Wang, N., Li, S., Hong, M., Wang, X. & Feng, Y. The Reactive Oxygen Species in Macrophage Polarization: Reflecting Its Dual Role in Progression and Treatment of Human Diseases. *Oxid. Med. Cell. Longev.* **2016,** 1–16 (2016).

206. Nishimura, F. de C. Y., de Almeida, A. C., Ratti, B. A., Ueda-Nakamura, T., Nakamura, C. V., Ximenes, V. F. & Silva, S. de O. Antioxidant Effects of Quercetin and Naringenin Are Associated with Impaired Neutrophil Microbicidal Activity. *Evid. Based Complement. Alternat. Med.* **2013,** 1–7 (2013).

207. Kim, B.-H., Choi, J. S., Yi, E. H., Lee, J.-K., Won, C., Ye, S.-K. & Kim, M.-H. Relative antioxidant activities of quercetin and its structurally related substances and their effects on NF-κB/CRE/AP-1 signaling in murine macrophages. *Mol. Cells* **35,** 410–420 (2013).

208. Guimarães-Ferreira, L. Role of the phosphocreatine system on energetic homeostasis in skeletal and cardiac muscles. *Einstein São Paulo* **12,** 126–131 (2014).

209. O'Connor, R. S., Steeds, C. M., Wiseman, R. W. & Pavlath, G. K. Phosphocreatine as an energy source for actin cytoskeletal rearrangements during myoblast fusion: Phosphocreatine regulates cell fusion. *J. Physiol.* **586,** 2841–2853 (2008).

210. Loike, J. D., Somes, M. & Silverstein, S. C. Creatine uptake, metabolism, and efflux in human monocytes and macrophages. *Am. J. Physiol.-Cell Physiol.* **251,** C128–C135 (1986).

211. Fang, Y., Cao, W., Xia, M., Pan, S. & Xu, X. Study of Structure and Permeability Relationship of Flavonoids in Caco-2 Cells. *Nutrients* **9,** 1301 (2017).

212. Cho, S.-Y., Park, S.-J., Kwon, M.-J., Bok, S.-H., Choi, W.-Y., Jeong, W.-I., Ryu, S.-Y., Do, S.-H., Lee, C.-S., Song, J.-C. & Jeong, K.-S. Quercetin suppresses proinflammatory cytokines production through MAP kinases and NF-κB pathway in lipopolysaccharide-stimulated macrophage. *Molecular and Cellular Biochemistry,* **243,** 153-160 (2003)

SUPPLEMENTARY INFORMATION

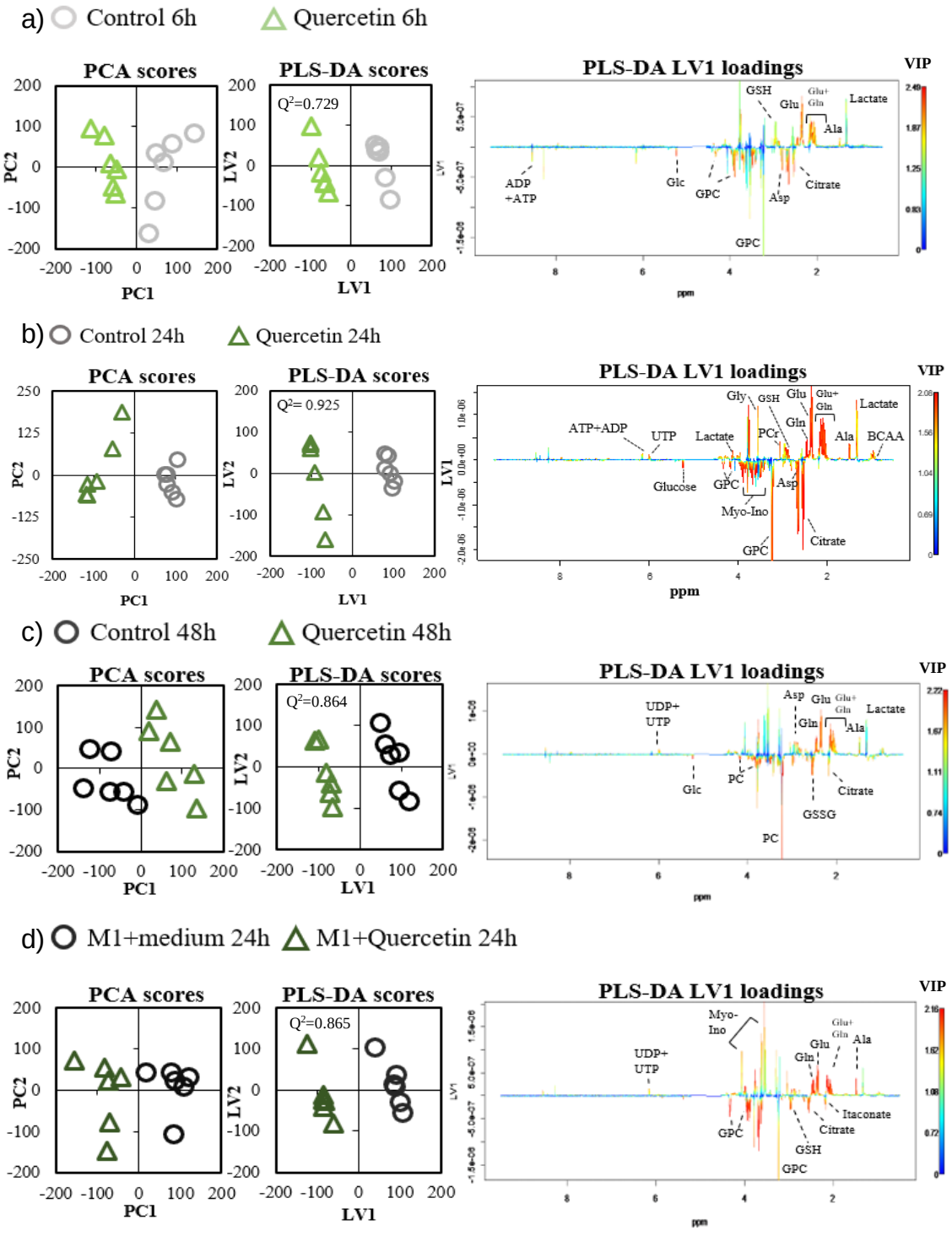

Figure S1: Multivariate analysis of ^{1}H-NMR spectra from the polar extracts of THP-1 derived macrophages comparing M0 macrophages (grey) and Quercetin-treated macrophages (green) , incubated for: a) 6h, b) 24h and c) 48h. M1 macrophages treated with Quercetin for 24h (d). PCA and PLS-DA scores scatter plots (left and center, respectively) and LV1 loadings *w* (right), colored according to variable importance to projection (VIP).

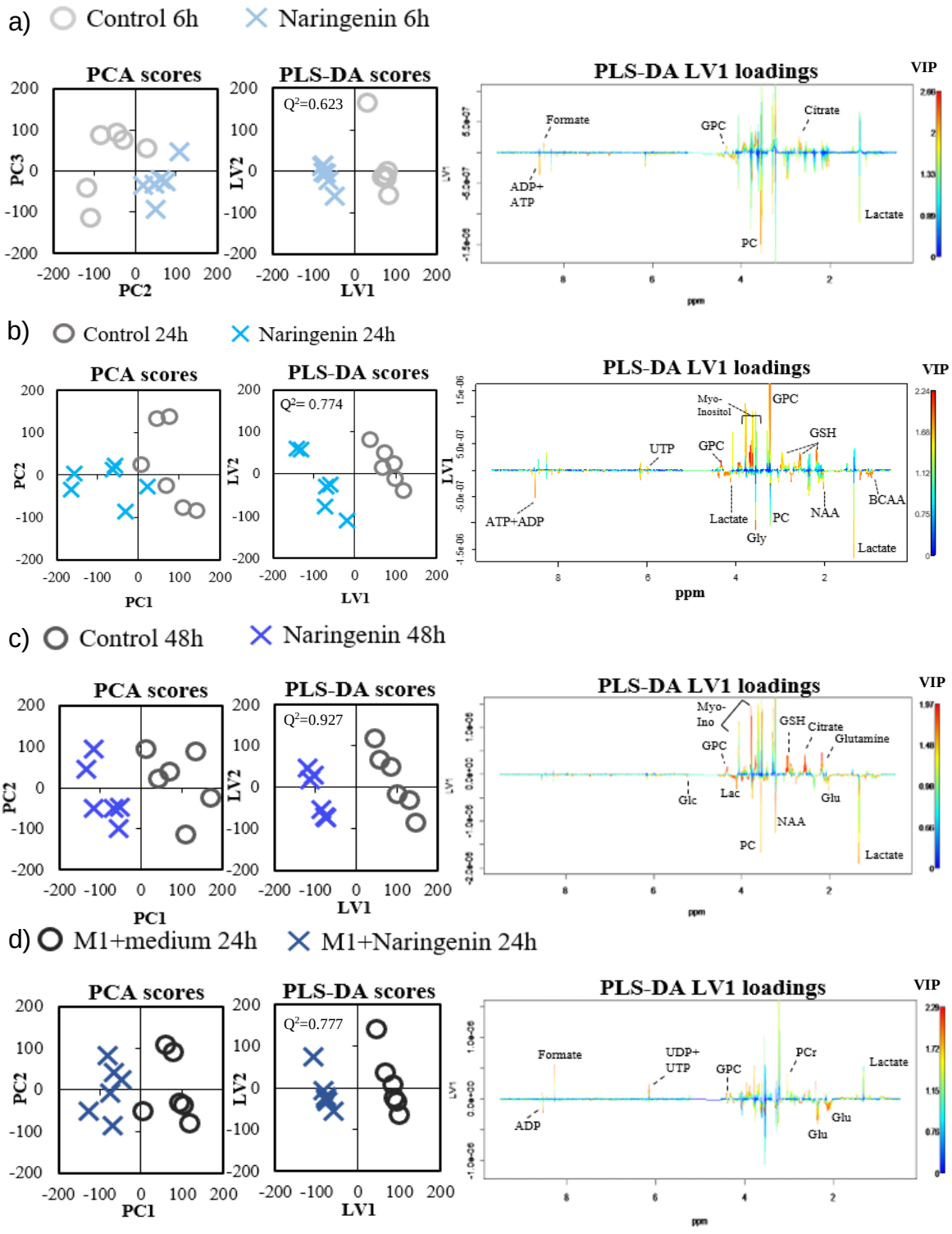

Figure S2: Multivariate analysis of ^{1}H-NMR spectra from the polar extracts of THP-1 derived macrophages comparing M0 macrophages (grey) and Naringenin-treated macrophages (blue) , incubated for: a) 6h, b) 24h and c) 48h. M1 macrophages treated with Naringenin for 24h (d). PCA and PLS-DA scores scatter plots (left and center, respectively) and LV1 loadings w (right), colored according to variable importance to projection (VIP).

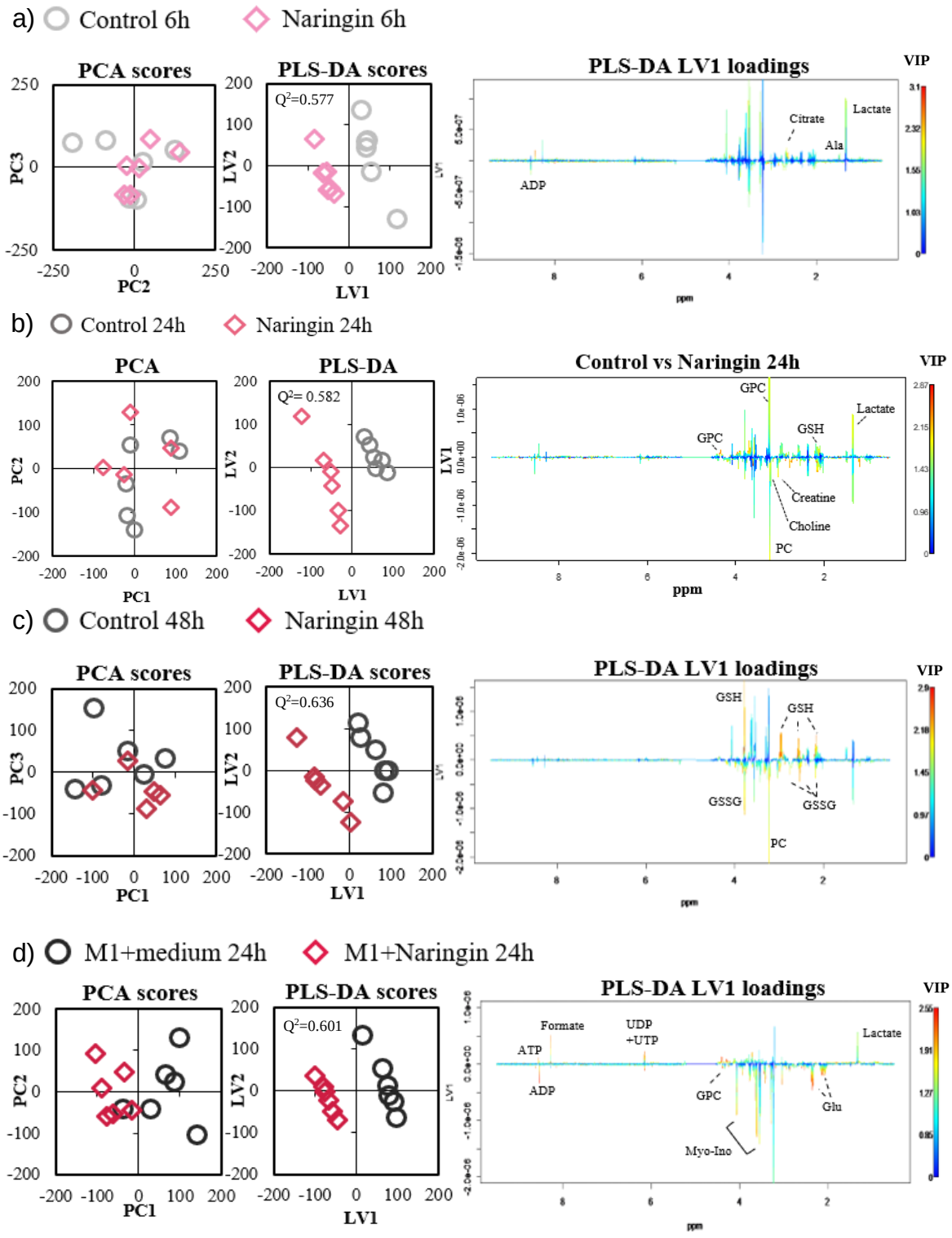

Figure S3: Multivariate analysis of ^{1}H-NMR spectra from the polar extracts of THP-1 derived macrophages comparing M0 macrophages (grey) and Naringin-treated macrophages (pink) , incubated for: a) 6h, b) 24h and c) 48h. M1 macrophages treated with Naringin for 24h (d). PCA and PLS-DA scores scatter plots (left and center, respectively) and LV1 loadings w (right), colored according to variable importance to projection (VIP).

Table S1: Assignment of resonances in the ^{1}H-NMR profile of polar extracts from THP-1 derived macrophages. Multiplicity: s, singlet; d, doublet; t, triplet; q, quartet; m, multiplet; dd, doublet of doublets; dt, doublet of triplets; td, triplet of doublets.

No.	Compound	δ ^{1}H in ppm (multiplicity, assignment)
1	Acetate	1.926 (s, β-CH_3)
2	Acetone	2.236 (s, CH_3)
3	ADP	4.235 (m, C5'H, ribose); 4.40 (m, C4'H, ribose); 4.60 (m, C2'H, ribose); 6.155 (d, C1'H, ribose); 8.285 (s, C8H, ring); 8.53 (s, C2H, ring)
4	Alanine	1.487 (d, β-CH_2); 3.781 (q, α-CH)
5	Arginine	1.659 (m, γ-CH_2); 1.92 (m, β-CH_2); 3.254 (t, δ-CH_2); 3.784 (t, α-CH)
6	Asparagine	2.881 (m, β-CH); 2.931 (m, β'-CH); 4.012 (dd, α-CH)
7	Aspartate	2.672 (dd, β-CH); 2.802 (dd, β'-CH); 3.903 (dd, α-CH)
8	ATP	4.222 (m, C5'H, ribose); 4.296 (m. C5''H, ribose); 4.41 (m, C4'H, ribose); 4.61 (m, C2'H, ribose); 6.155 (d, C1'H, ribose); 8.825 (s, C8H, ring); 8.534 (s, C2H, ring)
9	Choline	3.214 (s, $N(CH_3)_3$); 3.523 (m, CH_2 (NH)); 4.067 (m, CH_2(OH))
10	Citraconate	1.938 (d, C7H); 5.513 (d, C2H)
11	Citrate	2.536 (d, α-CH_2 / β-CH_2); 2.662 (d, α'-CH_2 / β'-CH_2)
12	Creatine	3.039 (s, CH_3); 3.939 (s, N-CH_3)
13	Formate	8.465 (s, CH)
14	Fumarate	6.526 (s, CH)
15	Glucose	3.239 (dd, C3H); 3.405 (m, C5H); 3.464 (m, C6H); 3.535 (dd, C3H); 3.72 (m, C4H, C11H); 3.827 (m, C6H, C11H); 3.895 (dd, C11H); 4.658 (d, C2H); 5.235 (d, C2H)
16	Glutamate	2.044 (m, β-CH); 2.12 (β'-CH); 2.333 (m, γ-CH_2); 3.77 (dd, α-CH)

Table S1 (cont.): Assignment of resonances in the ^{1}H-NMR profile of polar extracts from THP-1 derived macrophages. Multiplicity: s, singlet; d, doublet; t, triplet; q, quartet; m, multiplet; dd, doublet of doublets; dt, doublet of triplets; td, triplet of doublets.

No.	Compound	δ ^{1}H in ppm (multiplicity, assignment)
17	Glutamine	2.142 (m, β-CH_2); 2.454 (m, γ-CH_2); 3.78 (t, α-CH)
18	Glycine	3.575 (s, α-CH_2)
19	Glutathione, oxidized (GSSG)	2.17 (m, β-CH_2, Glu); 2.535 (m, γ-CH_2, Glu); 2.988 (m, β-CH_2, Cys); 3.314 (m, β-CH_2, Cys'); 3.783 (m, α-CH_2, Gly); 3.783 (m, α-CH, Glu)
20	Glutathione, reduced (GSH)	2.175 (m, β-CH_2, Glu); 2.564 (m, γ-CH_2, Glu); 2.96 (m, β-CH_2, Cys); 3.783 (m, α-CH, Gly); 4.603 (q, α-CH, Cys)
21	Glycerophosphocholine	3.24 (s, N(CH_3)$_3$); 3.675 (m, β'-CH_2(N) / γ-CH_2(OH)); 3.917 (s, α-CH_2 / β-CH_2); 4.326 (m, α'-CH_2(P))
22	Histidine	3.232 (m, β-CH_2); 4.00 (m, α-CH_2); 7.165 (s, C4H, ring); 8.072 (s, C2H, ring)
23	Isoleucine	0.944 (t, δ-CH_3); 1.013 (d, β-CH_3); 1.258 (m, γ-CH_2); 1.470 (m, γ'-CH_2); 1.984 (m, β-CH); 3.673 (d, α-CH)
24	Itaconate	3.158 (m, α-CH_2), 5.382 (m, CH_2); 5.860 (m, CH_2')
25	Lactate	1.329 (d, β-CH_3); 4.125 (q, α-CH)
26	Leucine	0.963 (t, δ-CH_3); 1.699 (m, γ-CH / β-CH_2); 3.736 (m, α-CH)
27	Lysine	1.439 (m, γ-CH_2); 1.725 (m, δ-CH_2); 1.904 (m, β-CH_2); 3.001 (t, ε-CH_2); 3.765 (t, α-CH)
28	Methylguanidine	2.845 (s, CH_3(N))
29	*myo*-Inositol	3.286 (t, C5H); 3.544 (dd, C1'H / C3H); 3.632 (t, C4H / C6H); 4.072 (t, C2H)
30	NAD+	4.230 (m, A5'H); 4.357 (m, A4'H); 4.383 (m, A4'H / N5'H); 4.411 (dd, N3'H); 4.469 (m, A3'H); 4.513 (m, N2'H); 6.031 (d, N1'H); 6.104 (d, A1'H); 8.172 (s, A2H / N5H); 8.827 (d, N4H); 9.122 (d, N6H); 9.339 (s, N2H)
31	*N*-Acetylaspartate	2.030 (s, CH_3); 2.507 (dd, β-CH_2); 2.69 (dd, β'-CH_2); 4.398 (dd, α-CH)

Table S1 (cont.): Assignment of resonances in the ^{1}H-NMR profile of polar extracts from THP-1 derived macrophages. Multiplicity: s, singlet; d, doublet; t, triplet; q, quartet; m, multiplet; dd, doublet of doublets; dt, doublet of triplets; td, triplet of doublets.

No.	Compound	δ ^{1}H in ppm (multiplicity, assignment)
32	Pantothenate	0.905 (s, CH_3); 0.925 (s,CH_3); 2.435 (t, α-CH_2); 3.416 (d, CH_2); 3.438 (q, β-CH_2); 3.510 (d, CH_2); 3.99 (s, CH)
33	Phenylalanine	3.146 (m, β-CH); 3.280 (dd, β'-CH); 4.00 (m, α-CH); 7.384 (d, C2H / C6H, ring); 7.39 (d, C4H, ring); 7.43 (t, C3H / C5H, ring)
34	Phosphocholine	3.23 (s, $N(CH_3)_3$); 3.62 (m, N-CH_2); 4.172 (m, PO_3-CH_2)
35	Phosphocreatine	3.04 (s, CH_3); 3.955 (s, CH_2)
36	Phosphoethanolamine	3.232 (t, CH_2(O)); 4.005 (td, N-CH_2)
37	Proline	2.014 (m, γ-CH_2); 2.08 (m, β-CH); 2.35 (m, β'-CH); 3.35 (dt, δ-CH); 3.418 (dt-δ'-CH); 4.137 (dd, α-CH)
38	Pyroglutamate	2.05 (m, β-CH_2); 2.40 (m, γ-CH_2); 2.495 (m, β'-CH_2); 4.17 (dd, α-CH)
39	Serine	3.852 (dd, α-CH); 3.99 (m, β-CH_2)
40	Succinate	2.41 (s, CH_2)
41	Taurine	3.27 (t, S-CH_2); 3.43 (t, N-CH_2)
42	Threonine	1.341 (d, γ-CH_3); 3.950 (d, α-CH); 4.269 (m, β-CH)
43	Tyrosine	3.07 (m, β'-CH); 3.21 (m, β-CH); 3.95 (m, α-CH); 6.91 (d, C3H / C5H, ring); 7.21 (d, C2H / C6H, ring)
44	UDP	4.231 (m, C5'H, ribose); 4.280 (m, C4'H, ribose); 4.398 (t, C2'H, ribose); 4.44 (t, C3'H, ribose); 5.97 (s, C1'H, ribose); 5.98 (d, C6H, ring); 7.995 (d, C5H, ring)
45	UTP	4.26 (m, C5'H, ribose); 4.295 (m, C4'H, ribose); 4.416 (t, C2'H, ribose); 4.45 (t, C3'H, ribose); 5.98 (s, C1'H, ribose); 5.995 (d, C6H, ring); 7.982 (d, C5H, ring)
46	Valine	1.027 (d, γ-CH_2); 2.265 (m, β-CH); 3.625 (d, α-CH)